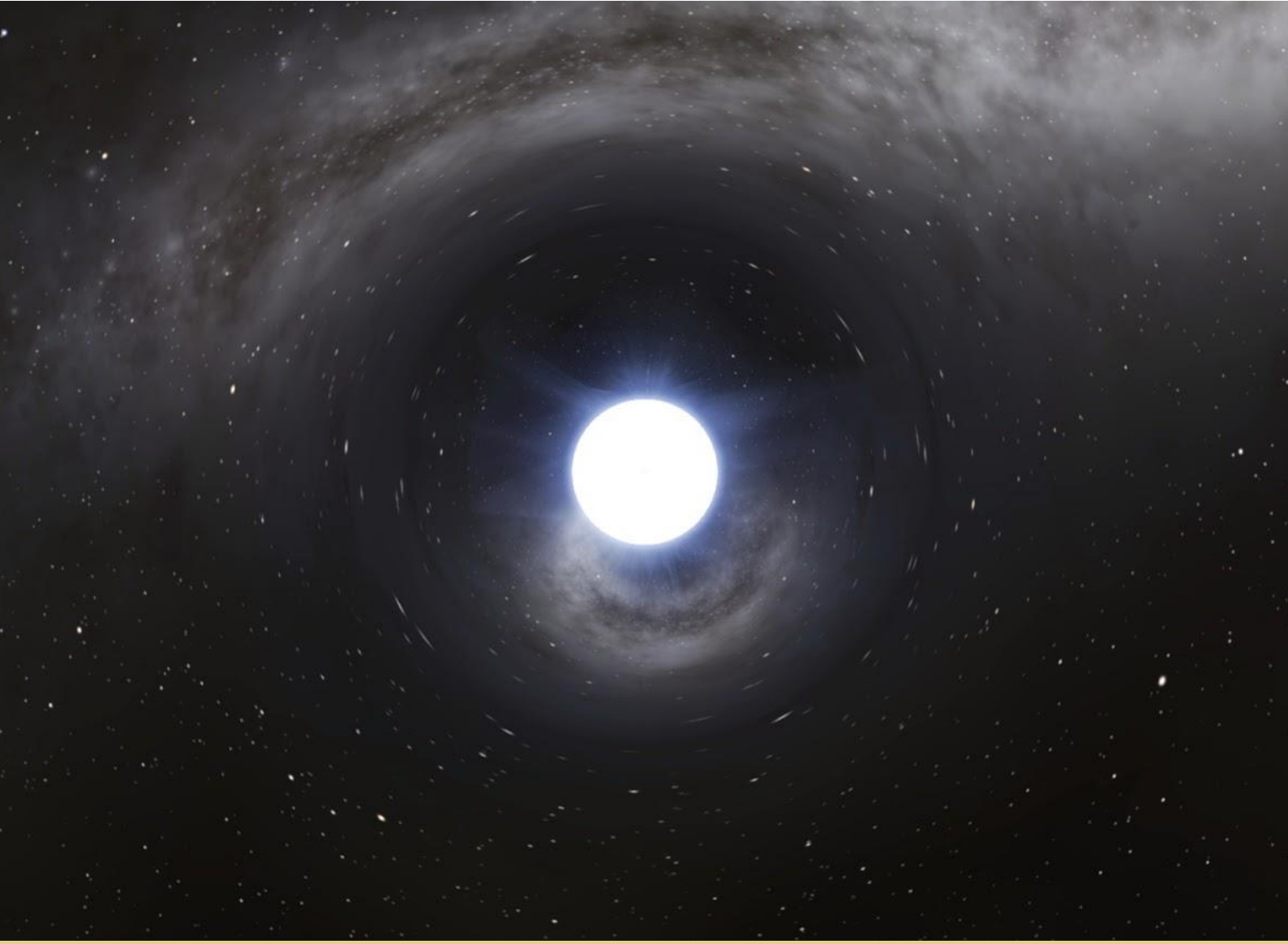

André Marques Pina de Oliveira Duarte

Two Phase Model for Warm Stellar Matter

Tese de Mestrado em Física

Setembro/2017

· U C ·

Universidade de Coimbra

Cover photo rendered with Space Engine
(spaceengine.org)

Two phase model for warm stellar matter

An equation of state for compact stars

AUTHOR: André Duarte

SUPERVISOR: Constança Providência

A thesis submitted for the degree of
Master of Science in Physics

• U  C •

Departmento de Física
Faculdade de Ciência e Tecnologia
Universidade de Coimbra
September 15th, 2017

Abstract

In this work a two-phase model for warm dense stellar matter is presented and used to study the properties and structure of neutron stars. In this approach two effective models of dense matter, the NL3$\omega\rho$ model of hadronic matter, and the NJL model for quark matter, are used to describe matter at low (around nuclear saturation density) and high (much higher than saturation density) densities, respectively. These are unified in a single model by treating each as a model of a separate phase (the confined and deconfined phases) of dense matter, with the two phases coexisting in thermodynamic equilibrium.

This two-phase approach predicts an interval of densities at which both hadronic and deconfined matter coexist, the so called "mixed phase", as well as purely hadronic matter at low densities and pure quark matter at high densities. At very low densities matter no longer exists as uniform matter in the ground state; it exists instead as a lattice of nuclei: the neutron star crust. This is accounted for with an approximation scheme that yields very good results for stars with masses of astrophysical interest.

The parametrization of the models in terms of experimental quantities is discussed. The properties and structure of neutron stars made of this matter are calculated, and the effect of varying the parameters of the models is studied. It is shown that the model predicts neutron stars of mass and radius compatible with the latest astronomical observations, provided that the NJL model vector coupling constant lies in a certain interval. It is concluded that it is possible for the heavier stars predicted by this model to have a hybrid or even pure quark core.

Furthermore, proto-neutron stars are idealized as constant-entropy stars and their properties are studied. This enables conclusions to be drawn about the formation and evolution of neutron stars via a purely stationary analysis. Proto-neutron stars at various stages of formation are thus modelled, and their properties discussed.

Resumo

Neste trabalho estudou-se um modelo de duas fases para matéria estelar densa e quente, e aplicou-se esse modelo ao estudo das propriedades e estrutura de estrelas de neutrões. Nesta abordagem dois modelos de matéria densa, o modelo NL3$\omega\rho$ para matéria hadrónica e o modelo NJL para matéria de quarks, são usados para descrever matéria a baixas (cerca da densidade nuclear) e altas densidades (várias vezes a densidade nuclear), respectivamente. Estes modelos são unificados num só tratando cada um destes como modelos de uma dada fase (fase confinada e desconfinada) de matéria densa, com as duas fases em equilíbrio termodinâmico.

Esta abordagem prevê um intervalo de densidades em que coexistem matéria confinada e desconfinada, na chamada "fase mista", bem como matéria puramente hadrónica a baixas densidades e puramente de quarks a altas densidades. A densidades muito baixas o estado mais favorável deixa de ser matéria uniforme no estado fundamental mas sim uma lattice de núcleos: a crosta da estrela de neutrões. Isto é tido em conta através de uma aproximação que tem muito boa precisão para estrelas de massas astrofisicamente realistas.

A parametrização dos modelos em termos de grandezas experimentais é discutida. As propriedades e a estrutura das estrelas de neutrões compostas desta matéria é estudada. Mostra-se que o modelo prevê estrelas de neutrões de massa e raio compatíveis com as observações astronómicas mais recentes, dado que a constante de acoplamento vectorial do modelo NJL esteja num certo intervalo. Conclui-se que é possível que as estrelas mais pesadas previstas por este modelo tenham um núcleo de matéria híbrida ou até puramente de quarks.

Para além disso, idealizam-se proto-estrelas de neutrões como estrelas de entropia constante e estudam-se as suas propriedades. Isto permite que sejam tiradas conclusões sobre a formação e evolução de estrelas de neutrões através de uma análise puramente estacionária. Constroem-se assim estrelas de neutrões em diferentes estágios de fornação, e discutem-se as suas propriedades.

Agradecimentos

Em primeiro lugar, quero agradecer à Prof[a]. Doutora Constança Providência, pela dedicação e constante disponibilidade que demonstrou para me ajudar ao longo deste trabalho. Sem as suas sugestões e o seu apoio jamais teria sido possível completar este projecto. Também a todos os professores do Departamento de Física da Universidade de Coimbra devo uma palavra, por tudo o que me transmitiram ao longo destes cinco anos de estudo.

Aos meus pais e avó, pelo amor e apoio incondicional que me sempre me deram; no fundo por me terem aturado estes 22 anos. Não há-de ter sido nada fácil. Ao meu irmão por ser um bom amigo, e um excelente parceiro de Mario Kart.

À Margarida, por ser uma das pessoas mais fantásticas que alguma tive o prazer de conhecer.

Aos meus colegas de curso que me acompanharam durante todo ou parte do meu precurso académico. Foi um privilégio ter cruzado caminho convosco.

Por fim, uma palavra a todas aquelas pessoas que de uma forma ou outra deixaram a sua marca na minha vida até agora. São mais do que se possa contar.

Contents

Units and conventions

In this work we use natural units,

$$\hbar = c = k_B = 1$$

where $\hbar$ is the reduced Planck constant, c is the speed of light, and k_B is the Boltzmann constant.

Energy, mass, momentum and temperature have the same units, commonly expressed in MeV ($1.6022 \times 10^{-13}\,\mathrm{J}$), and length and time have inverse units, usually expressed in fm ($10^{-15}\,\mathrm{m}$). The following conversion factor is useful:

$$\hbar c = 1 = 197.326\,\mathrm{MeV\,fm}$$

In SI units:

$$\begin{aligned} 1\,\mathrm{MeV} &= 1.7827 \times 10^{-30}\,\mathrm{kg} \\ &= 1.1605 \times 10^{10}\,\mathrm{K} \\ 1\,\mathrm{fm} &= 3.3356 \times 10^{-24}\,\mathrm{s} \end{aligned}$$

The metric tensor is defined in the time-positive convention.

$$\eta^{\mu\nu} = \eta_{\mu\nu} = \mathrm{diag}(+1, -1, -1, -1)$$

Throughout this work we will employ the Einstein summation convention whereby sums are performed over repeated upper and lower indices, e.g.

$$a^\mu b_\mu \equiv \sum_\mu a^\mu b_\mu$$

Unless otherwise explicitly noted, greek indices (μ, ν, etc.) are assumed to go through $0, 1, 2, 3$, while latin letters i, j, etc. are assumed to go only through the space indices $1, 2, 3$.

The identity matrix of dimension N is denoted

$$\mathbb{1}_N \equiv \mathrm{diag}(\underbrace{1, \ldots, 1}_{N\mathrm{times}})$$

the subscript may be omitted when its value is obvious from context.

Outline

In Chapter 1 we motivate the study of neutron stars, briefly describe their overall properties and establish experimental limits to their properties. We develop the theory of neutron star structure from general relativity and establish the need for a model of neutron star matter, from which we can obtain an equation of state. We discuss the conditions of stability, and we describe a method for calculating crust mass and thickness without a crust EoS.

In Chapter 2 we develop the formalism of quantum field theory which we need in order to describe our models of neutron star matter. We present the theory of Quantum Chromodynamics and examine its properties and symmetries, which will guide our attempts to write an effective model. We introduce the mean field approximation. We introduce the concept of grand canonical ensemble which will enable us to analyse the thermodynamics of a model, and show how to calculate it for a mean field model.

In Chapter 3 we present a model of neutron star matter, based on a two-model approach of nucleons in a confined state through a model of hadrons and interaction-mediating mesons, and of matter in a deconfined state through an effective theory of quark matter interacting via four-point interactions. We describe how to build a complete equation of state by combining the two models in a two-phase construction in thermodynamic equilibrium. We derive the zero-temperature limit of the model.

In Chapter 4 we present the results from our work, and in Chapter 5 we draw conclusions and discuss future directions of research.

The raw data files generated in the course of this work can be freely accessed at `https://github.com/andrepd/masterthesis-data`.

Chapter 1

Neutron Stars

1.1 Introduction

Neutron stars are some of the most extreme objects in the universe, in that they are the smallest and densest stars known to exist. Neutrons stars are formed after a massive star ($M > 8\,\mathrm{M}_\odot$) undergoes core collapse. In the process, the supernova explosion ejects the outer layers of the star while the core is compressed. The remnant core left after the star goes nova is the neutron star [1].

During their life stars burn hydrogen through nuclear fusion, producing heat and heavier elements. The pressure from this process balances the gravitational pressure, and thus the star is stable. When the fuel — hydrogen — is exhausted, the star starts burning helium since that reaction is now the most energetically favourable, thus producing even heavier elements. When the helium is exhausted the star proceeds to undergo fusion of still heavier elements until they are exhausted, and so on until it eventually reaches iron. Beyond iron, nuclear fusion is no longer exothermic and thus will no longer occur in the star. Absent the pressure from the heat generated by fusion, the gravitational force is unbalanced and star collapses. Depending on its mass, it may evolve to become a white dwarf, either directly or passing through a red giant stage first, or if massive enough may explode in a supernova, giving birth to a neutron star or a black hole [1].

Given their extreme conditions neutron stars are naturally occurring "laboratories" or "testbeds" of physics. Many interesting physical processes are though to take place in neutron stars, and given their extreme density they provide conditions which we cannot reproduce by any means here on Earth, since we do not have the technology for that. Thus studying neutron stars may give us valuable insights into physics at very high energy scales, and even a possibility to test our hypotheses in high-energy physics in these natural laboratories.

Namely, the properties and behaviour of dense matter are an open problem in physics (where by dense we mean above the nuclear saturation density). Studying neutron stars is a way to test the validity of models of dense matter and strong interactions: by constructing neutron stars from models of dense matter and comparing with experimental data we can deduce constraints on our theory of dense matter.

1.2 General properties

Mass

Two theoretical limits of the mass of a neutron star are the Chandrasekhar limit at $1.4\,M_\odot$ and the Tolman–Oppenheimer–Volkov limit at $\approx 3\,M_\odot$ [2]. The Chandrasekhar limit gives the upper bound on the mass of a stable white dwarf star, as modelled by a degenerate electron gas. White dwarfs are stable due to the balance between gravitational attraction and electron degeneracy pressure. The Chandrasekhar limit corresponds to the mass at which the electron degeneracy pressure becomes insufficient to balance the gravitational self-attraction. The exact value of this limit depends on the specific model of matter but it's generally taken to be $\approx 1.4\,M_\odot$ [3]. Since no white dwarf can exist in a stable state at a higher mass, such a white dwarf would continue to evolve to a different type of star such as a neutron star. Conversely, compact stars below that limit should be white dwarfs (although it's important to realize there is an interval of a few tenths of a solar mass where the masses of low-mass neutron stars and high-mass white dwarfs can overlap; there can exist neutron stars as light as $1.1\,M_\odot$ [4]).

On the other hand, the Tolman–Oppenheimer–Volkoff limit is an analogous upper bound on the mass of a stable neutron star. It is the point at which gravity overcomes the balancing forces in a star composed of neutron degenerate matter resulting in collapse to a black hole. Once again it depends on the specific equation of state that is used to model the dense matter in the star, but modern treatments give the value of this limit in the range from approximately 2 to 3 solar masses [5].

Furthermore, another important constraint is imposed on the admissible values for the mass of a neutron star: an observational one. The maximum observed value for the mass of a neutron star is $\approx 2\,M_\odot$, as measured in the PSR J0348+0432 and PSR J1614–2230 pulsars [4]. This gives an empirical range for the masses which the hypothetical models need to reproduce. Any theoretical model we develop must produce stars compatible with these observational constraints, namely it must predict stable stars of $M \gtrsim 2\,M_\odot$ in its sequence. Figure 1.1 shows measurements of the masses of several neutron stars and respective uncertainties [6].

Radius

The relation between the mass and radius of a neutron star is a consequence of the properties of the matter that makes up the star. As such, the predicted size of a neutron star of a certain mass may vary quite a bit between different models. In general, neutron stars have radii in the order of magnitude of $\sim 10\,\mathrm{km}$.

The radius of a neutron star is difficult to measure empirically. There are significant challenges both in making measurements and in accurately assessing their uncertainty. Nevertheless, there have been a growing number of radius measurements of neutron stars made with modern X-ray instruments in the past few years; recent studies have also included a careful assessment of the statistical and systematic uncertainties in such measurements [4,7]. The most reliable and constraining of these have come from neutron

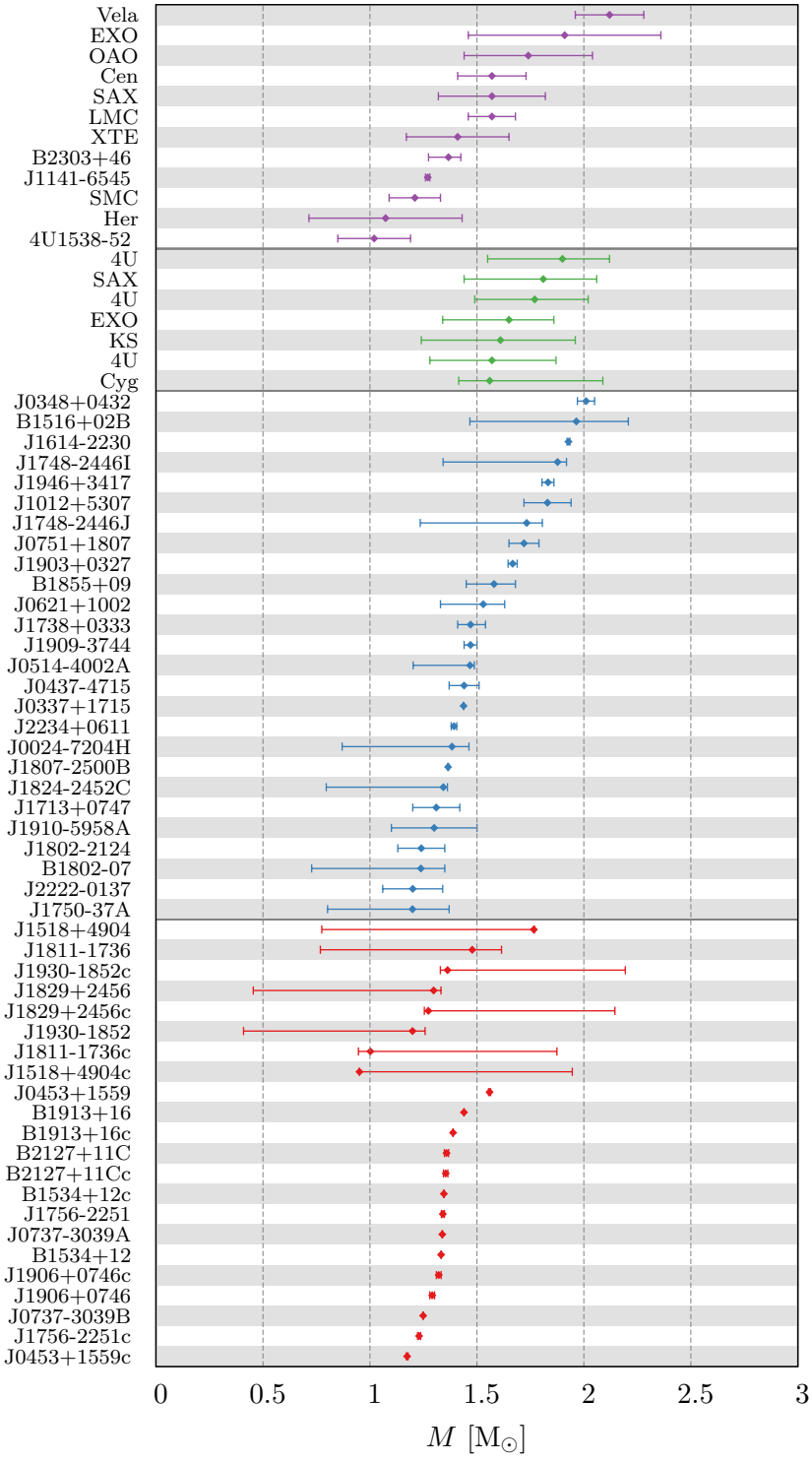

Figure 1.1: Observed neutron star masses. Red: neutron star binaries, blue: recycled pulsars, green: bursters, purple: slow pulsars. [6]

stars in binaries with low-mass companions. Based on these measurements we can put an observational constraint on the likely mass–radius relation [4].

The next generation of X-ray telescopes currently being built are expected to provide even more accurate measurements [4].

Temperature

The temperature inside a newly formed neutron star can be as high as 10^{12} K, however the star rapidly diffuses away a great number of neutrinos, which carry away so much energy that in a short amount of time (seconds/minutes) the star will cool down to temperatures on the range of 10^5 to 10^9 K ($\sim 10^{-1}$ to 10^{-5} MeV), cold on a nuclear scale [1].

Density and pressure

Neutron stars have densities in the order of magnitude of the nuclear density: in the order of $10^{14}\,\mathrm{g/cm^3}$. These are *global* densities ($M_{\mathrm{total}}/V_{\mathrm{total}}$); the local density at a given point (close to the centre for example) can be even higher. By comparison, the Sun has a density of about $1.4\,\mathrm{g/cm^3}$.

The pressure inside the star can range up to $\sim 10^{35}$ Pa in the inner core [1].

Rotation

Since in the formation process the neutron star retains its parent star's angular momentum while having a sharply reduced size, it is common for the resulting neutron star to be formed with a very high rotation speed: the period of rotation can vary between milliseconds and tens of seconds; the fastest known pulsar spins at 716 Hz [8]. In this work, however, we will only consider static stars.

Magnetic field

Neutron stars are known to have strong magnetic fields. The magnetic field strength at the surface of neutron stars has been estimated to lie in the range from 10^4 to 10^{11} T [1] (magnetars, a class of neutron stars, have the strongest observed magnetic fields in the universe; compare to the Earth magnetic field of about 25 to 65 µT, or the Sun's, at $\sim 10^{-2}$ T). The origin of such a strong magnetic field is still uncertain.

Gravitational field

By virtue of their density neutron stars have very strong gravitational fields. The gravitational field at the surface of a neutron star is in the order of $10^{12}\,\mathrm{m/s^2}$. Another measure of the star's gravitational pull is the escape velocity, which can range from 100 000 to 150 000 km/s, over a third of the speed of light. One consequence of this fact is that objects impacting the star do so at such tremendous speeds that almost certainly

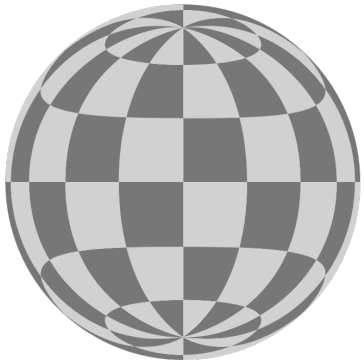

Figure 1.2: Gravitational distortion of a sphere with a radius equal to twice its Schwarzschild radius. It is possible to view more than half of the surface from any position.

the atoms disintegrate on impact, thus rendering the matter identical to the rest of the neutron stars.

The star's gravity induces a visible gravitational lensing effect (Figure 1.2). Also, because of their strong gravitational fields, it is thought that neutron star binaries are one of the strongest sources of gravitational waves in the universe [9].

In order to treat the strong gravity in neutron stars, we will necessarily have to use the formalism of general relativity, the most accurate theory of gravity we currently possess; neutron stars are too dense to admit a Newtonian approximation [1].

1.3 Structure

The detailed internal structure of neutron stars is not currently known. Experimental data about the interior of a neutron star, particularly its core, is scant, and as such not many details are known about it. As a rule of thumb, the closer to the center we get the less knowledge we have: we have a good idea of the composition of the atmosphere and outer crust, but predictions about the composition of the inner core vary widely. Nevertheless we can give an overview of the structure of the star [1] (see Figure 1.3).

Neutron stars have a thin atmosphere, hypothesized to be only micrometers thick; its dynamics are fully controlled by the star's magnetic field [10]. Below, the outermost part of the star is the solid crust, with an extremely smooth surface due to the gravitational field. The crust is formed by a solid lattice of heavy atomic nuclei with a gas of electrons flowing through the gaps. Proceeding inwards, the density increases, the nuclei become more neutron-rich due to beta capture (being prevented from decaying by the tremendous pressures) until a point where the energy levels for neutrons become filled up to the rest mass of the neutron. At this point, new neutrons produced by beta capture will become free: this is the neutron drip point. This marks the transition to the inner crust, where there is now a neutron fluid flowing in between the nuclei.

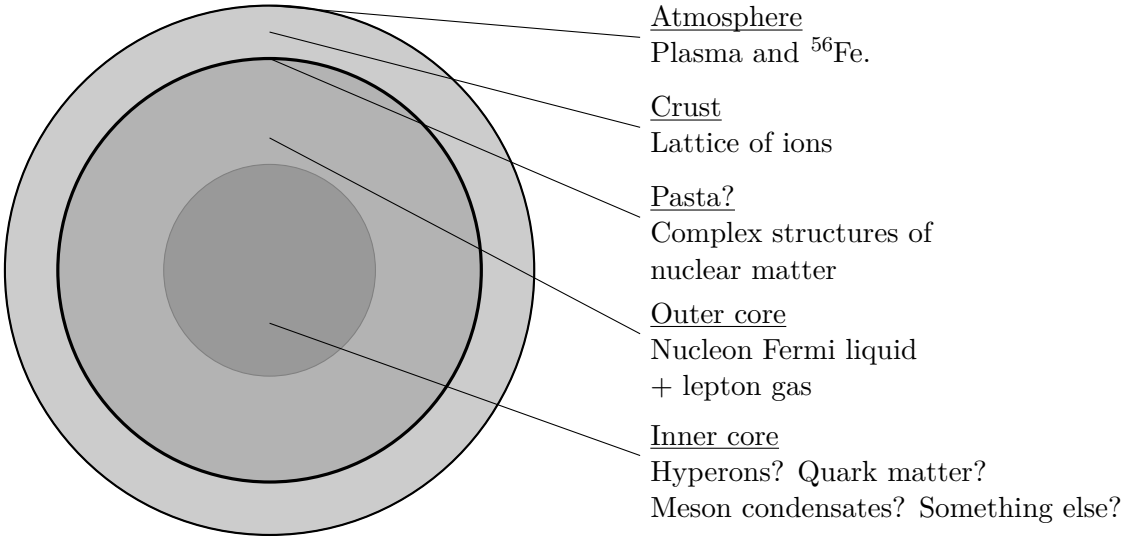

Figure 1.3: Structure of a neutron star.

As the density increases, more and more neutrons "drip" out of the nuclei until eventually all neutrons are free. This marks the beginning of the core region, where matter is in the form of free nucleons and leptons. In the transition, several intermediate configurations of matter may exist, called nuclear pasta, in which the most favourable configurations of nuclear matter immersed in the neutron liquid may be, for example, droplets, long rods, or sheets of nuclear matter.

Finally, in the inner core the composition of matter remains an unknown. Proposed models' predictions include superfluid neutron-degenerate matter, degenerate strange matter, a quark-gluon plasma, or other exotic phases of matter. In this work we propose a model in which the inner core of the star may contain pure quark matter.

1.4 General relativity

The most accurate description of gravity we have is given by the theory of General Relativity [11]. This theory elegantly describes gravity using geometry, by relating the curvature of spacetime at a given point to the energy–momentum content in that point. The force of gravity arises from that curvature, which bends the geodesic trajectories bodies in freefall take in spacetime.

The theory is contained in a single, elegant tensor equation [11]: the Einstein field equation:

$$G_{\mu\nu} = 8\pi G T_{\mu\nu} \tag{1.1}$$

Often called *gnocchi phase*, *spaghetti phase*, and *lasagna phase*, respectively, hence the name nuclear pasta.

Despite its simple appearance, when fully spelled out the Einstein field equations consist of 10 coupled non-linear partial differential equations.

where $G_{\mu\nu}$, the Einstein tensor, encodes the curvature of spacetime and $T_{\mu\nu}$, the stress–energy tensor, represents the energy–momentum content. Both are tensor fields over spacetime.

The Einstein tensor is a symmetric, divergenceless rank 2 tensor that expresses the curvature of spacetime. It is written

$$G_{\mu\nu} = R_{\mu\nu} - \frac{1}{2}Rg_{\mu\nu} \tag{1.2}$$

where $R_{\mu\nu}$ is the Ricci tensor and R is the Ricci scalar. Both can be calculated by contracting the Riemann curvature tensor,

$$R^{\rho}{}_{\sigma\mu\nu} = \partial_\mu \Gamma^{\rho}{}_{\nu\sigma} - \partial_\nu \Gamma^{\rho}{}_{\mu\sigma} + \Gamma^{\rho}{}_{\mu\lambda}\Gamma^{\lambda}{}_{\nu\sigma} - \Gamma^{\rho}{}_{\nu\lambda}\Gamma^{\lambda}{}_{\mu\sigma} \tag{1.3}$$

where Γ represents the symmetric Christoffel symbol (of the second kind), which encodes the metric connection such that covariant derivatives of vector fields can be written

$$\nabla_\mu V^\nu = \partial_\mu V^\nu + \Gamma^{\nu}{}_{\lambda\mu} V^\lambda \tag{1.4}$$

It can be written in terms of the metric as

$$\Gamma^{\sigma}{}_{\alpha\beta} = \frac{1}{2} g^{\mu\nu}(\partial_\alpha g_{\beta\nu} + \partial_\beta g_{\alpha\nu} - \partial_\nu g_{\alpha\beta}) \tag{1.5}$$

The Ricci tensor is then obtained by contracting the Riemann tensor thusly:

$$R_{\mu\nu} = R^{\sigma}{}_{\mu\sigma\nu} \tag{1.6}$$

while the Ricci scalar is the trace of this latter.

$$R = R^{\mu}{}_{\mu} \tag{1.7}$$

A general definition of $T^{\mu\nu}$ can be said to be "the flux of four-momentum p^μ through a surface of constant x^ν" [11]; we will present a more practical way to write it when we attempt to solve the equations.

The Einstein field equations can therefore be used to find the geometry of spacetime (i.e. the metric tensor) given an configuration of energy and momentum in spacetime. Then, the inertial trajectories of particles are given by an equation of motion called the geodesic equation:

$$\frac{\mathrm{d}^2 x^\mu}{\mathrm{d}s^2} + \Gamma^{\mu}{}_{\alpha\beta} \frac{\mathrm{d}x^\alpha}{\mathrm{d}s} \frac{\mathrm{d}x^\beta}{\mathrm{d}s} = 0 \tag{1.8}$$

These equations tell us that the content of matter and energy in any given point affects the curvature of spacetime in that point (Einstein field equations); in turn the curvature controls the distribution of matter and energy (geodesic equation). This mutual effect makes the theory very hard to solve. Nonetheless, depending on the problem, there are often numerous symmetries and assumptions that we can exploit to reduce the complexity of the equations. We will find that for an idealized static star we are able to analytically solve these equations.

1.4.1 The Tolman–Oppenheimer–Volkoff equation

In 1939 J. Robert Oppenheimer and George Volkoff, building upon earlier work by Richard Tolman, derived their namesake equation by solving the Einstein field equations for a static, isotropic, spherically symmetric perfect fluid in hydrostatic equilibrium [12]. We will first examine if these are reasonable assumptions upon which to model a neutron star, and then we will attempt to obtain the Tolman–Oppenheimer–Volkoff equation following their derivation.

We can consider a static or slowly rotating star to be isotropic and spherically symmetric, but neutron stars actually often have a high frequency of rotation, as mentioned before. However we can consider a static star since we are mainly interested in calculating the mass and radius of the star and not in the effects of rotation (the corrections on those, for typical rotation speeds, are small, on the order of a few percent [4,13]). As for hydrostatic equilibrium, this is a reasonable assumption for stars after enough time has passed from their formation; they have settled and can be treated as a perfect fluid in hydrostatic equilibrium [1].

Let us now follow the derivation. The line element in a given metric is written

$$\mathrm{d}s^2 = g_{\mu\nu}\,\mathrm{d}x^\mu\,\mathrm{d}x^\nu \tag{1.9}$$

For a static (no time dependence) and spherically symmetric (no angular dependence) metric, the most general line element is

$$\mathrm{d}s^2 = A(r)\,\mathrm{d}t^2 - B(r)\,\mathrm{d}r^2 - r^2\,\mathrm{d}\theta^2 - r^2\sin^2\theta\,\mathrm{d}\phi^2 \tag{1.10}$$

in spherical coordinates. Anticipating a more useful form we write the metric as

$$\mathrm{d}s^2 = e^{2\nu(r)}\,\mathrm{d}t^2 - e^{2\lambda(r)}\,\mathrm{d}r^2 - r^2\,\mathrm{d}\theta^2 - r^2\sin^2\theta\,\mathrm{d}\phi^2 \tag{1.11}$$

In this metric the nonvanishing Christoffel symbols are

$$\begin{aligned}
\Gamma^1_{00} &= \nu' e^{2(\nu-\lambda)} & \Gamma^0_{10} &= \nu' \\
\Gamma^1_{11} &= \lambda' & \Gamma^2_{12} &= \Gamma^3_{13} = 1/r \\
\Gamma^1_{22} &= -re^{-2\lambda} & \Gamma^3_{23} &= \cot\theta \\
\Gamma^1_{33} &= -r\sin^2\theta e^{-2\lambda} & \Gamma^2_{33} &= -\sin\theta\cos\theta
\end{aligned} \tag{1.12}$$

so that the nonvanishing Ricci curvature tensor elements are

$$\begin{aligned}
R_{00} &= -e^{2(\nu-\lambda)}\left[\nu'' - \lambda'\nu' + \nu'^2 + \frac{2\nu'}{r}\right] \\
R_{11} &= \nu'' - \lambda'\nu' + \nu'^2 - \frac{2\lambda'}{r} \\
R_{22} &= e^{-2\lambda}(1 + r(\nu' - \lambda')) - 1 \\
R_{33} &= R_{22}\sin^2\theta
\end{aligned} \tag{1.13}$$

A perfect fluid is a fluid which can be completely characterized by its rest mass density and isotropic pressure (isotropic meaning the pressure is the same in every direction). Specifically, perfect fluids have no shear stresses, viscosity, or heat conduction.

Commonly abbreviated TOV equation or just TOV.

and the scalar curvature

$$R = e^{-2\lambda}\left[-2\nu'' + 2\lambda'\nu' - 2\nu'^2 - \frac{2}{r^2} + \frac{4}{r}(\lambda' - \nu')\right] + \frac{2}{r^2} \tag{1.14}$$

where the prime ($'$) denotes differentiation with respect to r.

Now, the energy–momentum tensor of a perfect fluid is

$$T^{\mu\nu} = -Pg^{\mu\nu} + (\rho + P)u^\mu u^\nu \tag{1.15}$$

where u is the four-velocity of the fluid element. Since it's always possible to find a frame in which the fluid is at rest (the co-moving frame), then working in that frame $g^{\mu\nu} = \mathrm{diag}(1, -1, -1, -1)$ and $u = \mathrm{diag}(1, 0, 0, 0)$, so the energy-momentum tensor becomes

$$T^{00} = \rho\,, \qquad\qquad T^{ii} = P \tag{1.16}$$

Now we can solve the Einstein field equations. It is more convenient to work with mixed tensors. Using the results above the (mixed) Einstein tensor $G^\mu_\nu = R^\mu_\nu - \frac{1}{2}R$ is

$$\begin{aligned} r^2 G^0_0 &= e^{-2\lambda}(1 - 2r\lambda') - 1 = \frac{\mathrm{d}}{\mathrm{d}r}\left(re^{-2\lambda}\right) - 1 \\ r^2 G^1_1 &= e^{-2\lambda}(1 + 2r\nu') - 1 \\ G^2_2 = G^3_3 &= e^{-2\lambda}\left(\nu'' + \nu'^2 - \nu'\lambda' + \frac{\nu' - \lambda'}{r}\right) \end{aligned} \tag{1.17}$$

while the mixed energy–momentum tensor becomes

$$T^0_0 = \rho\,, \qquad\qquad T^i_i = -P \tag{1.18}$$

So the $^0_0$ component of the Einstein equation becomes

$$G^0_0 = -8\pi G T^0_0 \tag{1.19}$$

$$\frac{1}{r^2}\frac{\mathrm{d}}{\mathrm{d}r}\left(re^{-2\lambda} - r\right) = -8\pi G\rho \tag{1.20}$$

Integrating immediately yields

$$e^{-2\lambda(r)} = 1 - \frac{8\pi G}{r}\int_0^r \rho(r) r^2\,\mathrm{d}r \tag{1.21}$$

$$= 1 - \frac{2Gm(r)}{r}, \quad m(r) \equiv \int_0^r 4\pi r^2 \rho(r)\,\mathrm{d}r \tag{1.22}$$

whereas for the the $^1_1$ component

$$\frac{e^{-2\lambda}(1 + 2r\nu') - 1}{r^2} = 8\pi G P \tag{1.23}$$

$$\nu' = \frac{e^{2\lambda}(8\pi G P r^2 + 1) - 1}{2r} \tag{1.24}$$

Plugging the result from (1.22) we obtain

$$\frac{\mathrm{d}\nu}{\mathrm{d}r} = \frac{1}{2r}\left[1 - \frac{2Gm}{r}\right]^{-1}(8\pi GPr^2 + 1) - 1 \tag{1.25}$$

$$= \frac{1}{2r}\left[1 - \frac{2Gm}{r}\right]^{-1}\left[8\pi GPr^2 + \frac{2Gm}{r}\right] \tag{1.26}$$

We obtain a second equation by demanding that the stress–energy tensor be divergenceless: $\nabla_\mu T^\mu{}_\nu = 0$. Considering one component in particular

$$\nabla_\mu T^\mu_1 = -\frac{\mathrm{d}P}{\mathrm{d}r} - (\rho + P)\frac{\mathrm{d}\nu}{\mathrm{d}r} = 0 \tag{1.27}$$

or

$$\frac{\mathrm{d}P}{\mathrm{d}r} = -(\rho + P)\frac{\mathrm{d}\nu}{\mathrm{d}r} \tag{1.28}$$

Eliminating $\mathrm{d}\nu/\mathrm{d}r$ by combining equations (1.26) and (1.27) we obtain

$$\frac{\mathrm{d}P}{\mathrm{d}r} = -\frac{1}{2r}[\rho + P]\left[1 - \frac{2Gm}{r}\right]^{-1}\left[8\pi GPr^2 + \frac{2Gm}{r}\right] \tag{1.29}$$

or, rearranging,

$$\boxed{\frac{\mathrm{d}P(r)}{\mathrm{d}r} = -\frac{G}{r^2}\left[\rho(r) + P(r)\right]\left[4\pi r^3 P(r) + m(r)\right]\left[1 - \frac{2Gm(r)}{r}\right]^{-1}} \tag{1.30}$$

This is the Tolman–Oppenheimer–Volkoff equation.

1.4.2 Integrating the TOV equation

Looking at equation (1.30) we see that it depends on three functions of r: the pressure at radial distance r, $P(r)$, the mass/energy density at radial distance r, $\rho(r)$, and the total mass inside the sphere of radius r, $m(r)$. $m(r)$ we can write in terms of $\rho(r)$ following the definition in (1.26). If we just supply a relation between ρ and P we can, in principle, by writing one in function of the other like $P(\rho)$, integrate the TOV equation to find the $P(r)$ function for the star — and consequently $\rho(r)$ — called the *profile* of the star. Such a relation of the form $F(P, \rho) = 0$ comes from the properties of matter, and is called the *equation of state*.

We can integrate the TOV equation as follows: we set $m(0) = 0$ and $P(0) = P_c = P(\rho_c)$ for some central density and pressure. Then we integrate until such R as the pressure $P(R)$ is zero. This is the limit of the star since zero pressure can support no overlying matter against gravitational attraction [1]. This R is the radius of the star and $M = m(R)$ its mass. Repeating this process for different central densities/pressures we can find a family (corresponding to a M–R curve) of acceptable stars. This family is called the *sequence* of stars corresponding to a given equation of state.

Manifestly, the bulk of the work is in working out the equation of state of star matter. To this end, and this is the main objective of this work, we will develop a model of the

matter inside the neutron star, and calculate the equation of state of matter in that model, and finally use it to calculate the properties of a neutron star made of that matter. For this, we will need to make use of the formalism of quantum field theory, which we will develop in the succeeding chapter.

1.5 Validity of the flat spacetime approximation

In particle physics, gravity is almost always neglected. Gravity is much weaker than the other forces, and at a quantum level can be ignored for any but a handful of systems of interest (e.g. black holes).

However neutron stars are extremely massive objects, and therefore it's not unreasonable at first glance to suggest that gravity must be taken into account when describing stellar matter, and the laws of physics that govern matter inside the neutron stars be formulated in a curved spacetime.

The equivalence principle states that an inertial Lorentz frame (where the metric is that of Minkowsky) can always be erected *locally*, that is, in the neighbourhood of any point, for spacetime is a Lorentzian manifold. Of course, it's manifestly not possible to erect a *global* Lorentz frame everywhere. The smallness of that neighbourhood depends on the curvature at that point: the greater the curvature, the smaller the region around that point where we can consider spacetime to be flat without incurring in significant error; conversely, if the curvature is only slight, we may be able to consider that spacetime is negligibly close to flat in a large region around a given point. What we want to know is if, in the context of a neutron star, we can erect such a frame in a sufficiently large neighbourhood so that it's justified to formulate and solve the equations of particle fields in flat spacetime.

We present an argument following [1] (pp. 75–77). We can calculate the relative change in the metric in a star just near the limit of gravitational collapse. The metric for the space outside the star is the Schwarzschild metric [11]:

$$\mathrm{d}s^2 = \left(1 - \frac{R_S}{r}\right)\mathrm{d}t^2 - \left(1 - \frac{R_S}{r}\right)^{-1}\mathrm{d}r^2 - r^2\,\mathrm{d}\theta^2 - r^2\sin^2\theta\,\mathrm{d}\phi^2\,, \quad R_s \equiv 2GM \tag{1.31}$$

while the interior metric is (1.11). The relative change in the metric, along the radial direction, across the radius of the star, is

$$\frac{g_{11}(R)}{g_{11}(0)} = \left(1 - \frac{2M}{R}\right)^{-1} = \left(1 - \frac{6}{10}\right)^{-1} = 2.5 \tag{1.32}$$

The metric changes by a factor of 2.5 over the dimension of the star. Taking the internucleon spacing to be $r_0 \approx 0.5\,\mathrm{fm}$, the relative change in the metric across a nucleon

One interesting way to quantify the relative strength of forces is to look at typical decay timescales of their bound states; the strength of the interaction is inversely proportional to the decay time. Strong force decays in $\sim 10^{-22}\,\mathrm{s}$, weak force in $\sim 10^{-8}$ to $10^{-13}\,\mathrm{s}$, electromagnetism in $\sim 10^{-14}$ to $10^{-20}\,\mathrm{s}$, while the bound states of gravity (planets, solar systems) can take many millions of years to decay. Alternatively, see Table 1.1.

We know that $g_{11}(0) = -1$ by looking at (1.11) and (1.22).

Table 1.1: Relative strength of forces acting on two protons in intranuclear distance [14]

Force	Rel. strength
Gravity	10^{-37}
Weak force	10^{-13}
Electromagnetism	10^{-2}
Strong force	1

is only $2.5r_0/R \approx 10^{-19}$. This means the metric would, say, change only 1 part in 10^9 over a radial distance of 10^{10} nucleon spacings. This is completely negligible. As such, we find it completely satisfactory to apply, in the context of a neutron star, a nuclear model derived in a Lorentz frame.

1.6 Electrical neutrality

We expect matter in a neutron star, or in any large body held together by gravity, to be charge neutral. Since electromagnetic repulsion is so much stronger than gravitational attraction, if the body was not electrically neutral, or very nearly so, the electric potential energy would overwhelm the gravitational forces holding it together. and it would easily disintegrate.

Let us make this reasoning more rigorous. A star can hold a net charge so long as the repulsive Coulomb force on a particle is less than the gravitational attraction.

$$\frac{Ze}{R^2} < G\frac{Mm}{R^2} \tag{1.33}$$

where Z is the net charge in the star, M and R the mass and the radius of the star, respectively, and m and e the mass and charge of a baryon. If the number of baryons in a star is A then $M < Am$ because of the gravitational binding energy. Hence

$$\frac{Ze}{R^2} < G\frac{(Am)m}{R^2} \;\Leftrightarrow\; Z < AeG\left(\frac{m}{e}\right)^2 \tag{1.34}$$

For a proton, $m/e \approx 1.0440 \times 10^{-8}\,\mathrm{kg/C}$, so

$$Z/A < 10^{-36}e \tag{1.35}$$

In other words the net charge per nucleon must be less than 10^{-36} times the charge of a proton, therefore the average charge of the star must be very very small, essentially zero. Therefore in our model we must always impose that the matter be charge neutral.

1.7 Stability

The solutions to the TOV equations correspond to stars which are in equilibrium. However, these are not necessarily stable equilibria. We will prove that along the sequence

$(M(\rho_c), R(\rho_c))$ of allowed stars the stars pass from being stable to being unstable only at a point where the mass is stationary with respect to the central density,

$$\frac{\partial M(\rho_c)}{\partial \rho_c} = 0 \tag{1.36}$$

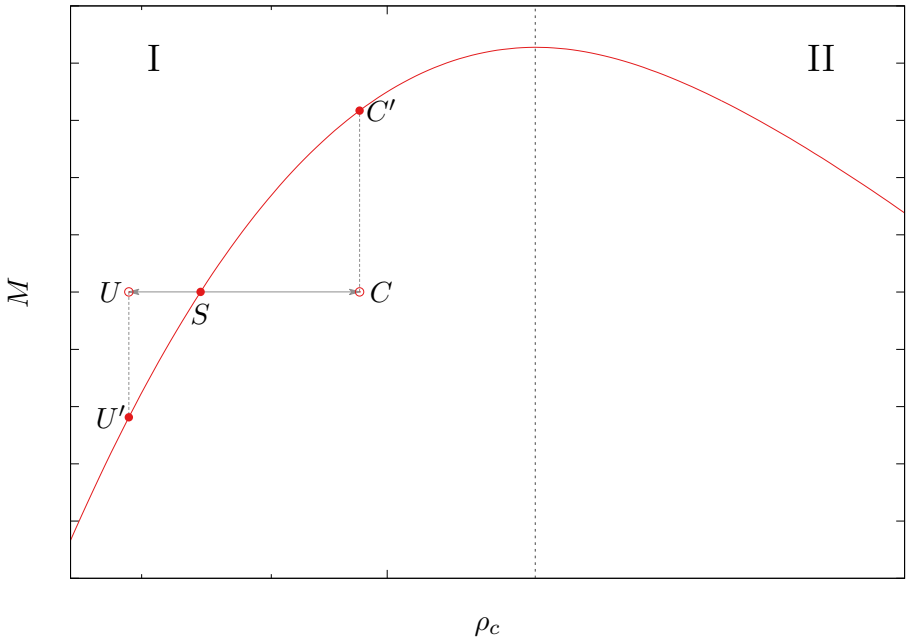

Figure 1.4: Illustration of the heuristic argument for a necessary criterion for star stability.

This follows from the following argument. Suppose an equilibrium solution in the region where $\partial M/\partial \rho_c > 0$ (region I in Figure 1.4) is perturbed. Suppose it is compressed (to C in the figure). It now has a deficit of mass respective to the corresponding equilibrium configuration (C^*), that is to say, it has less mass than it should given its density, and thus the gravity is weaker than it should. The star will thus expand, back to equilibrium.

Similarly, a star that undergoes a perturbation wherein it is uncompressed relative to an equilibrium solution (U) will have a surplus of mass respective to U^*. Thus the gravity is stronger than it "should", and the force of gravity acting upon it will act to compress it and return it to S.

An equivalent analysis done for the region where $\partial M/\partial \rho_c < 0$ (region II in the figure) shows the opposite: if the equilibrium configuration is compressed or decompressed, it will tend away from equilibrium, for if it is compressed it will have a surplus of mass, which will cause the force of gravity to compress it further, and if it is decompressed it will have a deficit of mass, and the force of gravity will be weak and it will evolve to further away from equilibrium.

Therefore, a necessary condition for a star to be stable is that

$$\frac{\partial M(\rho_c)}{\partial \rho_c} > 0 \tag{1.37}$$

For a star outside this region, any radial perturbation would be enhanced, ripping it apart.

This is a necessary, but not sufficient, condition for stability. A sufficient condition for stability can be obtained by analysing the the normal radial vibrational modes of oscillation of the star [1].

1.8 Neutron star crust

The crust of a neutron star is fundamentally different from the rest of the star, as discussed in section 1.3. It is a solid lattice of nuclei rather than the homogeneous nuclear matter that composes the core. In any model of neutron stars this must be taken into account. One standard approach is to use two separate models of matter: one for the core matter an another for the crust matter. This raises issues mainly because it's not certain that the two equations of state link smoothly. Besides, one must carefully account for the aforementioned "pasta phase" structures that arise in the transition between the core and the inner crust. This can be done in the framework of a Thomas–Fermi approach, for a given nuclear matter model [15].

We present an alternative approach, put forward in [16]. This approach hinges on the fact that the crust of a neutron star is small in thickness and mass compared to the star, namely $l_{\text{crust}}/R \sim 0.1$ and $M_{\text{crust}}/M \sim 0.01$, where l_{crust} is the thickness of the crust and M_{crust} is the mass of the crust, compared to the radius of the star R and its mass M (Figure 1.5). Therefore, for the region $R_{\text{core}} < r < R$ (that is, inside the crust) the TOV equation can be simplified by neglecting small terms, and we can obtain the following expressions for the mass and thickness of the crust, respectively:

$$M_{\text{crust}} = \frac{4\pi P_* R_{\text{core}}^4}{G M_{\text{core}}}\left(1 - \frac{2GM_{\text{core}}}{R_{\text{core}}}\right) \tag{1.38}$$

$$l_{\text{crust}} = \gamma R_{\text{core}} \frac{1 - R_s/R_{\text{core}}}{1 - \gamma(1 - R_s/R_{\text{core}})}, \quad \gamma \equiv \left[\left(\frac{\mu_*}{\mu_0}\right)^2 - 1\right]\frac{R_{\text{core}}}{R_s}, \quad R_s \equiv 2GM \tag{1.39}$$

where M_{core} and R_{core} is the mass and radius of the core, respectively, P_* and μ_* is the pressure and baryonic chemical potential, respectively, at the core–crust transition point, and μ_0 is the baryonic chemical potential in the vacuum (at $P = 0$). No more information is required about the crust, namely, no knowledge of the crust EoS is needed. The total mass and radius of the star are simply

$$M = M_{\text{core}} + M_{\text{crust}} \tag{1.40}$$

$$R = R_{\text{core}} + l_{\text{crust}} \tag{1.41}$$

For the derivations of these expressions see appendix A.1

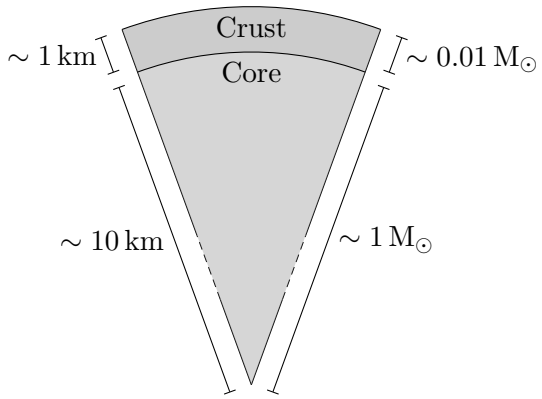

Figure 1.5: Order of magnitude of mass and radius of the core and crust of a neutron star.

Despite the apparent simplicity this approach yields very accurate results for the overall mass and radius of the star while forgoing the need for knowledge of the equation of state of the crust. If studying the detailed structure of the crust is not the primary objective, beyond basic mass and radius, this approach is very satisfactory. Since in this work this is the case, this was the chosen approach to analysing the crust.

The question remains on how to determine the parameters for this approximation. First, we need to find the density n_* at which the fundamental state of matter goes from being a homogeneous state ($n < n_*$) to a solid lattice of nuclei ($n > n_*$). There are various approaches to this problem, but a meta-analysis of several methods applied to several models found that, for matter in β-equilibrium, it was always found that $0.38n_0 < n_* < 0.63n_0$ [17], where n_0 is the saturation density of matter in the model.

It's important to know how sensitive this approximation is to finding the exact transition point. Given that it can be unclear when exactly does the transition occur, we want to know if we can justify using a rough estimate inside the aforementioned interval. To assess this we performed the calculations for an equation of state obtained in the NL3$\omega\rho$ model (section 3.2) taking the transition point to be $0.38n_0$, $0.5n_0$, and $0.63n_0$, to see how the end result varies. We obtained the mass–radius curves displayed in Figure 1.6.

As we can see, there is little variation in the predicted mass–radius curve when we vary the transition density across the interval of values given by [17]. In fact, since we are only interested in astrophysically significant masses, above $\approx 1\,\mathrm{M}_\odot$ at least, the difference in very small, with a maximum variation in the predicted radius no greater than 0.17% (or 24 m) at $1\,\mathrm{M}_\odot$, falling to only 0.04% (or 5 m) at $2\,\mathrm{M}_\odot$ (see Table 1.2) in this example.

We therefore conclude that the approximation is tolerant to a great deal of uncertainty with respect to the exact transition point. This, coupled with the fact that it is found that

Knowing n_* we can find P_* and μ_*.

In the nuclear model used in this work, $n_0 = 0.148\,\mathrm{fm}^{-3}$ (see Table 4.5).

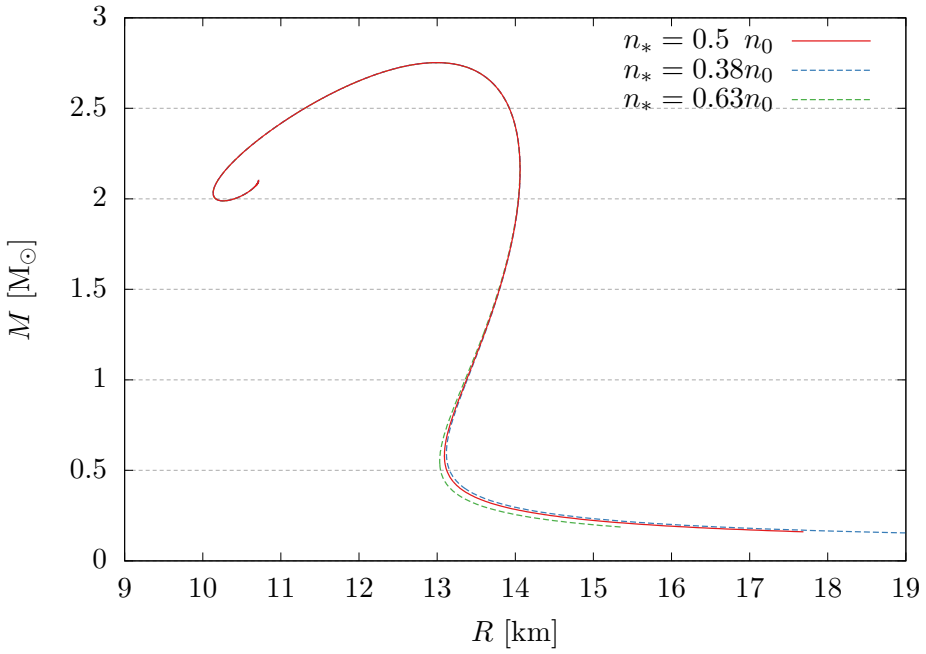

Figure 1.6: Mass–radius curves obtained via the small-crust approximation with varying transition densities, with an equation of state obtained in the NL3$\omega\rho$ model.

Table 1.2: Change in radius as a function of the choice of n_*. Superscript denotes n_* in units of n_0.

M [M$_\odot$]	$R^{0.5}$ [km]	$R^{0.38}$ [km]	$R^{0.63}$ [km]	δR^-	δR^+
1.0	13.382	13.385	13.361	0.02%	0.15%
1.5	13.798	13.803	13.790	0.03%	0.06%
2.0	14.043	14.045	14.040	0.01%	0.03%

for models in β-equilibrium the transition point lies in the interval $0.38n_0 < n_* < 0.63n_0$, means that, lacking a better estimate, we can set $n_* = 0.5n_0$ and obtain a very accurate result.

Finally, we also need to know $\mu_0 = \mu(P = 0)$. For this we used the energy per nucleon of iron-56 [16], which is at zero temperature the isotope with the lowest energy per nucleon:

$$\mu_0 = \frac{m(^{56}\mathrm{Fe})}{56} = 930.4\,\mathrm{MeV} \tag{1.42}$$

Chapter 2

Quantum Field Theory

Quantum field theory (abbr. QFT) is the most accurate theoretical framework we currently have for constructing quantum mechanical models of subatomic particles and their interactions. It arises as a necessary consequence of reconciling quantum mechanics and special relativity. A theory of resounding experimental success, it enables us to make some of the most accurate predictions in all of science, starting from arguably few fundamental principles.

In this chapter we will lay out how to build models in this framework; then we will examine the fundamental theories relevant to neutron star matter.

2.1 Introduction

The standard way to quantize fields is analogous to the canonical quantization of quantum mechanics, hence the name "second quantization". In quantum mechanics we promote the generalized coordinates q_a and their conjugate momenta p^a of classical mechanics to operators which obey the following commutation relations:

$$[q_a, q_b] = [p^a, p^b] = 0 \tag{2.1}$$

$$[q_a, p^b] = i\hbar\delta^b{}_a \tag{2.2}$$

while the Poisson bracket structure of classical mechanics is replaced by the commutator by the following recipe [18]:

$$\{A, B\} \mapsto \frac{1}{i\hbar}[A, B] \tag{2.3}$$

In quantum field theory we do the same thing with classical field theory. The classical fields $\phi_a(\vec{x})$ and their momentum conjugates $\pi^a(\vec{x})$ are promoted to operators with similar commutation relations [19],

$$[\phi_a(\vec{x}), \phi_b(\vec{y})] = [\pi^a(\vec{x}), \pi^b(\vec{y})] = 0 \tag{2.4}$$

$$[\phi_a(\vec{x}), \pi^b(\vec{y})] = i\hbar\delta(\vec{x} - \vec{y})\delta^b{}_a \tag{2.5}$$

for bosons (integer spin fields), while fermions (half-integer spin fields) obey equivalent *anti*commutation relations

$$\{\phi_a(\vec{x}), \phi_b(\vec{y})\} = \{\pi^a(\vec{x}), \pi^b(\vec{y})\} = 0 \tag{2.6}$$

$$\{\phi_a(\vec{x}), \pi^b(\vec{y})\} = i\hbar\delta(\vec{x} - \vec{y})\delta^b{}_a \tag{2.7}$$

The dynamics of the fields are formulated by means of a Lagrangian, a function of the fields and their derivatives such that the action is

$$S = \int L(\phi_a, \partial_\mu \phi_a)\, \mathrm{d}t \tag{2.8}$$

It is actually more convenient to work with a Lagrangian *density*,

$$S = \int \mathcal{L}(\phi_a, \partial_\mu \phi_a)\, \mathrm{d}^4x \tag{2.9}$$

Throughout this work we will work with the Lagrangian density though we will simply call it the Lagrangian.

The equations of motion are obtained by the action principle, which tells us that the system's evolution is the solution for which the action is stationary.

$$\frac{\delta S}{\delta \phi_a} = 0 \tag{2.10}$$

By enforcing this principle, the Euler–Lagrange equations are obtained [19]:

$$\partial_\mu \frac{\partial \mathcal{L}}{\partial(\partial_\mu \phi_a)} - \frac{\partial \mathcal{L}}{\partial \phi_a} = 0 \tag{2.11}$$

The solutions to these are the equations of motion of the system.

2.2 Quantum Chromodynamics

The QCD Lagrangian is [20]

$$\mathcal{L} = \overline{\psi}(i\gamma^\mu \mathcal{D}_\mu - m)\psi - \frac{1}{4} F_a{}^{\mu\nu} F^a{}_{\mu\nu} \tag{2.12}$$

where ψ the quark field spinor ($\psi = (q_1, \ldots, q_{N_f})^T$), a vector of spinors of each flavour of quark, and $\overline{\psi} \equiv \psi^\dagger \gamma^0$; where N_f is the number of flavours of quarks. Each quark exists in $N_c = 3$ colours, as a colour triplet. m is a diagonal matrix in flavour space ($m = \mathrm{diag}(m_{q_1}, \ldots, m_{q_{N_f}})$) of the bare quark masses. γ^μ denotes the gamma matrices (see appendix B.1).

$\mathcal{D}_\mu$ denotes the gauge covariant derivative,

$$\mathcal{D}_\mu = \partial_\mu - igt_a \mathcal{A}^a{}_\mu \tag{2.13}$$

No higher than first order for locality.

It involves the massless gauge vector fields ${\mathcal{A}^a}_\mu$, one for each colour index $a \in \{1, \ldots, 8\}$. t_a are the generators of $\mathrm{SU}(3)_{\mathrm{colour}}$.

${F^a}_{\mu\nu}$ is the gluon field strength tensor, defined as

$$ {F^a}_{\mu\nu} = \partial_\mu \mathcal{A}^a_\nu - \partial_\nu \mathcal{A}^a_\mu + g {f^a}_{bc} \mathcal{A}^b_\mu \mathcal{A}^c_\nu \tag{2.14} $$

where g is the strong coupling constant and f_{abc} are the SU(3) structure constants (see appendix B.2). Note that the contravariance or covariance of indices is trivial in the case of colour indices (like a), while raising and lowering spacetime indices requires contraction with the metric.

Quarks in QCD exist in three colour charges, as a colour triplet $q_f = (q_{fr}, q_{fg}, q_{fb})^T$. and the action is invariant under a local $\mathrm{SU}(3)_{\mathrm{color}}$ gauge transformation in color space. It is by imposing that this gauge invariance be local that the 8 gauge fields arise, one for each of the generators of $\mathrm{SU}(3)_{\mathrm{color}}$. This is similar to how the local U(1) gauge invariance in QED necessarily gives rise to the photon gauge field, with one crucial difference: unlike U(1), SU(3) is non-abelian, which means that unlike in QED, where photons do not interact with photons, in QCD the gluon fields have self-interactions intrinsically (from the last term of $F_{\mu\nu}$, a consequence of the non-commutativity of the elements of $\mathfrak{su}(3)$; no such term in abelian QED). This implies that, unlike photons which have no charge, the 8 gluon fields *do* carry colour charge.

Therefore, according to the rules of quantum field theory, the above theory gives rise to three basic interactions: a quark may emit (or absorb) a gluon, a gluon may emit (or absorb) a gluon, and two gluons may directly interact [20] (the processes in Figure 2.1). This contrasts with QED, in which only the first kind of interaction occurs, since photons have no charge.

QCD also has two peculiar properties:

- **Confinement**, whereby particles carrying a colour charge such as quarks cannot exist as free particles. The force between quarks does not diminish with separation. Because of this, if you attempt to separate a quark (a coloured state) from other quarks, the energy in the gluon field between the two coloured quarks grows linearly with separation [20], and eventually surpasses the energy for creating a quark–antiquark pair out of the vacuum, which will promptly form a colourless bound hadron. Quarks are thus forever bound in colourless states. If you attempt to pull a quark out of a hadron, you will just pull a jet of hadrons [21]. Although widely believed to be true since it explains the failure of free quark searches, and because it is verified in lattice QCD calculations, there is as of yet no rigorous analytical proof of confinement from first principles.

- **Asymptotic freedom**, whereby in very high-energy reactions, quarks and gluons interact very weakly. In fact the theory's coupling constant becomes asymptotically weaker as energy or momentum transfer increases and distance decreases. This is

To first order; they can of course interact via higher-order processes.

$\mathfrak{su}(3)$ denotes the associated Lie algebra of the generators of SU(3).

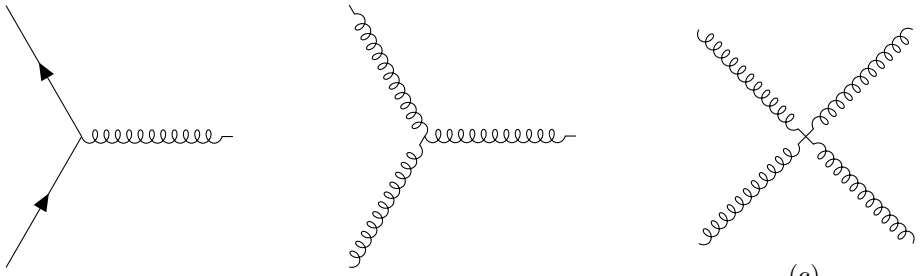

Figure 2.1: Basic leading-order diagrams of QCD.

manifested in the fact that quarks seem to be nearly free inside the short-distance confines of the hadron. This property can be derived by calculating the beta-function, which encodes the dependency of the theory's coupling constant on the energy scale.

$$\beta(g) = \mu \frac{\partial g}{\partial \mu}, \quad \mu = p/\Lambda_{\mathrm{QCD}} \tag{2.15}$$

To first order

$$\beta(g) = -\frac{g^3}{(4\pi)^2}\left(\frac{11N_c}{6} + \frac{2N_f}{3}\right) \tag{2.16}$$

which means that for $N_c = 3$ and $N_f = 6$, $\beta < 0$ thus the coupling constant goes to zero as the momentum scale increases, thus the theory is asymptotically free [20].

Unlike the vast majority of physical theories formulated before or since, QCD is non-perturbative at low energies. The standard method of expansion in the coupling constant only works at high energy when asymptotic freedom kicks in. At low energies we must use another approach. This is what motivates the use of effective theories, theories that aim to reproduce the essential features of the fundamental theory in a simplified and mathematically tractable model (see Chapter 3).

QCD in $N_f = 3$

The standard model of particle physics recognizes six flavours of quarks, in three generations (see Table 2.1).

We can classify them in two "light" quarks (u, d) and three "heavy" quarks (c, t, b), in comparison to the strong interaction scale of $\approx 200\,\mathrm{MeV}$ [20]. The strange quark is at the treshold, and can be considered part of the light quarks or not in different models.

Because of their mass, heavy quarks will never appear in ground state matter such as exists in our model of neutron star matter. Therefore, even though full, standard model QCD has $N_f = 6$ quark flavours, we will be able to consider a version where $N_f = 3$, where only the lightest three quarks enter. Henceforth in this work we will always consider QCD in 3 flavours.

Table 2.1: Experimental values for quark masses [22].

Generation	Quark (symbol)	Mass [MeV]
1st	Up (u)	$2.2\,^{+0.6}_{-0.4}$
	Down (d)	$4.7\,^{+0.5}_{-0.4}$
2nd	Charm (c)	1280 ± 30
	Strange (s)	$96\,^{+8}_{-4}$
3rd	Top (t)	173100 ± 600
	Bottom (b)	$4180\,^{+40}_{-30}$

The quark field spinor is

$$\psi(x) = \begin{pmatrix} u(x) \\ d(x) \\ s(x) \end{pmatrix} \tag{2.17}$$

The mass matrix is diagonal in flavour space, as noted before.

$$m = \mathrm{diag}(m_u, m_d, m_s) \tag{2.18}$$

2.2.1 Symmetries of QCD

The colour group $\mathrm{SU}(3)_{\mathrm{color}}$ represents the *local* gauge symmetry that gives rise to quantum chromodynamics. QCD also has CPT symmetry (symmetry under *simultaneous* global charge conjugation, parity transformation and time reversal). Of course, it also enjoys the spacetime symmetries of the Poincaré group (group of translations in time and space, rotations, and Lorentz boosts.). These are all exact symmetries, and valid for QCD in any number of flavours.

In addition, QCD contains an approximate, *global* flavour symmetry represented by the group $\mathrm{U}(N_f) = \mathrm{SU}(N_f)_L \otimes \mathrm{SU}(N_f)_R \otimes \mathrm{U}(1)_V \otimes \mathrm{U}(1)_A$. This is only an approximate symmetry, exactly valid, as we will see below, only in the massless limit. Let us examine this, for the particular case where $N_f = 3$.

Consider

$$\mathcal{L} = \mathcal{L}^0 + \delta\mathcal{L} \tag{2.19}$$

where $\mathcal{L}^0$ is the limit of $\mathcal{L}$ when $m \to 0$, and $\delta\mathcal{L}$ is the remaining term, $-m\overline{\psi}\psi$. Let us introduce the left and right handed fields,

$$\psi_L = \frac{1-\gamma^5}{2}\psi \qquad \overline{\psi}_L = \overline{\psi}\frac{1+\gamma^5}{2} \tag{2.20}$$

$$\psi_R = \frac{1+\gamma^5}{2}\psi \qquad \overline{\psi}_R = \overline{\psi}\frac{1-\gamma^5}{2} \tag{2.21}$$

The massless Lagrangian neatly separates like so

$$\begin{aligned}\mathcal{L}^0 &= i\bar{\psi}\not{\mathcal{D}}\psi - \frac{1}{4}F^{\mu\nu}F_{\mu\nu} \\ &= i\bar{\psi}_L\not{\mathcal{D}}\psi_L + i\bar{\psi}_R\not{\mathcal{D}}\psi_R - \frac{1}{4}F^{\mu\nu}F_{\mu\nu}\end{aligned} \tag{2.22}$$

where $\not{\mathcal{D}} \equiv \gamma^\mu\mathcal{D}_\mu$, the Feynmann slash notation. It is evidently invariant under separate global U(1) transformations of left- and right-handed fields.

$$\mathrm{U}(1)_L : \psi_L \to e^{i\alpha_L}\psi_L \tag{2.23}$$

$$\mathrm{U}(1)_R : \psi_R \to e^{i\alpha_R}\psi_R \tag{2.24}$$

for some (real number) phases α_L, α_R (global, independent of x). This is referred to as chiral $\mathrm{U}(1)_L \otimes \mathrm{U}(1)_R$ symmetry. Noether's theorem tells us that continuous symmetries give rise to conserved currents (see appendix A.2). The corresponding Noether currents to these symmetries are

$$j_L{}^\mu(x) = \bar{\psi}_L(x)\gamma^\mu\psi_L(x) \tag{2.25}$$

$$j_R{}^\mu(x) = \bar{\psi}_R(x)\gamma^\mu\psi_R(x) \tag{2.26}$$

where $\partial_\mu\, j_L{}^\mu = \partial_\mu\, j_R{}^\mu = 0$.

We can cast this in an alternative form. Let

$$V^\mu(x) = j_R{}^\mu(x) + j_L{}^\mu(x) = \bar{\psi}(x)\gamma^\mu\psi(x) \tag{2.27}$$

$$A^\mu(x) = j_R{}^\mu(x) - j_L{}^\mu(x) = \bar{\psi}(x)\gamma^\mu\gamma_5\psi(x)\,, \tag{2.28}$$

called respectively the vector and axial currents. Both these currents are trivially also conserved, and correspond to the following symmetry transformations:

$$\mathrm{U}(1)_V : \psi \to e^{i\alpha_V}\psi \tag{2.29}$$

$$\mathrm{U}(1)_A : \psi \to e^{i\gamma_5\alpha_A}\psi \tag{2.30}$$

again for some real phases α_V, α_A. The transformations of group $\mathrm{U}(1)_V$ rotate the left- and right-handed fields by equal phases, while the transformations of the group $\mathrm{U}(1)_A$ act with opposite sign on left- and right-handed fields:

$$\mathrm{U}(1)_V : \begin{cases}\psi_L \to e^{i\alpha_V}\psi_L \\ \psi_R \to e^{i\alpha_V}\psi_R\end{cases} \tag{2.31}$$

$$\mathrm{U}(1)_A : \begin{cases}\psi_L \to e^{-i\alpha_A}\psi_L \\ \psi_R \to e^{i\alpha_A}\psi_R\end{cases} \tag{2.32}$$

Chiral L/R symmetry is therefore equivalent to V/A symmetry:

$$\mathrm{U}(1)_L \otimes \mathrm{U}(1)_R = \mathrm{U}(1)_V \otimes \mathrm{U}(1)_A \tag{2.33}$$

However, the mass term breaks the axial symmetry explicitly, for if we reintroduce the mass term we have, as we can check

$$\partial_\mu A^\mu = 2m\overline{\psi} i\gamma_5 \psi \tag{2.34}$$

whereas the $\mathrm{U}(1)_V$ vector symmetry remains untouched. This is because the mass term mixes handedness:

$$\overline{\psi} m \psi = \overline{\psi}_R m \psi_L + \overline{\psi}_L m \psi_R \tag{2.35}$$

While in the massless limit the left- and right-handed fields are completely decoupled, the mass term plays the role of an interaction that mixes left- and right-handed quarks. Therefore the action is not invariant in general under separate transformations of the left- and right-handed fields.

Furthermore, the massless Lagrangian is also invariant under the following transformations:

$$\mathrm{SU}(3)_L : \psi_L \to e^{i\lambda_n \alpha_L^n/2} \psi_L \tag{2.36}$$

$$\mathrm{SU}(3)_R : \psi_R \to e^{i\lambda_n \alpha_R^n/2} \psi_R \tag{2.37}$$

where $\lambda_n, n = 1, \ldots, 8$ are the Gell-Mann matrices of $\mathrm{SU}(3)_{\text{flavour}}$ (see appendix B.2), and $\alpha_{L/R}^n$ are again arbitrary real phases. The currents are

$$j_{Ln}{}^\mu(x) = \overline{\psi}_L(x)\gamma^\mu \frac{\lambda_n}{2} \psi_L(x) \tag{2.38}$$

$$j_{Rn}{}^\mu(x) = \overline{\psi}_R(x)\gamma^\mu \frac{\lambda_n}{2} \psi_R(x) \tag{2.39}$$

and similarly to before, we can cast this symmetry in a vector/axial form:

$$\mathrm{SU}(3)_V : \psi \to e^{i\lambda_n \alpha_V^n/2} \psi \tag{2.40}$$

$$\mathrm{SU}(3)_A : \psi \to e^{i\lambda_n \alpha_A^n \gamma_5/2} \psi \tag{2.41}$$

where, again, $\mathrm{SU}(3)_V$ transformations act on left- and right-handed quarks identically, and those of $\mathrm{SU}(3)_A$ act opposite on opposite handedness.

The mass term breaks $\mathrm{SU}(3)_A$ symmetry, while $\mathrm{SU}(3)_V$ symmetry is kept **if** all masses are equal ($m_u = m_d = m_s \equiv m_q \Leftrightarrow m = \mathrm{diag}(m_q, m_q, m_q) = m_q \mathbb{1}$), such that

$$\overline{\psi} m \psi = m_q \overline{\psi} \psi \tag{2.42}$$

and broken if any masses differ.

Finally, we should note that $\mathrm{U}(1)_A$ symmetry is broken right away at a quantum level, even in the massless limit, by instanton effects [23].

To summarize: massless QCD has $\mathrm{SU}(N_f)_V \otimes \mathrm{SU}(N_f)_A \otimes \mathrm{U}(1)_V \otimes \mathrm{U}(1)_A$ symmetry (at a classical level). At a quantum level there is an anomaly that breaks the symmetry to $\mathrm{SU}(N_f)_V \otimes \mathrm{SU}(N_f)_A \otimes \mathrm{U}(1)_V$. The mass term explicitly breaks $\mathrm{SU}(N_f)_A$ symmetry (as well as $\mathrm{U}(1)_A$). If the masses are not equal, the $\mathrm{SU}(N_f)_V$ symmetry is also broken.

For $N_f = 3$. This is trivially generalizable for any number of flavours by replacing the generators with the generators of $\mathrm{SU}(N_f)$.

Physical interpretation

The only one of the above symmetries that is exact in all cases is the $\mathrm{U}(1)_V$ symmetry. The associated conserved current is the baryon number, which is conserved in the strong interaction.

The $\mathrm{SU}(3)_V$ symmetry, on the other hand, is only approximate: it is valid only if the masses of all the quarks in the theory are equal. This is a reasonable approximation in $N_f = 2$, where it gives rise to the familiar concept of isospin, in which this invariance under flavour rotations enables us to treat proton and neutron as two states of the same "particle" (just as if they were spin states of a spin-1/2 particle, hence the name isospin). In $N_f = 3$ the symmetry is less exact due to the strange quark being much heavier than the other two, but still yields the "Eightfold Way" theory of hadrons [21]. This symmetry explains why mesons and baryons occur in nearly degenerate multiplets: the splitting is due only to the (small) differences in mass between the quarks, since the strong interaction with the gluons is the same for all flavours.

The axial $\mathrm{SU}(3)_A$ symmetry does not seem to correspond to any familiar conserved quantity of strong interactions. For one, it is slightly broken by the mass term (but this is a small perturbation so that the symmetry could still be considered an approximate one). Crucially, as shown by Nambu in his Nobel Prize-winning work, it is also *spontaneously* broken in nature, as follows. In QCD, quarks and antiquarks have strong attractive interactions; also, the first two or three quarks at least, are light in comparison to the strong interaction scale. If quarks are light, then the energy cost of creating a quark-antiquark pair is small, then we expect there to exist a finite condensate of quark-antiquark pairs in the QCD vacuum:

$$\langle 0|\overline{\psi}\psi|0\rangle = \langle 0|\overline{\psi}_R\psi_L + \overline{\psi}_L\psi_R|0\rangle \neq 0 \tag{2.43}$$

which is invariant under $\mathrm{U}(3)_V$ transformations but not under $\mathrm{U}(3)_A$. The nonvanishing condensate signals that the vaccum mixes handedness and is not invariant under general separate transformations of the left- and right-handed fields [20]. This mechanism generates an effective mass for the quarks. Inside a nucleon, the bare quark masses only contribute $\sim 1\%$ of the mass of the nucleon; the remaining 99% comes from the condensate.

The existence of this quark condensate can be attested in several ways, namely: in lattice QCD calculations [24], which show that indeed the quark scalar density in the vaccum is different from zero, and through the observation of the Goldstone bosons. Goldstone's theorem states that the spontaneous breaking of a continuous symmetry generates massless spinless particles, called the Goldstone bosons, one for each of the generators of the broken symmetry (section A.3). Here we would expect nine such

And also different electroweak interactions due to the different charge.

Spontaneous symmetry breaking happens when the ground state does not share the symmetries of the Hamiltonian. A familiar example is ferromagnetism: even though there is no perferred direction for the magnetic moments to align (i.e. rotational symmetry in the Hamiltonian), the lowest energy state is one where all the moments are aligned in one direction (which breaks rotational symmetry).

$\langle \bar{u}u\rangle \approx \langle \bar{d}d\rangle = -(283(2)\,\mathrm{MeV})^3$ and $\langle \bar{s}s\rangle = -(290(15)\,\mathrm{MeV})^3$ [24].

particles, from the breakdown of $\mathrm{U}(3)_L \otimes \mathrm{U}(3)_R$ to $\mathrm{U}(3)_V$. In reality, since the quarks are massive, and therefore the symmetry is also slightly broken explicitly, these particles are not massless, but only relatively light (so-called pseudo-Goldstone bosons).

The $\mathrm{U}(1)_A$ symmetry is explicitly broken by a quantum anomaly, shown by 't Hooft to be related to the existence of instanton solutions that couple to the quarks, creating an induced interaction that breaks this symmetry [23]. Then, we expect there to exist only eight light pseudo-Goldstone bosons (from the spontaneously broken $\mathrm{SU}(3)_A$ symmetry but not the explicitly broken $\mathrm{U}(1)_A$). We identify these with the pseudoscalar meson octet (Figure 2.2), which are by far the lightest mesons in the spectrum of the theory [22]. This explains why the η (from the octet) and η' (the SU(3) singlet) have such different masses even though they should be degenerate (the η' puzzle).

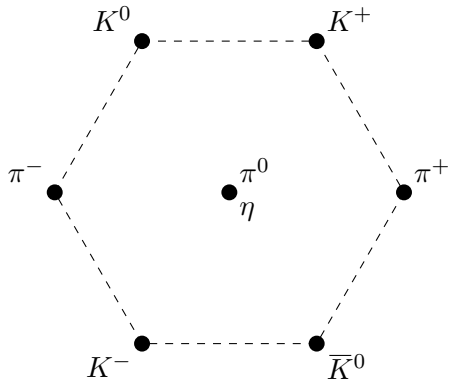

Figure 2.2: The meson octet.

The masses of the pseudo-Goldstone mesons can be calculated with chiral perturbation theory, and they match experimental results [25].

2.3 The mean field approximation

The relativistic mean field approximation is an approximation framework where fields are replaced by their expectation values in the vacuum. This amounts to removing all quantum fluctuations of those fields, treating them simply as classical fields (c-number-valued instead of operator-valued).

For instance, given a theory of fermion fields ψ_a and auxiliary fields ϕ_b, one can study the approximation of fermions moving in the mean field of the ϕ_b by substituting in the Lagrangian

$$\phi_b \to \langle \phi_b \rangle \tag{2.44}$$

while keeping the fermion fields as full quantum fields. The theory then becomes a quantum field theory of fermions moving subject to a mean field potential generated by the auxiliary fields.

The explicit and spontaneous symmetry breakings are assumed to occur separately, at a different energy scales, and to be unrelated mechanisms.

Also, if the theory contains *products* of Dirac bilinears, we can linearise the action by writing them as their expectation values plus a perturbation,

$$\hat{A} = \langle \hat{A} \rangle + \delta \hat{A}, \quad A = \overline{\psi}_1 M \psi_2 \tag{2.45}$$

developing the products of operators, dropping the terms that are second order or more in the perturbation, and substituting back $\delta \hat{A} = \hat{A} - \langle \hat{A} \rangle$. We find

$$\hat{A} \quad = \hat{A} \tag{2.46}$$

$$\hat{A}\hat{B} \quad \approx \hat{A}\langle \hat{B} \rangle + \langle \hat{A} \rangle \hat{B} - \langle \hat{A} \rangle \langle \hat{B} \rangle \tag{2.47}$$

$$\hat{A}\hat{B}\hat{C} \approx \hat{A}\langle \hat{B} \rangle \langle \hat{C} \rangle + \langle \hat{A} \rangle \hat{B} \langle \hat{C} \rangle + \langle \hat{A} \rangle \langle \hat{B} \rangle \hat{C} - 2\langle \hat{A} \rangle \langle \hat{B} \rangle \langle \hat{C} \rangle \tag{2.48}$$

$$\dots$$

(see appendix A.4 for the calculations). This corresponds to approximating a four-point interaction, six-point interaction, etc, with two-point interactions:

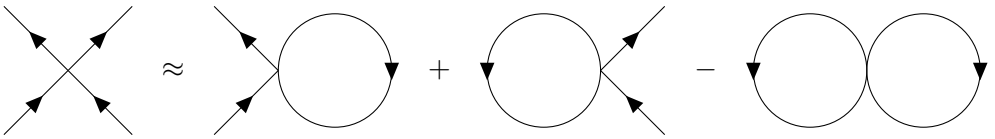

(2.49)

and so on. We then have an action that is first-order in the Dirac bilinears.

2.4 Thermodynamics of quantum field theory

At this point we must introduce the concept of temperature. All we've developed so far is valid for $T = 0$; however a realistic model of the real world must necessarily be formulated at finite temperature, since the actual phenomena we wish to study take place at those conditions (despite the fact that for many classes of phenomena and regimes the approximation that $T = 0$ is a good approximation to make and yields very good theoretical predictions).

2.4.1 The grand canonical ensemble

In order to treat quantum field theory at finite temperature we introduce the concept of a grand canonical ensemble: the statistical ensemble that is used to represent a system of particles in thermodynamic (thermal and chemical) equilibrium with a reservoir, with which the system can exchange energy and particles.

The thermodynamic variables in this system are the temperature, T, and the chemical potentials, μ_i, one for each conserved quantity: electric charge, baryonic number, etc; these control the transfer of heat and of particles of the species i (or, in general, of conserved charge of species i) with the reservoir, respectively. Also the volume of the system, V, is fixed. In the formalism of equilibrium statistical physics, the fundamental object is the density matrix [26]:

$$\hat{\rho} = \exp[(H - \sum_i \mu_i N_i)/T] \tag{2.50}$$

where N_i, μ_i are the conserved number operators and the associated chemical potentials, respectively, for each conserved quantity, and H denotes the Hamiltonian. It is equal to $\int \mathcal{H}\,\mathrm{d}^3x$ where $\mathcal{H}$ is the Hamiltonian density, which is expressed as a Legendre transformation of the Lagrangian density in the usual fashion:

$$\mathcal{H} = \sum_n \frac{\partial \mathcal{L}}{\partial \dot{\psi}_n}\dot{\psi}_n - \mathcal{L}, \quad \dot{\psi}_n = \frac{\partial \psi_n}{\partial t} \tag{2.51}$$

In terms of this function the expectation value of an operator can be calculated as follows:

$$\langle \hat{O} \rangle = \frac{\operatorname{Tr} \hat{\rho}\,\hat{O}}{\operatorname{Tr} \hat{\rho}} \tag{2.52}$$

The trace in the expression above is carried over all states of the system: momentum, spin, colour, flavour, etc.

We define a function, called the grand canonical potential, as

$$\Omega = -T \ln \mathcal{Z}, \quad \mathcal{Z} = \operatorname{Tr} \hat{\rho} \tag{2.53}$$

where $\mathcal{Z}$ is called the grand canonical partition function. From the former, all quantities of interest can be derived thusly [26]:

$$N_i = -\frac{\partial \Omega}{\partial \mu_i} \tag{2.54}$$

$$P = -\frac{\partial \Omega}{\partial V} \tag{2.55}$$

$$S = -\frac{\partial \Omega}{\partial T} \tag{2.56}$$

$$E = -PV + TS + \sum_i \mu_i N_i \tag{2.57}$$

where N_i is the number of particles of species i (or generally, the charge i associated with the chemical potential μ_i), P is the pressure, S is the entropy and E is the energy of the system.

However we do not want to work with particle numbers and the total energy of the system, for example, but instead with particle *densities* and the energy *density* of the system. Thus, alternatively to the above, we can work instead with the grand canonical potential density:

$$\Omega = -\frac{T}{V} \ln \mathcal{Z} \tag{2.58}$$

such that, in terms of this latter,

$$n_i = -\frac{\partial \Omega}{\partial \mu_i} \tag{2.59}$$

$$P = -\frac{\partial (\Omega V)}{\partial V} \tag{2.60}$$

$$S = -\frac{\partial \Omega}{\partial T} \tag{2.61}$$

$$E = -P + TS + \sum_i \mu_i n_i \tag{2.62}$$

where n_i is the density associated with chemical potential μ_i, P is the pressure, S is the entropy density, and E is the energy density. Note we have reused some of the symbols, but henceforth they shall always refer to the (intensive) densities, not the (extensive) total quantities.

2.4.2 Fermi–Dirac distribution

Let us apply this formalism to a simple system of non-interacting fermions. Due to the fact that the particles in the system don't interact, we are able to consider as if each particle was its own thermodynamic system in contact with the reservoir. This one-particle system has only two possible states: particle or no particle, as a consequence of the Pauli exclusion principle, which prohibits two particles from sharing the same state. Thus

$$\mathcal{Z} = e^{-(0-0\mu)/T} + e^{-(E-1\mu)/T} = 1 + e^{-(E-\mu)/T} \tag{2.63}$$

and

$$\Omega = -\frac{T}{V} \ln\Big(1 + e^{-(E-\mu)/T}\Big) \tag{2.64}$$

The particle number is simply

$$N = -V\frac{\partial \Omega}{\partial \mu} = T\frac{\frac{1}{T}e^{-(E-\mu)/T}}{1 + e^{-(E-\mu)/T}} = \frac{1}{1 + e^{(E-\mu)/T}} \tag{2.65}$$

This is called the Fermi–Dirac distribution, and is denoted $\mathscr{f}$. The corresponding distribution for antiparticles is simply the above with $\mu \mapsto -\mu$, and is denoted $\bar{\mathscr{f}}$. Summarizing:

$$\mathscr{f}(E, \mu, T) = \frac{1}{1 + e^{(E-\mu)/T}} \tag{2.66}$$

$$\bar{\mathscr{f}}(E, \mu, T) = \frac{1}{1 + e^{(E+\mu)/T}} \tag{2.67}$$

Pair production implies the chemical potential of a particle and its antiparticle must be symmetric.

2.4.3 The chemical potential

Noether's theorem implies that symmetries in the Lagrangian correspond to conserved currents. For instance, the free fermion Lagrangian

$$\mathcal{L} = \overline{\psi}(i\partial\!\!\!/ - m)\psi \tag{2.68}$$

or one with interactions that preserve U(1) symmetry has the following conserved current

$$\partial_\mu j^\mu = 0, \quad j^\mu = \overline{\psi}\gamma^\mu\psi \tag{2.69}$$

This implies the existence of a conserved charge:

$$Q = \int \mathrm{d}^3x\, j^0 = \int \mathrm{d}^3x\, \psi^\dagger\psi \tag{2.70}$$

which in this case is the baryonic number.

In the grand canonical ensemble, however, the system can exchange particles, even if conserved, with a reservoir, constrained by a chemical potential, which acts as a Lagrange multiplier [26]. The chemical potential term in (2.50) will be a term of the form

$$\mu \int \mathrm{d}^3x\, \psi^\dagger\psi \tag{2.71}$$

Note that even though there can exist several types of particles, each one with its own associated chemical potential, there are at most as many independent chemical potentials as there are conserved charges. We will make this concrete when we study a system in particular in the next chapter.

2.4.4 Calculating the grand canonical potential in the mean field approximation

The Lagrangian of a free fermion system is

$$\mathcal{L} = \overline{\psi}(i\gamma^\mu\partial_\mu - m)\psi \tag{2.72}$$

which corresponds to the Hamiltonian density

$$\mathcal{H} = -\overline{\psi}(i\gamma^i\partial_i - m)\psi \tag{2.73}$$

such that

$$\hat{\rho} = \exp[-(H - \mu N)/T] = \exp\left[\int \mathrm{d}^3x\, \overline{\psi}(i\gamma^i\partial_i - m + \gamma^0\mu)\psi/\,T\right] \tag{2.74}$$

We can calculate this integral, calculate the partition function, and arrive at an analytic expression for the grand canonical potential density [26]:

$$\Omega = -2T\,\mathrm{Tr}\int \frac{\mathrm{d}^3\vec{p}}{(2\pi)^3}\left[\frac{\omega}{T} + \ln\left(1 + e^{-(\omega+\mu)/T}\right) + \ln\left(1 + e^{-(\omega-\mu)/T}\right)\right] + \Omega_0 \tag{2.75}$$

By this we mean transformations $\psi \to A\psi$ where $A \in \mathrm{U}(1)$.

where $\omega = \sqrt{|\vec{p}|^2 + m^2}$.

On the other hand, we find that the linearised Lagrangian of fermion system with auxiliary fields in the mean field approximation can be written

$$\mathcal{L} = \overline{\psi}(i\gamma^\mu\partial_\mu - m)\psi - \mathcal{S}(\overline{\psi}\psi) - \mathcal{V}(\psi^\dagger\psi) + U \tag{2.76}$$

$$= \overline{\psi}[i\gamma^\mu\partial_\mu - \gamma^0\mathcal{V} - (m + \mathcal{S})]\psi + U \tag{2.77}$$

where $\mathcal{S}$, $\mathcal{V}$ and U are just c-numbers — in general functions of the expectation values of auxiliary fields. The Hamiltonian density is thus

$$\mathcal{H} = -\overline{\psi}[i\gamma^i\partial_i - \gamma^0\mathcal{V} - (m + \mathcal{S})]\psi - U \tag{2.78}$$

such that

$$\hat{\rho} = \exp[-(H - \mu N)/T] = \exp\left[\int \mathrm{d}^3x \left(\overline{\psi}[i\gamma^i\partial_i - \underbrace{(m + \mathcal{S})}_{M} + \gamma^0 \underbrace{(\mu - \mathcal{V})}_{\tilde{\mu}}]\psi + U\right)/T\right] \tag{2.79}$$

This is exactly the same form as (2.74) with $\mu \mapsto \tilde{\mu} = \mu - \mathcal{V}$ and $m \mapsto M = m + \mathcal{S}$, plus the added potential energy term U. As such, the grand canonical potential density of a fermion system in the mean field potential is

$$\Omega = -2T\,\mathrm{Tr}\int \frac{\mathrm{d}^3\vec{p}}{(2\pi)^3}\left[\frac{\omega}{T} + \ln\left(1 + e^{-(\omega+\tilde{\mu})/T}\right) + \ln\left(1 + e^{-(\omega-\tilde{\mu})/T}\right)\right] - U + \Omega_0 \tag{2.80}$$

where $\omega = \sqrt{|\vec{p}|^2 + M^2}$, $M = m + \mathcal{S}$ is the interpreted as an effective mass, and $\tilde{\mu} = \mu - \mathcal{V}$ as an effective chemical potential. The trace is taken over any internal indices the fermion field has, i.e. colour, flavour, etc.

We can interpret the terms as the contribution of particles (2nd term), and antiparticles (3rd term), as well the Dirac sea (1st term). Note also the factor of 2, corresponding to the spin-degeneracy factor for particles of spin-1/2 ($2s + 1 = 2$).

Ω_0 is an arbitrary constant (all quantities (2.59)–(2.62) are defined up to a constant term in Ω). It is usually defined such that in the vacuum ($P = 0, T = 0$) the grand canonical potential density vanishes (it corresponds to the vacuum energy density, or the symmetric of the vacuum pressure).

Chapter 3

Effective Models

3.1 The Nambu–Jona-Lasinio model

First proposed in 1961 by Yoichiro Nambu and Giovanni Jona-Lasinio, the NJL model is a theory of baryons and mesons constructed from interacting Dirac fermions, in a way that closely parallels the construction of Cooper pairs from electrons in the then recently developed Bardeen–Cooper–Schrieffer theory of superconductivity [28]. Although initially believed by the authors to be a fundamental theory, it has since been supplanted by QCD since the former does not model features known to exist in nature such as confinement or asymptotic freedom; also, it is non-renormalizable. Nevertheless it remains a very useful effective theory of quantum chromodynamics in the chiral limit, when supplemented by an appropriate regularization procedure.

The NJL model (in $N_f = 3$) is based on the following ideas [29]:

a) Consider the "light" quarks, u, d, s, as the only fundamental degrees of freedom;

b) Replace the gluon degrees of freedom by a local effective interaction;

c) Write the interaction so that the NJL Lagrangian reproduces the symmetries of QCD.

The Lagrangian has the form

$$\mathcal{L} = \overline{\psi}(i\partial\!\!\!/ - m)\psi + \mathcal{L}_{\text{int}} \tag{3.1}$$

where $\psi = (u, d, s)^T$ is a vector of Dirac spinors for each flavour of quark, and $m = \text{diag}(m_u, m_d, m_s)$ is a matrix of bare quark masses.

A mention must be made that the model was independently invented by Soviet physicists Valentin Vaks and Anatoly Larkin around the same time [27].

3.1.1 Interactions

We want to write an interaction based on the local coupling between two currents that has the same symmetries as the strong interaction of QCD (section 2.2.1), namely $\mathrm{U}(1)_V \otimes \mathrm{SU}(3)_V \otimes \mathrm{SU}(3)_A$ (the latter two are approximate symmetries of QCD slightly broken by the mass term but still symmetries of the strong interaction)

Since the fundamental quark currents in QCD are color currents $J_{a\mu} = \overline{\psi}\gamma_\mu t_a \psi$ we can start by writing a simple, four-point interaction based on the local coupling between two such currents [29]:

$$\mathcal{L}_{\text{int}}^{(4)} = -G \sum_{a=1}^{8} (\overline{\psi}\gamma_\mu t_a \psi)^2 \tag{3.2}$$

where γ_μ are the Dirac gamma matrices and t_a are the $\mathrm{SU}(3)_{\text{color}}$ generators (normalized such that $\mathrm{Tr}(t_a t_b) = 2\delta_{ab}$. Such an interaction is manifestly invariant under transformations of $\mathrm{SU}(3)_V \otimes \mathrm{SU}(3)_A \otimes \mathrm{U}(1)_V \otimes \mathrm{U}(1)_A$, as well as under $\mathrm{SU}(3)_{\text{color}}$ transformations.

A very useful tool to understand exactly what this interaction consists of is the Fierz transform (see appendix A.5). We can use it to decompose a four-point interaction. This method will allow us to derive a general interaction, naturally arising from the above term.

Applying the Fierz identity to the colour gauge symmetry generators,

$$\mathcal{L}_{\text{int}}^{(4)} = -\frac{2(N_c^2-1)}{N_c^2} G(\overline{\psi}\gamma_\mu\psi)^2 + \frac{1}{N_c} G(\overline{\psi}\gamma_\mu t_a \psi)^2 \tag{3.3}$$

then to SU(3) in flavour space

$$\begin{aligned}\mathcal{L}_{\text{int}}^{(4)} = &-\frac{2(N_c^2-1)}{N_c^2 N_f} G(\overline{\psi}\gamma_\mu\psi)^2 - \frac{(N_c^2-1)}{N_c^2} G(\overline{\psi}\gamma_\mu\lambda_n\psi)^2 \\ &+ \frac{1}{N_c N_f} G(\overline{\psi}\gamma_\mu t_a\psi)^2 + \frac{1}{2N_c} G(\overline{\psi}\gamma_\mu t_a\lambda_n\psi)^2\end{aligned} \tag{3.4}$$

where λ_n are the generators of $\mathrm{SU}(N_f)_{\text{flavour}}$, also normalized so that $\mathrm{Tr}\,\lambda_n\lambda_m = 2\delta_{nm}$. Then finally:

$$\begin{aligned}\mathcal{L}_{\text{int}}^{(4)} = &-\frac{2(N_c^2-1)}{N_c^2 N_f} G\Big[(\overline{\psi}\psi)^2 + (\overline{\psi}i\gamma_5\psi)^2 - \frac{1}{2}(\overline{\psi}\gamma_\mu\psi)^2 - \frac{1}{2}(\overline{\psi}\gamma_\mu\gamma_5\psi)^2\Big] \\ &- \frac{(N_c^2-1)}{N_c^2} G\Big[(\overline{\psi}\lambda_n\psi)^2 + (\overline{\psi}i\gamma_5\lambda_n\psi)^2 - \frac{1}{2}(\overline{\psi}\gamma_\mu\lambda_n\psi)^2 - \frac{1}{2}(\overline{\psi}\gamma_\mu\gamma_5\lambda_n\psi)^2\Big] \\ &+ \frac{1}{N_c N_f} G\Big[(\overline{\psi}t_a\psi)^2 + (\overline{\psi}i\gamma_5 t_a\psi)^2 - \frac{1}{2}(\overline{\psi}\gamma_\mu t_a\psi)^2 - \frac{1}{2}(\overline{\psi}\gamma_\mu\gamma_5 t_a\psi)^2\Big] \\ &+ \frac{1}{2N_c} G\Big[(\overline{\psi}t_a\lambda_n\psi)^2 + (\overline{\psi}i\gamma_5 t_a\lambda_n\psi)^2 - \frac{1}{2}(\overline{\psi}\gamma_\mu t_a\lambda_n\psi)^2 - \frac{1}{2}(\overline{\psi}\gamma_\mu\gamma_5 t_a\lambda_n\psi)^2\Big]\end{aligned} \tag{3.5}$$

Note that in in the preceding expressions there's an implied summation over $a = 1, \ldots, N_c^2 - 1$ and $n = 1, \ldots, N_f^2 - 1$.

Let us look at the colour singlet terms (first two lines of the above expression) and disregard the colour octet terms. Let us also work in the concrete case of 3 colours and 3 flavours ($N_c = 3$, $N_f = 3$). We can group them as

$$\begin{aligned}\mathcal{L}^{(4)}_{\text{int}} =& -\frac{2}{3}\cdot\frac{8}{9}G\Big[[(\overline{\psi}\psi)^2+(\overline{\psi}i\gamma_5\psi)^2]-\frac{1}{2}[(\overline{\psi}\gamma_\mu\psi)^2+(\overline{\psi}\gamma_\mu\gamma_5\psi)^2]\Big]\\ &-\frac{8}{9}G\Big[[(\overline{\psi}\lambda_n\psi)^2+(\overline{\psi}i\gamma_5\lambda_n\psi)^2]-\frac{1}{2}[(\overline{\psi}\gamma_\mu\lambda_n\psi)^2+(\overline{\psi}\gamma_\mu\gamma_5\lambda_n\psi)^2]\Big]\end{aligned} \tag{3.6}$$

$$\begin{aligned}=& -G_{S\text{-}IS}\Big[(\overline{\psi}\lambda_0\psi)^2+(\overline{\psi}i\gamma_5\lambda_0\psi)^2\Big]\\ &-G_{S\text{-}IV}\Big[(\overline{\psi}\lambda_n\psi)^2+(\overline{\psi}i\gamma_5\lambda_n\psi)^2\Big]\\ &+G_{V\text{-}IS}\Big[(\overline{\psi}\gamma_\mu\lambda_0\psi)^2+(\overline{\psi}\gamma_\mu\gamma_5\lambda_0\psi)^2\Big]\\ &+G_{V\text{-}IV}\Big[(\overline{\psi}\gamma_\mu\lambda_n\psi)^2+(\overline{\psi}\gamma_\mu\gamma_5\lambda_n\psi)^2\Big]\end{aligned} \tag{3.7}$$

where $G_{S\text{-}IS} = G_{S\text{-}IV} = \frac{8}{9}G$ and $G_{V\text{-}IS} = G_{V\text{-}IV} = \frac{1}{2}\frac{8}{9}G$. $\lambda_0 \equiv \sqrt{\frac{2}{3}}\mathbb{1}_3$, so that $\{\lambda_0, ..., \lambda_8\}$ forms the $\mathfrak{u}(3)$ algebra with $\operatorname{Tr}\lambda_n\lambda_m = 2\delta_{nm}$.

General interaction

We derived the above interaction starting from a single term and a single coupling constant in (3.2). As a matter of fact we have no *a priori* reason to consider that there is any relationship between the coupling constants above. In fact a general four-point interaction that does not break any symmetry of QCD is [29]

$$\begin{aligned}\mathcal{L}^{(4)}_{\text{int}} =& +G_S\Big[(\overline{\psi}\lambda_0\psi)^2+(\overline{\psi}i\gamma_5\lambda_0\psi)^2+(\overline{\psi}\lambda_n\psi)^2+(\overline{\psi}i\gamma_5\lambda_n\psi)^2\Big]\\ &-G_V\Big[(\overline{\psi}\gamma_\mu\lambda_0\psi)^2+(\overline{\psi}\gamma_\mu\gamma_5\lambda_0\psi)^2+(\overline{\psi}\gamma_\mu\lambda_n\psi)^2+(\overline{\psi}\gamma_\mu\gamma_5\lambda_n\psi)^2\Big]\\ &-\delta G_{V\text{-}IS}(\overline{\psi}\gamma_\mu\lambda_0\psi)^2-\delta G_{A\text{-}IS}(\overline{\psi}\gamma_\mu\gamma_5\lambda_0\psi)^2\end{aligned} \tag{3.8}$$

with the coupling constants in the above expression all independent. We have defined the signs of the coupling parameters in a way consistent with the usual in literature. The parameters $\delta G_{V\text{-}IS}$ and $\delta G_{A\text{-}IS}$ are set equal to 0 for the remainder of this work, even though strictly speaking we *can* tune them separately without breaking symmetry. Thus our four-point interaction becomes succinctly

$$\begin{aligned}\mathcal{L}^{(4)}_{\text{int}} =& +G_S\Big[(\overline{\psi}\lambda_n\psi)^2+(\overline{\psi}i\gamma_5\lambda_n\psi)^2\Big]\\ &-G_V\Big[(\overline{\psi}\gamma_\mu\lambda_n\psi)^2+(\overline{\psi}\gamma_\mu\gamma_5\lambda_n\psi)^2\Big]\end{aligned} \tag{3.9}$$

now with $n = 0, 1, \ldots, 8$.

Both coupling constants have dimensions of inverse energy squared.

Breaking the $\mathrm{U}(1)_A$ symmetry

The interaction $\mathcal{L}_{\text{int}}^{(4)}$ we have written thus far still contains an unwanted $\mathrm{U}(1)_A$ symmetry. In order to break it while conserving the remaining symmetries, 't Hooft proposed adding the following six-point interaction [23]:

$$\mathcal{L}_{\text{int}}^{(6)} = G_D\Big(\det[\overline{\psi}_i(1+\gamma_5)\psi_j] + \det[\overline{\psi}_i(1-\gamma_5)\psi_j]\Big) \tag{3.10}$$

where the determinants are taken over flavour space. It is a maximally flavour-mixing interaction [29] that breaks $\mathrm{U}(1)_A$ symmetry while leaving the remaining $\mathrm{SU}(3)_V \otimes \mathrm{SU}(3)_A \otimes \mathrm{U}(1)_V$ symmetry intact.

The G_D parameter has dimensions of inverse energy to the fifth.

3.1.2 Regularization procedure

Due to its local current-current interactions the NJL model has divergences which mean it is non-renormalizable [29]. As such it needs an appropriate regularization procedure so the integrals converge. This can be done in a number of ways.

There are several possible regularization schemes [20]. In this work we opt for a simple 3-momentum cutoff, where the integrations in $\vec{p}$ are done up to $|\vec{p}| \leq \Lambda$.

We can interpret this cutoff by saying that the interaction is "on" for low momenta $|\vec{p}| \leq \Lambda$ and turned off for large momenta $|\vec{p}| > \Lambda$. In this view, this can be seen as a rough way of implementing an "asymptotic freedom" of sorts: at large momenta the strong interaction is suppressed.

This regularization scheme suffers from limitations; namely, it breaks Lorentz invariance. To see why notice that imposing a cutoff on the momentum is the same as imposing a discrete lattice on spacetime: an upper limit on the momentum is a lower limit on the wavelength, which (by the sampling theorem) implies a discrete lattice spacing, inversely proportional to the momentum cutoff. This means that, for example, the rotation and translation symmetries of the Poincaré group are immediately broken; we can no longer rotate or translate by any angle or vector we wish, only those compatible with the lattice points.

The model, then, is only applicable in the low energy regime, below the cutoff. At the zero-temperature limit, this amounts to the condition that $p_{Fi} = \sqrt[3]{n_i \pi^2} < \Lambda,\ f = u, d, s$ (see section 3.4.1), since the momenta are distributed only up to the Fermi level. If not, the Fermi distribution is nonzero above that, and care must be taken that the energy is not so big that a significant portion of the particles have momenta above Λ, for example by saying

$$\int_{\Lambda}^{\infty} \not{f}_i \, \mathrm{d}p \tag{3.11}$$

must be very small.

3.1.3 Mean field approximation

As mentioned before, applying the mean field approximation to the model is equivalent to linearising the Lagrangian in the manner explained in section 2.3. First, the four-point

interaction; it becomes

$$\begin{aligned}\mathcal{L}_{\text{int}}^{(4)} = &+ G_S\Big[2(\bar{\psi}\lambda_n\psi)\langle\bar{\psi}\lambda_n\psi\rangle - \langle\bar{\psi}\lambda_n\psi\rangle^2 \\ &\quad + 2(\bar{\psi}i\gamma_5\lambda_n\psi)\langle\bar{\psi}i\gamma_5\lambda_n\psi\rangle - \langle\bar{\psi}i\gamma_5\lambda_n\psi\rangle^2\Big] \\ &- G_V\Big[2(\bar{\psi}\gamma_\mu\lambda_n\psi)\langle\bar{\psi}\gamma_\mu\lambda_n\psi\rangle - \langle\bar{\psi}\gamma_\mu\lambda_n\psi\rangle^2 \\ &\quad + 2(\bar{\psi}\gamma_\mu\gamma_5\lambda_n\psi)\langle\bar{\psi}\gamma_\mu\gamma_5\lambda_n\psi\rangle - \langle\bar{\psi}\gamma_\mu\gamma_5\lambda_n\psi\rangle^2\Big]\end{aligned} \tag{3.12}$$

with $n = 0, \ldots, 8$.

Now, the ground state has well-defined charge, spin and parity. Any operators that mix flavour states will change these properties when applied to the ground state, therefore their expectation values will be zero. The only non-vanishing terms will be those corresponding to states diagonal in flavour space. Furthermore, only the timelike components of vectors will exist; since we are considering static matter all currents will vanish.

The only terms with nonvanishing expectation value are:

$$\langle\bar{\psi}\lambda_0\psi\rangle = \sqrt{\frac{2}{3}}(\sigma_u + \sigma_d + \sigma_s) \tag{3.13}$$

$$\langle\bar{\psi}\lambda_3\psi\rangle = \sigma_u - \sigma_d \tag{3.14}$$

$$\langle\bar{\psi}\lambda_8\psi\rangle = \frac{1}{\sqrt{3}}(\sigma_u + \sigma_d - 2\sigma_s) \tag{3.15}$$

$$\langle\bar{\psi}\gamma^0\lambda_0\psi\rangle = \langle\psi^\dagger\lambda_0\psi\rangle = \sqrt{\frac{2}{3}}(n_u + n_d + n_s) \tag{3.16}$$

$$\langle\bar{\psi}\gamma^0\lambda_3\psi\rangle = \langle\psi^\dagger\lambda_3\psi\rangle = n_u - n_d \tag{3.17}$$

$$\langle\bar{\psi}\gamma^0\lambda_8\psi\rangle = \langle\psi^\dagger\lambda_8\psi\rangle = \frac{1}{\sqrt{3}}(n_u + n_d - 2n_s) \tag{3.18}$$

where we denote $\sigma_i \equiv \langle\bar{\psi}_i\psi_i\rangle$ and $n_i \equiv \langle\psi_i^\dagger\psi_i\rangle$. The (linearised) NJL four-point interaction in the mean field approximation becomes

$$\begin{aligned}\mathcal{L}_{\text{int}}^{(4)} \approx &+ G_S\Big[2(\bar{\psi}\lambda_0\psi)\sqrt{\frac{2}{3}}(\sigma_u + \sigma_d + \sigma_s) - \frac{2}{3}(\sigma_u + \sigma_d + \sigma_s)^2 \\ &\quad + 2(\bar{\psi}\lambda_3\psi)(\sigma_u - \sigma_d) - (\sigma_u - \sigma_d)^2 \\ &\quad + 2(\bar{\psi}\lambda_8\psi)\frac{1}{\sqrt{3}}(\sigma_u + \sigma_d - 2\sigma_s) - \frac{1}{3}(\sigma_u + \sigma_d - 2\sigma_s)^2\Big] \\ &- G_V\Big[2(\psi^\dagger\lambda_0\psi)\sqrt{\frac{2}{3}}(n_u + n_d + n_s) - \frac{2}{3}(n_u + n_d + n_s)^2 \\ &\quad + 2(\psi^\dagger\lambda_3\psi)(n_u - n_d) - (n_u - n_d)^2 \\ &\quad + 2(\psi^\dagger\lambda_8\psi)\frac{1}{\sqrt{3}}(n_u + n_d - 2n_s) - \frac{1}{3}(n_u + n_d - 2n_s)^2\Big]\end{aligned} \tag{3.19}$$

As for the 't Hooft determinant, we can write it using the Levi-Civita symbol (also called the completely antisymmetric tensor; see appendix B.4). We have

$$\det \hat{A} = \sum_{\substack{i=\{u,d,s\}\\ j=\{u,d,s\}\\ k=\{u,d,s\}}} \varepsilon_{ijk} \hat{A}_{ui} \hat{A}_{dj} \hat{A}_{sk} \tag{3.20}$$

where A_{ij} stands for $\overline{\psi}_i(1 \pm \gamma_5)\psi_j$. Explicitly:

$$\begin{aligned} \det \hat{A} = {} & \hat{A}_{uu}\hat{A}_{dd}\hat{A}_{ss} + \hat{A}_{ud}\hat{A}_{ds}\hat{A}_{su} + \hat{A}_{us}\hat{A}_{du}\hat{A}_{sd} \\ & - \hat{A}_{us}\hat{A}_{dd}\hat{A}_{su} - \hat{A}_{uu}\hat{A}_{ds}\hat{A}_{sd} - \hat{A}_{ud}\hat{A}_{du}\hat{A}_{ss} \end{aligned} \tag{3.21}$$

The vacuum expectation value of $\langle \hat{A}_{ij} \rangle$ is

$$\langle \hat{A}_{ij} \rangle = \langle \overline{\psi}_i(1 \pm \gamma_5)\psi_j \rangle = \langle \overline{\psi}_i \psi_j \rangle \pm \langle \overline{\psi}_i \gamma_5 \psi_j \rangle = \sigma_i \delta_{ij} \tag{3.22}$$

for, as discussed before, flavour mixing condensates vanish in the vacuum ($\langle \overline{\psi}_i \psi_j \rangle = 0$ if $i \neq j$) and, since we are assuming a static configuration, $\langle \overline{\psi}_i \gamma_5 \psi_j \rangle = 0$.

In the mean field approximation, the product between three operators is approximated by (2.48), so

$$\begin{aligned} \det \hat{A} \approx {} & \hat{A}_{uu}\langle \hat{A}_{dd} \rangle \langle \hat{A}_{ss} \rangle + \langle \hat{A}_{uu} \rangle \hat{A}_{dd} \langle \hat{A}_{ss} \rangle + \langle \hat{A}_{uu} \rangle \langle \hat{A}_{dd} \rangle \hat{A}_{ss} - 2\langle \hat{A}_{uu} \rangle \langle \hat{A}_{dd} \rangle \langle \hat{A}_{ss} \rangle \\ & \hat{A}_{ud}\langle \hat{A}_{ds} \rangle \langle \hat{A}_{su} \rangle + \langle \hat{A}_{ud} \rangle \hat{A}_{ds} \langle \hat{A}_{su} \rangle + \langle \hat{A}_{ud} \rangle \langle \hat{A}_{ds} \rangle \hat{A}_{su} - 2\langle \hat{A}_{ud} \rangle \langle \hat{A}_{ds} \rangle \langle \hat{A}_{su} \rangle \\ & \hat{A}_{us}\langle \hat{A}_{du} \rangle \langle \hat{A}_{sd} \rangle + \langle \hat{A}_{us} \rangle \hat{A}_{du} \langle \hat{A}_{sd} \rangle + \langle \hat{A}_{us} \rangle \langle \hat{A}_{du} \rangle \hat{A}_{sd} - 2\langle \hat{A}_{us} \rangle \langle \hat{A}_{du} \rangle \langle \hat{A}_{sd} \rangle \\ & - \hat{A}_{us}\langle \hat{A}_{dd} \rangle \langle \hat{A}_{su} \rangle - \langle \hat{A}_{us} \rangle \hat{A}_{dd} \langle \hat{A}_{su} \rangle - \langle \hat{A}_{us} \rangle \langle \hat{A}_{dd} \rangle \hat{A}_{su} + 2\langle \hat{A}_{us} \rangle \langle \hat{A}_{dd} \rangle \langle \hat{A}_{su} \rangle \\ & - \hat{A}_{uu}\langle \hat{A}_{ds} \rangle \langle \hat{A}_{sd} \rangle - \langle \hat{A}_{uu} \rangle \hat{A}_{ds} \langle \hat{A}_{sd} \rangle - \langle \hat{A}_{uu} \rangle \langle \hat{A}_{ds} \rangle \hat{A}_{sd} + 2\langle \hat{A}_{uu} \rangle \langle \hat{A}_{ds} \rangle \langle \hat{A}_{sd} \rangle \\ & - \hat{A}_{ud}\langle \hat{A}_{du} \rangle \langle \hat{A}_{ss} \rangle - \langle \hat{A}_{ud} \rangle \hat{A}_{du} \langle \hat{A}_{ss} \rangle - \langle \hat{A}_{ud} \rangle \langle \hat{A}_{du} \rangle \hat{A}_{ss} + 2\langle \hat{A}_{ud} \rangle \langle \hat{A}_{du} \rangle \langle \hat{A}_{ss} \rangle \end{aligned} \tag{3.23}$$

Since $\langle A_{ij} \rangle = 0$ if $i \neq j$ we have

$$\det \hat{A} \approx \hat{A}_{uu}\langle \hat{A}_{dd} \rangle \langle \hat{A}_{ss} \rangle + \langle \hat{A}_{uu} \rangle \hat{A}_{dd} \langle \hat{A}_{ss} \rangle + \langle \hat{A}_{uu} \rangle \langle \hat{A}_{dd} \rangle \hat{A}_{ss} - 2\langle \hat{A}_{uu} \rangle \langle \hat{A}_{dd} \rangle \langle \hat{A}_{ss} \rangle \tag{3.24}$$

since all other terms vanish. Thus the 't Hooft interaction in the mean field approximation is

$$\begin{aligned} \mathcal{L}^{(6)}_{\text{int}} &= G_D\Big(\det[\overline{\psi}(1+\gamma_5)\psi] + \det[\overline{\psi}(1-\gamma_5)\psi]\Big) \\ &\approx 2G_D\Big(\overline{\psi}_u\psi_u\langle\overline{\psi}_d\psi_d\rangle\langle\overline{\psi}_s\psi_s\rangle + \langle\overline{\psi}_u\psi_u\rangle\overline{\psi}_d\psi_d\langle\overline{\psi}_s\psi_s\rangle \\ &\qquad + \langle\overline{\psi}_u\psi_u\rangle\langle\overline{\psi}_d\psi_d\rangle\overline{\psi}_s\psi_s - 2\langle\overline{\psi}_u\psi_u\rangle\langle\overline{\psi}_d\psi_d\rangle\langle\overline{\psi}_s\psi_s\rangle\Big) \\ &= 2G_D\Big(\overline{\psi}_u(\sigma_d\sigma_s)\psi_u + \overline{\psi}_d(\sigma_u\sigma_s)\psi_d + \overline{\psi}_s(\sigma_u\sigma_d)\psi_s - 2\sigma_u\sigma_d\sigma_s\Big) \end{aligned} \tag{3.25}$$

All put together, the NJL Lagrangian in the mean field approximation becomes

$$\begin{aligned}
\mathcal{L} &= \overline{\psi}(i\partial\!\!\!/ - m)\psi + \mathcal{L}_{\text{int}}^{(4)} + \mathcal{L}_{\text{int}}^{(6)} \\
&\approx \overline{\psi}(i\partial\!\!\!/ - m)\psi \\
&\quad + G_S\Big[2(\overline{\psi}\lambda_0\psi)\sqrt{\frac{2}{3}}(\sigma_u+\sigma_d+\sigma_s) - \frac{2}{3}(\sigma_u+\sigma_d+\sigma_s)^2 \\
&\quad\quad + 2(\overline{\psi}\lambda_3\psi)(\sigma_u-\sigma_d) - (\sigma_u-\sigma_d)^2 \\
&\quad\quad + 2(\overline{\psi}\lambda_8\psi)\frac{1}{\sqrt{3}}(\sigma_u+\sigma_d-2\sigma_s) - \frac{1}{3}(\sigma_u+\sigma_d-2\sigma_s)^2\Big] \\
&\quad - G_V\Big[2(\psi^\dagger\lambda_0\psi)\sqrt{\frac{2}{3}}(n_u+n_d+n_s) - \frac{2}{3}(n_u+n_d+n_s)^2 \\
&\quad\quad + 2(\psi^\dagger\lambda_3\psi)(n_u-n_d) - (n_u-n_d)^2 \\
&\quad\quad + 2(\psi^\dagger\lambda_8\psi)\frac{1}{\sqrt{3}}(n_u+n_d-2n_s) - \frac{1}{3}(n_u+n_d-2n_s)^2\Big] \\
&\quad - 2G_D\Big[\overline{\psi}\Big(^{\sigma_d\sigma_s}{}_{\sigma_s\sigma_u}{}_{\sigma_u\sigma_d}\Big)\psi - 2\sigma_u\sigma_d\sigma_s\Big]
\end{aligned} \tag{3.26}$$

3.1.4 Thermodynamics

Casting the mean field Lagrangian in the form of (2.77):

$$\mathcal{L} = \overline{\psi}[i\partial\!\!\!/ - \gamma^0\mathcal{V} - (m+\mathcal{S})]\psi + U \tag{3.27}$$

we arrange it like so:

$$\begin{aligned}
\mathcal{L} \approx \overline{\psi}\Bigg[&i\partial\!\!\!/ - \gamma^0\Bigg(2G_V\Bigg(\sqrt{\frac{2}{3}}\lambda_0(n_u+n_d+n_s) + \lambda_3(n_u-n_d) + \frac{1}{\sqrt{3}}\lambda_8(n_u+n_d-2n_s)\Bigg)\Bigg) \\
&- \Bigg(m - 2G_S\Bigg(\sqrt{\frac{2}{3}}\lambda_0(\sigma_u+\sigma_d+\sigma_s) + \lambda_3(\sigma_u-\sigma_d) + \frac{1}{\sqrt{3}}\lambda_8(\sigma_u+\sigma_d-2\sigma_s)\Bigg) + \Big(^{\sigma_d\sigma_s}{}_{\sigma_s\sigma_u}{}_{\sigma_u\sigma_d}\Big)\Bigg)\Bigg]\psi \\
&- G_S\Bigg(\frac{2}{3}(\sigma_u+\sigma_d+\sigma_s)^2 + (\sigma_u-\sigma_d)^2 + \frac{1}{3}(\sigma_u+\sigma_d-2\sigma_s)^2\Bigg) \\
&+ G_V\Bigg(\frac{2}{3}(n_u+n_d+n_s)^2 + (n_u-n_d)^2 + \frac{1}{3}(n_u+n_d-2n_s)^2\Bigg) + 4G_D\sigma_u\sigma_d\sigma_s
\end{aligned} \tag{3.28}$$

I.e.:

$$\begin{aligned}
\mathcal{S} = &-2G_S\Bigg(\sqrt{\frac{2}{3}}\lambda_0(\sigma_u+\sigma_d+\sigma_s) + \lambda_3(\sigma_u-\sigma_d) + \frac{1}{\sqrt{3}}\lambda_8(\sigma_u+\sigma_d-2\sigma_s)\Bigg) \\
&+ 2G_D\Big(^{\sigma_d\sigma_s}{}_{\sigma_s\sigma_u}{}_{\sigma_u\sigma_d}\Big)
\end{aligned} \tag{3.29}$$

$$\mathcal{V} = 2G_V\Bigg(\sqrt{\frac{2}{3}}\lambda_0(n_u+n_d+n_s) + \lambda_3(n_u-n_d) + \frac{1}{\sqrt{3}}\lambda_8(n_u+n_d-2n_s)\Bigg) \tag{3.30}$$

$$U = -2G_S({\sigma_u}^2 + {\sigma_d}^2 + {\sigma_s}^2) + 2G_V({n_u}^2 + {n_d}^2 + {n_s}^2) + 4G_D\sigma_u\sigma_d\sigma_s \tag{3.31}$$

Simplifying:

$$\begin{aligned}
\mathcal{S} &= -2G_S\left[\frac{2}{3}\begin{pmatrix}1 & & \\ & 1 & \\ & & 1\end{pmatrix}(\sigma_u+\sigma_d+\sigma_s) + \begin{pmatrix}1 & & \\ & -1 & \\ & & 0\end{pmatrix}(\sigma_u-\sigma_d) + \frac{1}{3}\begin{pmatrix}1 & & \\ & 1 & \\ & & -2\end{pmatrix}(\sigma_u+\sigma_d-2\sigma_s)\right] \\
&\quad + 2G_D\begin{pmatrix}\sigma_d\sigma_s & & \\ & \sigma_s\sigma_u & \\ & & \sigma_u\sigma_d\end{pmatrix} \\
&= -2G_S\begin{pmatrix}\frac{2}{3}(\sigma_u+\sigma_d+\sigma_s)+\sigma_u-\sigma_d+\frac{1}{3}(\sigma_u+\sigma_d-2\sigma_s) & & \\ & \frac{2}{3}(\sigma_u+\sigma_d+\sigma_s)-\sigma_u+\sigma_d+\frac{1}{3}(\sigma_u+\sigma_d-2\sigma_s) & \\ & & \frac{2}{3}(\sigma_u+\sigma_d+\sigma_s)-\frac{2}{3}(\sigma_u+\sigma_d-2\sigma_s)\end{pmatrix} \\
&\quad + 2G_D\begin{pmatrix}\sigma_d\sigma_s & & \\ & \sigma_s\sigma_u & \\ & & \sigma_u\sigma_d\end{pmatrix} \\
&= -2G_S\begin{pmatrix}2\sigma_u & & \\ & 2\sigma_d & \\ & & 2\sigma_s\end{pmatrix} + 2G_D\begin{pmatrix}\sigma_d\sigma_s & & \\ & \sigma_s\sigma_u & \\ & & \sigma_u\sigma_d\end{pmatrix}
\end{aligned} \tag{3.32}$$

and

$$\begin{aligned}
\mathcal{V} &= 2G_V\left[\frac{2}{3}\begin{pmatrix}1 & & \\ & 1 & \\ & & 1\end{pmatrix}(n_u+n_d+n_s) + \begin{pmatrix}1 & & \\ & -1 & \\ & & 0\end{pmatrix}(n_u-n_d) + \frac{1}{3}\begin{pmatrix}1 & & \\ & 1 & \\ & & -2\end{pmatrix}(n_u+n_d-2n_s)\right] \\
&= 2G_V\begin{pmatrix}\frac{2}{3}(n_u+n_d+n_s)+n_u-n_d+\frac{1}{3}(n_u+n_d-2n_s) & & \\ & \frac{2}{3}(n_u+n_d+n_s)-n_u+n_d+\frac{1}{3}(n_u+n_d-2n_s) & \\ & & \frac{2}{3}(n_u+n_d+n_s)-\frac{2}{3}(n_u+n_d-2n_s)\end{pmatrix} \\
&= 2G_V\begin{pmatrix}2n_u & & \\ & 2n_d & \\ & & 2n_s\end{pmatrix}
\end{aligned} \tag{3.33}$$

Such that the effective masses and the effective chemical potentials, as defined in section section 2.4.4, are

$$M = m + \mathcal{S} = \begin{pmatrix}m_u & & \\ & m_d & \\ & & m_s\end{pmatrix} - 4G_S\begin{pmatrix}\sigma_u & & \\ & \sigma_d & \\ & & \sigma_s\end{pmatrix} + 2G_D\begin{pmatrix}\sigma_d\sigma_s & & \\ & \sigma_s\sigma_u & \\ & & \sigma_u\sigma_d\end{pmatrix} \tag{3.34}$$

$$\tilde{\mu} = \mu - \mathcal{V} = \begin{pmatrix}\mu_u & & \\ & \mu_d & \\ & & \mu_s\end{pmatrix} - 4G_V\begin{pmatrix}n_u & & \\ & n_d & \\ & & n_s\end{pmatrix} \tag{3.35}$$

These are the mass gap equations and the effective chemical potentials, respectively:

$$\begin{cases} M_u = m_u - 4G_S\sigma_u + 2G_D\sigma_d\sigma_s \\ M_d = m_d - 4G_S\sigma_d + 2G_D\sigma_s\sigma_u \\ M_s = m_s - 4G_S\sigma_s + 2G_D\sigma_u\sigma_d \end{cases} \tag{3.36}$$

$$\begin{cases} \tilde{\mu}_u = \mu_u - 4G_V n_u \\ \tilde{\mu}_d = \mu_d - 4G_V n_d \\ \tilde{\mu}_s = \mu_s - 4G_V n_s \end{cases} \tag{3.37}$$

or more compactly

$$M_i = m_i - 4G_S\sigma_i + 2G_D\sigma_j\sigma_k, \quad i,j,k \text{ even permutations of } u,d,s \tag{3.38}$$

$$\tilde{\mu}_i = \mu_i - 4G_V n_i, \quad i = u,d,s \tag{3.39}$$

We can finally write the grand canonical potential density as indicated in expression (2.80):

$$\Omega = -2T\,\mathrm{Tr}\int \frac{\mathrm{d}^3\vec{p}}{(2\pi)^3}\left[\frac{\omega}{T} + \ln\!\left(1+e^{-(\omega+\tilde{\mu})/T}\right) + \ln\!\left(1+e^{-(\omega-\tilde{\mu})/T}\right)\right] - U + \Omega_0 \tag{3.40}$$

where the trace is taken over flavour and colour indices. The trace over colour simply yields a factor of 3 ($= N_c$). Taking the trace over flavour amounts to summing over the flavour indices, since all matrices in flavour space are diagonal.

$$\begin{aligned}\Omega = -6T\sum_{f=u,d,s}\int \frac{\mathrm{d}^3\vec{p}}{(2\pi)^3}\left[\frac{\omega_f}{T} + \ln\!\left(1+e^{-(\omega_f+\tilde{\mu}_f)/T}\right) + \ln\!\left(1+e^{-(\omega_f-\tilde{\mu}_f)/T}\right)\right] \\ + 2G_S({\sigma_u}^2 + {\sigma_d}^2 + {\sigma_s}^2) - 2G_V({n_u}^2 + {n_d}^2 + {n_s}^2) - 4G_D\sigma_u\sigma_d\sigma_s + \Omega_0\end{aligned} \tag{3.41}$$

where $\omega_f = \sqrt{|\vec{p}|^2 + M_f^2}$.

From this, all quantities of interest can be derived ((2.59)–(2.62) on section 2.4.1). The particle densities, pressure, energy density and entropy density are:

$$\begin{aligned}E = 6\sum_{f=u,d,s}\int \frac{\mathrm{d}^3\vec{p}}{(2\pi)^3}\left[\omega_f(\bar{\ell}_f + \ell_f - 1)\right] \\ + 2G_S({\sigma_u}^2 + {\sigma_d}^2 + {\sigma_s}^2) + 2G_V({n_u}^2 + {n_d}^2 + {n_s}^2) - 4G_D\sigma_u\sigma_d\sigma_s + \Omega_0\end{aligned} \tag{3.42}$$

$$\begin{aligned}P = 6\sum_{f=u,d,s}\int \frac{\mathrm{d}^3\vec{p}}{(2\pi)^3}\left[\omega_f + T\ln\!\left(1+e^{-(\omega_f+\tilde{\mu}_f)/T}\right) + T\ln\!\left(1+e^{-(\omega_f-\tilde{\mu}_f)/T}\right)\right] \\ - 2G_S({\sigma_u}^2 + {\sigma_d}^2 + {\sigma_s}^2) + 2G_V({n_u}^2 + {n_d}^2 + {n_s}^2) + 4G_D\sigma_u\sigma_d\sigma_s - \Omega_0\end{aligned} \tag{3.43}$$

The trace of a square matrix is the sum of the elements in its diagonal (equivalently, of its eigenvalues). It is a linear map: $\mathrm{Tr}(A+B) = \mathrm{Tr}\,A + \mathrm{Tr}\,B$. Also, if A is a diagonal matrix, ($A = \mathrm{diag}(a_{11}, a_{22}, \dots)$) we have that $\mathrm{diag}({a_{11}}^N, {a_{22}}^N, \dots)$, with N a real number. Then immediately $e^A = \mathrm{diag}(e^{a_{11}}, e^{a_{22}}, \dots)$, $\log A = \mathrm{diag}(\log a_{11}, \log a_{22}, \dots)$, etc., in general $f(A) = \mathrm{diag}(f(a_{11}), f(a_{22}), \dots)$ for any analytic function f. Thus $\mathrm{Tr}\,f(A) = \sum_i f(a_{ii})$, if A is a diagonal matrix and f an analytic function.

$$S = 6 \sum_{f=u,d,s} \int \frac{\mathrm{d}^3\vec{p}}{(2\pi)^3} \frac{1}{T} \Big[\omega_f (\bar{\not{f}}_f + \not{f}_f) + \tilde{\mu} (\bar{\not{f}}_f - \not{f}_f) + T \ln\Big(1 + e^{-(\omega_f + \tilde{\mu}_f)/T}\Big) + T \ln\Big(1 + e^{-(\omega_f - \tilde{\mu}_f)/T}\Big) \Big] \tag{3.44}$$

$$n_i = \langle \psi_i^\dagger \psi_i \rangle = 6 \int \frac{\mathrm{d}^3\vec{p}}{(2\pi)^3} (\not{f}_i - \bar{\not{f}}_i) \tag{3.45}$$

with $\not{f}_i \equiv \not{f}(\omega_i, \tilde{\mu}_i, T)$ and $\bar{\not{f}}_i \equiv \bar{\not{f}}(\omega_i, \tilde{\mu}_i, T)$.

As for the scalar densities $\sigma_i = \langle \overline{\psi}_i \psi_i \rangle$, these are found by imposing that the grand canonical potential be stationary with respect to variations of σ_i:

$$\frac{\partial \Omega}{\partial \sigma_i} = 0, \quad i = u, d, s \tag{3.46}$$

After some calculation (see appendix A.6) we have

$$\sigma_i = \langle \overline{\psi}_i \psi_i \rangle = 6 \int \frac{\mathrm{d}^3\vec{p}}{(2\pi)^3} \frac{M_i}{\omega_i} [\not{f}_f + \bar{\not{f}}_f - 1] \tag{3.47}$$

Note that the value of the condensates depends on the constituent masses, while the gap equations for the masses depend on the value of the condensate. These sets of equations form a self-consistent system that can be solved numerically through appropriate methods.

As discussed before, these integrals are divergent unless an appropriate regularization scheme is used. In our scheme the integrals are taken up to $|\vec{p}| = \Lambda$, as per section 3.1.2.

3.1.5 Leptonic contribution

In addition to quarks and their interactions, we must also consider the presence of electrons and potentially muons (the tau is too massive to appear; it's a bit heavier than the charm quark, which also does not appear in a neutron star [1]; see Table 3.1). These are fundamental to enforce charge neutrality in neutron star matter.

We will model them by adding the following term to the Lagrangian, corresponding to a free fermion field

$$\mathcal{L} = \overline{\psi}(i\partial\!\!\!/ - m)\psi \tag{3.48}$$

where $\psi = (e, \mu)^T$ represents the Dirac fields of the electron and the muon, and $m = \mathrm{diag}(m_e, m_\mu)$.

The equilibrium configuration of the system is attained when P is stationary with respect to variations of the fields [26], and we know that $P = -\Omega$.

This amounts to tacking on to each of the integrals a factor of $H(\Lambda - |\vec{p}|)$, where $H(x)$ is the Heaviside step function (see appendix B.5)

Table 3.1: Experimental values for lepton masses [22].

Particle	Mass [MeV]
Electron (e^-)	0.510 998 946 1(31)
Muon (μ^-)	105.658 374 5(24)
Tau (τ^-)	1776.86(12)

Thermodynamics

The free lepton Lagrangian we wrote has no interactions or auxiliary fields, so the grand canonical potential density is

$$\Omega = -2T\,\mathrm{Tr}\int\frac{\mathrm{d}^3\vec{p}}{(2\pi)^3}\left[\frac{\omega}{T}+\ln\left(1+e^{-(\omega+\mu)/T}\right)+\ln\left(1+e^{-(\omega-\mu)/T}\right)\right]+\Omega_0 \tag{3.49}$$

Again all matrices are diagonal so the trace is simply a sum:

$$\Omega = -2T\sum_{\ell=e,\mu}\int\frac{\mathrm{d}^3\vec{p}}{(2\pi)^3}\left[\frac{\omega_\ell}{T}+\ln\left(1+e^{-(\omega_\ell+\mu_\ell)/T}\right)+\ln\left(1+e^{-(\omega_\ell-\mu_\ell)/T}\right)\right]+\Omega_0 \tag{3.50}$$

with $\omega_\ell = \sqrt{|\vec{p}|^2+m_\ell^2}$.

From this we extract the following expressions (calculations in appendix A.8):

$$E = 2\sum_{\ell=e,\mu}\int\frac{\mathrm{d}^3\vec{p}}{(2\pi)^3}\omega_\ell(\bar{\rho}_\ell+\rho_\ell-1)+\Omega_0 \tag{3.51}$$

$$\begin{aligned}P = 2\sum_{\ell=e,\mu}\int\frac{\mathrm{d}^3\vec{p}}{(2\pi)^3}\Big[&\omega_\ell+T\ln\left(1+e^{-(\omega_\ell+\mu_\ell)/T}\right)\\&+T\ln\left(1+e^{-(\omega_\ell-\mu_\ell)/T}\right)\Big]-\Omega_0\end{aligned} \tag{3.52}$$

$$\begin{aligned}S = \frac{2}{T}\sum_{\ell=e,\mu}\int\frac{\mathrm{d}^3\vec{p}}{(2\pi)^3}\Big[&\omega_\ell(\bar{\rho}_\ell+\rho_\ell)+\tilde{\mu}_\ell(\bar{\rho}_\ell-\rho_\ell)\\&+T\ln\left(1+e^{-(\omega_\ell+\tilde{\mu}_\ell)/T}\right)+T\ln\left(1+e^{-(\omega_\ell-\tilde{\mu}_\ell)/T}\right)\Big]\end{aligned} \tag{3.53}$$

$$n_\ell = 2\int\frac{\mathrm{d}^3\vec{p}}{(2\pi)^3}(\rho_\ell-\bar{\rho}_\ell) \tag{3.54}$$

Note the lepton gas does not interact in any way with the rest of the particles. As such its contribution to the energy, pressure and entropy is purely additive: all we have to do is add this contribution to the quantities we previously derived for the NJL model.

3.1.6 Charge neutrality

As discussed in section 1.6, in a neutron star matter is electrically neutral. Therefore in our calculations in this model we will need to impose the constraint that matter has

zero net electric charge. In the NJL model with leptons, this amounts to

$$\begin{aligned}\sum q_i n_i &= q_u n_u + q_d n_d + q_s n_s + q_e n_e + q_\mu n_\mu \\ &= \tfrac{2}{3} n_u - \tfrac{1}{3} n_d - \tfrac{1}{3} n_s - n_e - n_\mu = 0\end{aligned} \tag{3.55}$$

This constraint will have to be satisfied when we calculate the EoS for neutron star matter.

3.1.7 Chemical potential

In section 2.4.3 we noted that even if there are many particle species we have at most as many linearly independent chemical potentials as there are conserved charges (more precisely, conserved on the timescale of the star, or even more generally, on a timescale greater than our observations). That is, we can always write the chemical potential of particle i as

$$\mu_i = \sum_j q_{ij} \mu_j \tag{3.56}$$

where q_{ij} is the charge of type j that particle i has, and μ_j is the chemical potential associated with charge j.

In this case, the only quantities that are conserved on this timescale are the baryon number and the electric charge (the lepton number is not conserved on the lifetime of the star [1]). Let the chemical potentials associated to these be μ_b and μ_q respectively. We know that

Particle	Baryon number	Electric charge
u	$1/3$	$2/3$
d	$1/3$	$-1/3$
s	$1/3$	$-1/3$
e^-	0	-1
μ^-	0	-1

(3.57)

which means

$$\begin{cases} \mu_u = \frac{1}{3}\mu_b + \frac{2}{3}\mu_q \\ \mu_d = \frac{1}{3}\mu_b - \frac{1}{3}\mu_q \\ \mu_s = \frac{1}{3}\mu_b - \frac{1}{3}\mu_q \\ \mu_e = -\mu_q \\ \mu_\mu = -\mu_q \end{cases} \Rightarrow \begin{cases} \mu_e = \mu_d - \mu_u \\ \mu_d = \mu_s \\ \mu_e = \mu_\mu \end{cases} \tag{3.58}$$

3.1.8 Beta equilibrium

Alternatively to the above, we can obtain an equivalent result by the following argument [26]:

In other words, the leptonic chemical potential is zero, for if was nonzero the leptons would quickly disappear and bring it back to zero. Since this happens on a quick timescale, the leptonic chemical potential is always essentially zero.

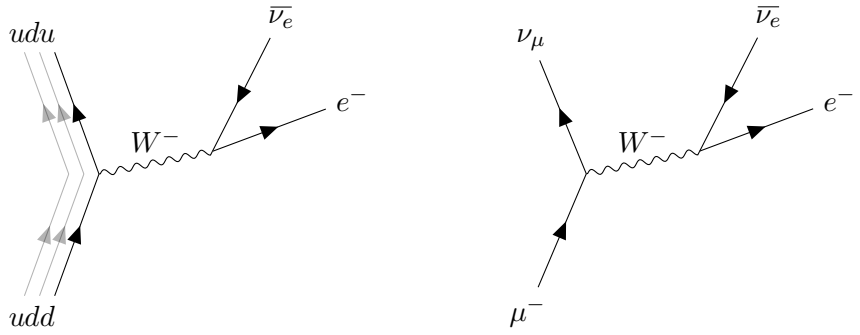

(a) Beta decay. (b) Muon decay.

Figure 3.1

In equilibrium, and if time reversal symmetry holds, if a reaction can happen it immediately follows that the reverse reaction must also happen, and at the same rate: a detailed balance must occur.

$$A + B + C + \cdots \rightleftharpoons X + Y + Z + \cdots \Rightarrow \tag{3.59}$$

$$\Rightarrow \mu_A + \mu_B + \mu_C + \cdots = \mu_X + \mu_Y + \mu_Z + \ldots \tag{3.60}$$

A detailed balance is translated into a relationship between chemical potentials: the chemical potentials of both sides of the reaction must be equal. This is another way of writing constraints between the chemical potentials of the different particles and thus showing they can be reduced to the chemical potentials of the independent conserved quantities/charges.

Consider beta decay (Figure 3.1a):

$$\begin{cases} d \rightleftharpoons u + e^- + \overline{\nu_e} \\ s \rightleftharpoons u + e^- + \overline{\nu_e} \end{cases} \tag{3.61}$$

If there is an equilibrium under this reaction then we have

$$\Rightarrow \begin{cases} \mu_d = \mu_u + \mu_e - \mu_{\nu_e} \\ \mu_s = \mu_u + \mu_e - \mu_{\nu_e} \end{cases} \tag{3.62}$$

Then, looking at muon decay (Figure 3.1b), whose dominant mode is

$$\mu^- \rightleftharpoons e^- + \overline{\nu_e} + \nu_\mu \tag{3.63}$$

we have that

$$\mu_\mu = \mu_e - \mu_{\nu_e} + \mu_{\nu_\mu} \tag{3.64}$$

Provided neutrinos have escaped the star (this happens in minutes since they interact so little with regular matter [1]), we can disregard their chemical potential, yielding equivalent constraints to those found above.

$$\begin{cases} \mu_d = \mu_u + \mu_e \\ \mu_d = \mu_s \\ \mu_e = \mu_\mu \end{cases} \tag{3.65}$$

3.1.9 Confinement

The NJL model is an effective field theory; despite its successes, it does not fully replicate the underlying fundamental theory. Crucially, it does not feature confinement, a critical feature of QCD to explain hadron physics. To solve this, we will use another, different effective field theory where the degrees of freedom are hadrons, instead of quarks, and combine the two in a unified theory.

3.2 The nonlinear NL3$\omega\rho$ model

Described by Walecka in [30], the (σ – ω) model is a nuclear field theory that was proposed as a theory to explain the properties of the nucleus. In this model, the degrees of freedom are the nucleons (proton and neutron; both fermion fields), a scalar meson field (called σ), and a vector meson field (denoted ω_μ). The interactions between nucleons are mediated by the exchange of mesons. It is intended to be studied in the mean field approximation. The Lagrangian of the theory has the form

$$\begin{aligned}\mathcal{L} &= \overline{\psi}(i\partial\!\!\!/ - m)\psi \\ &+ \frac{1}{2}(\partial_\mu\sigma)(\partial^\mu\sigma) - \frac{1}{2}m_\sigma^2\sigma^2 \\ &- \frac{1}{4}\omega_{\mu\nu}\omega^{\mu\nu} + \frac{1}{2}m_\omega^2\omega_\mu\omega^\mu \\ &+ \mathcal{L}_{\text{int}}\end{aligned} \tag{3.66}$$

where $\psi = (p, n)^T$, p and n the spinors for the proton and neutron, respectively, and $\omega_{\mu\nu} = \partial_\mu\omega_\nu - \partial_\nu\omega_\mu$ is the field strength tensor for the omega meson. Note that both proton and neutron have the same mass, m, such that we can consider them to be two orthogonal isospin states.

Now, we want the interaction to couple the scalar meson to the nucleon density, $\overline{\psi}\psi$, and the vector meson to the nucleon current, $\overline{\psi}\gamma^\mu\psi$. Therefore the interaction Lagrangian will have the following form:

$$\mathcal{L}_{\text{int}} = g_\sigma\sigma\overline{\psi}\psi - g_\omega\omega_\mu\overline{\psi}\gamma^\mu\psi \tag{3.67}$$

The Lagrangian of the model is then

$$\begin{aligned}\mathcal{L} = \overline{\psi}[i(\partial\!\!\!/ + ig_\omega\omega\!\!\!/) - (m - g_\sigma\sigma)]\psi \\ + \frac{1}{2}(\partial_\mu\sigma)(\partial^\mu\sigma) - \frac{1}{2}m_\sigma^2\sigma^2 - \frac{1}{4}\omega_{\mu\nu}\omega^{\mu\nu} + \frac{1}{2}m_\omega^2\omega_\mu\omega^\mu\end{aligned} \tag{3.68}$$

This is the linear (σ – ω) model.

The model has the following parameters: m, m_σ, m_ω, g_σ, g_ω. These can be determined by fitting to experimental properties. Indeed in this model we can derive algebraic relations between the aforementioned parameters and the following properties of nuclear matter: binding energy (per nucleon), saturation density, compression modulus, effective nucleon mass, and symmetry coefficient [1].

This model is too simplistic, however, and it fails to accurately account for the properties of nuclear matter [1,31]. Further improvements can be made.

Nonlinear interactions

To better replicate the properties of nuclear matter we add scalar self-interactions (cubic and quartic) controlled by two new parameters, κ and λ, in a term of the form

$$-\frac{1}{3}\kappa(g_\sigma\sigma)^3-\frac{1}{4}\lambda(g_\sigma\sigma)^4 \tag{3.69}$$

In addition, we can introduce also a quartic ω meson self-interaction

$$+\frac{1}{4!}\xi g_\omega^4(\omega_\mu\omega^\mu)^2 \tag{3.70}$$

The rho meson

Now, we introduce in this model another meson, the ρ meson, an isospin triplet vector field which couples to *isospin* current, via the term

$$-g_\rho\overline{\psi}\gamma^\mu\vec{\tau}\cdot\vec{\rho}_\mu\psi \tag{3.71}$$

where $\vec{\rho}=\{\rho^1,\rho^2,\rho^3\}$ and $\vec{\tau}=\{\tau_1,\tau_2,\tau_3\}$ are the generators of the $\mathrm{SU(2)_{isospin}}$ group, the Pauli matrices over two (see appendix B.3). This field is crucial to account for the properties of asymmetric matter.

The term for the free Lagrangian for this meson must of course also be included:

$$-\frac{1}{4}\vec{\rho}_{\mu\nu}\cdot\vec{\rho}^{\mu\nu}+\frac{1}{2}m_\rho^2\vec{\rho}_\mu\cdot\vec{\rho}^\mu \tag{3.72}$$

of the same form as the free Lagrangian for a vector field (like ω_μ), but with the three isospin components. Analogously, $\vec{\rho}_{\mu\nu}=\partial_\mu\vec{\rho}_\nu-\partial_\nu\vec{\rho}_\mu$

Finally, we also allow an interaction between the omega and rho mesons, through a term

$$+\Lambda_{\omega\rho}(g_\omega^2\omega_\mu\omega^\mu)(g_\rho^2\vec{\rho}_\nu\cdot\vec{\rho}^\nu) \tag{3.73}$$

All put together:

$$\begin{aligned}\mathcal{L}=&\,\overline{\psi}[i\gamma^\mu(\partial_\mu+ig_\omega\omega_\mu+ig_\rho\vec{\tau}\cdot\vec{\rho}_\mu)-(m-g_\sigma\sigma)]\psi\\&+\frac{1}{2}(\partial_\mu\sigma)(\partial^\mu\sigma)-\frac{1}{2}m_\sigma^2\sigma^2\\&-\frac{1}{4}\omega_{\mu\nu}\omega^{\mu\nu}+\frac{1}{2}m_\omega^2\omega_\mu\omega^\mu\\&-\frac{1}{4}\vec{\rho}_{\mu\nu}\cdot\vec{\rho}^{\mu\nu}+\frac{1}{2}m_\rho^2\vec{\rho}_\mu\cdot\vec{\rho}^\mu\\&-\frac{1}{3}\kappa(g_\sigma\sigma)^3-\frac{1}{4}\lambda(g_\sigma\sigma)^4+\frac{1}{4!}\xi g_\omega^4(\omega_\mu\omega^\mu)^2\\&+\Lambda_{\omega\rho}(g_\omega^2\omega_\mu\omega^\mu)(g_\rho^2\vec{\rho}_\nu\cdot\vec{\rho}^\nu)\end{aligned} \tag{3.74}$$

this is the NL3$\omega\rho$ model [32].

3.2.1 Mean field approximation and thermodynamics

As mentioned at the beginning, this model is intended for use in the context of a mean field approximation, where the meson fields are replaced by their mean values, and only nucleons are treated as quantum fields. This means these latter are treated as independent particles moving in the mean fields spawned by the mesons. We will also consider static matter.

Again, we follow the reasoning that only fields that preserve the properties of the vacuum can have nonvanishing expectation value (since operators that don't, necessarily have $\langle 0|\hat{A}|0\rangle = 0$). Furthermore, as we are working in a static configuration, no currents exist: the $i = 1, 2, 3$ components of the vector fields also vanish, as well as any derivatives.

As such, in the mean field only σ, ω_0 and ρ^3_0 exist (τ_3 is the only matrix diagonal in isospin). Thus we write as a shorthand

$$\sigma \equiv \langle \sigma \rangle \tag{3.75}$$
$$\omega \equiv \langle \omega_0 \rangle \tag{3.76}$$
$$\rho \equiv \langle \rho^3_0 \rangle \tag{3.77}$$

where these will henceforth denote the mean fields, not the quantum fields proper. Thus the Lagrangian, in the form of (2.77), is

$$\begin{aligned}\mathcal{L} \approx\ & \bar{\psi}[i\partial\!\!\!/ - \gamma^0(g_\omega\omega + g_\rho\tau_3\rho) - (m - g_\sigma\sigma)]\psi \\ & - \frac{1}{2}m_\sigma^2\sigma^2 + \frac{1}{2}m_\omega^2\omega^2 + \frac{1}{2}m_\rho^2\rho^2 \\ & - \frac{1}{3}\kappa(g_\sigma\sigma)^3 - \frac{1}{4}\lambda(g_\sigma\sigma)^4 + \frac{1}{4!}\xi g_\omega^4\omega^4 \\ & + \Lambda_{\omega\rho}(g_\omega^2\omega^2)(g_\rho^2\rho^2)\end{aligned} \tag{3.78}$$

or form (2.77) where

$$\mathcal{S} = -g_\sigma\sigma \tag{3.79}$$
$$\mathcal{V} = g_\omega\omega + g_\rho\tau_3\rho \tag{3.80}$$
$$\begin{aligned}U = & -\frac{1}{2}m_\sigma^2\sigma^2 + \frac{1}{2}m_\omega^2\omega^2 + \frac{1}{2}m_\rho^2\rho^2 - \frac{1}{3}\kappa(g_\sigma\sigma)^3 - \frac{1}{4}\lambda(g_\sigma\sigma)^4 \\ & + \frac{1}{4!}\xi g_\omega^4\omega^4 + \Lambda_{\omega\rho}(g_\omega^2\omega^2)(g_\rho^2\rho^2)\end{aligned} \tag{3.81}$$

Thus:

$$M = m + \mathcal{S} = \begin{pmatrix} m_p & \\ & m_n \end{pmatrix} - g_\sigma\sigma \begin{pmatrix} 1 & \\ & 1 \end{pmatrix} \tag{3.82}$$

and

$$\tilde{\mu} = \mu - \mathcal{V} = \begin{pmatrix} \mu_p & \\ & \mu_n \end{pmatrix} - g_\omega\omega \begin{pmatrix} 1 & \\ & 1 \end{pmatrix} - g_\rho\rho\frac{1}{2}\begin{pmatrix} 1 & \\ & -1 \end{pmatrix} \tag{3.83}$$

that is,

$$\begin{cases} M_p = m_p - g_\sigma \sigma \\ M_n = m_n - g_\sigma \sigma \end{cases} \tag{3.84}$$

and

$$\begin{cases} \tilde{\mu}_p = \mu_p - g_\omega \omega - \frac{1}{2} g_\rho \rho \\ \tilde{\mu}_n = \mu_n - g_\omega \omega + \frac{1}{2} g_\rho \rho \end{cases} \tag{3.85}$$

Once again, the grand canonical potential density is, following (2.80),

$$\Omega = -2T \operatorname{Tr} \int \frac{\mathrm{d}^3 \vec{p}}{(2\pi)^3} \left[\frac{\omega}{T} + \ln\left(1 + e^{-(\omega+\tilde{\mu})/T}\right) + \ln\left(1 + e^{-(\omega-\tilde{\mu})/T}\right) \right] - U + \Omega_0 \tag{3.86}$$

This time the trace corresponds to a sum over the neutron and proton states (over isospin states) since all matrices are diagonal over that index, yielding

$$\begin{aligned} \Omega = & -2T \sum_{i=p,n} \int \frac{\mathrm{d}^3 \vec{p}}{(2\pi)^3} \left[\frac{\omega_i}{T} + \ln\left(1 + e^{-(\omega_i+\tilde{\mu}_i)/T}\right) + \ln\left(1 + e^{-(\omega_i-\tilde{\mu}_i)/T}\right) \right] \\ & + \frac{1}{2} m_\sigma^2 \sigma^2 - \frac{1}{2} m_\omega^2 \omega^2 - \frac{1}{2} m_\rho^2 \rho^2 + \frac{1}{3} \kappa (g_\sigma \sigma)^3 + \frac{1}{4} \lambda (g_\sigma \sigma)^4 \\ & - \frac{1}{4!} \xi g_\omega^4 \omega^4 - \Lambda_{\omega\rho} (g_\omega^2 \omega^2)(g_\rho^2 \rho^2) + \Omega_0 \end{aligned} \tag{3.87}$$

The proton and neutron densities, the pressure, the energy density and the entropy density can all be derived as we did for the NJL model, through the formulas (2.59)–(2.62). Again, the calculations are done in the appendices (page 91). The results are

$$\begin{aligned} E = & 2 \sum_{i=p,n} \int \frac{\mathrm{d}^3 \vec{p}}{(2\pi)^3} \left[\omega_i (\bar{\ell}_i + \ell_i - 1) \right] + g_\omega \omega (n_p + n_n) + \frac{1}{2} g_\rho \rho (n_p - n_n) \\ & + \frac{1}{2} m_\sigma^2 \sigma^2 - \frac{1}{2} m_\omega^2 \omega^2 - \frac{1}{2} m_\rho^2 \rho^2 + \frac{1}{3} \kappa (g_\sigma \sigma)^3 + \frac{1}{4} \lambda (g_\sigma \sigma)^4 \\ & - \frac{1}{4!} \xi g_\omega^4 \omega^4 - \Lambda_{\omega\rho} (g_\omega^2 \omega^2)(g_\rho^2 \rho^2) + \Omega_0 \end{aligned} \tag{3.88}$$

$$\begin{aligned} P = & 2 \sum_{i=p,n} \int \frac{\mathrm{d}^3 \vec{p}}{(2\pi)^3} \left[\omega_i + T \ln\left(1 + e^{-(\omega_i+\tilde{\mu}_i)/T}\right) + T \ln\left(1 + e^{-(\omega_i-\tilde{\mu}_i)/T}\right) \right] \\ & - \frac{1}{2} m_\sigma^2 \sigma^2 + \frac{1}{2} m_\omega^2 \omega^2 + \frac{1}{2} m_\rho^2 \rho^2 - \frac{1}{3} \kappa (g_\sigma \sigma)^3 - \frac{1}{4} \lambda (g_\sigma \sigma)^4 \\ & + \frac{1}{4!} \xi g_\omega^4 \omega^4 + \Lambda_{\omega\rho} (g_\omega^2 \omega^2)(g_\rho^2 \rho^2) - \Omega_0 \end{aligned} \tag{3.89}$$

$$\begin{aligned} S = & \frac{2}{T} \sum_{i=p,n} \int \frac{\mathrm{d}^3 \vec{p}}{(2\pi)^3} \Big[\omega_i (\bar{\ell}_i + \ell_i) + \tilde{\mu}_i (\bar{\ell}_i - \ell_i) \\ & + T \ln\left(1 + e^{-(\omega_i+\tilde{\mu}_i)/T}\right) + T \ln\left(1 + e^{-(\omega_i-\tilde{\mu}_i)/T}\right) \Big] \end{aligned} \tag{3.90}$$

$$n_i = 2 \int \frac{\mathrm{d}^3 \vec{p}}{(2\pi)^3} \left(\ell_i - \bar{\ell}_i \right), \quad i = p, n \tag{3.91}$$

Minimizing the grand canonical potential with respect to the auxiliary fields, analogously to how we did with the NJL model (again, see appendix A.7), we obtain the following three equations:

$$2g_\sigma \sum_{i=p,n} \int \frac{\mathrm{d}^3\vec{p}}{(2\pi)^3} \frac{M}{\omega_i} \Big[\rho_i + \bar{\rho}_i - 1 \Big] = m_\sigma^2 \sigma + \kappa g_\sigma^3 \sigma^2 + \lambda g_\sigma^4 \sigma^3 \tag{3.92}$$

$$2g_\omega \sum_{i=p,n} \int \frac{\mathrm{d}^3\vec{p}}{(2\pi)^3} \Big[\rho_i - \bar{\rho}_i \Big] = m_\omega^2 \omega + \frac{1}{3!} \xi g_\omega^4 \omega^3 + 2\Lambda_{\omega\rho} (g_\omega^2 \omega)(g_\rho^2 \rho^2) \tag{3.93}$$

$$g_\rho \int \frac{\mathrm{d}^3\vec{p}}{(2\pi)^3} \Big[(\rho_p - \bar{\rho}_p) - (\rho_n - \bar{\rho}_n) \Big] = m_\rho^2 \rho + 2\Lambda_{\omega\rho} (g_\omega^2 \omega^2)(g_\rho^2 \rho) \tag{3.94}$$

3.2.2 "No sea" approximation

The presence of the term ω_i in the integral in the expression for the grand canonical potential density, corresponding to the infinite Dirac sea, causes the integral to be divergent. For example in the expression for the energy we can see we have a sum over the energy of particles and antiparticles, and over an infinite number of negative-energy states. Whereas this was not a problem in our treatment of the NJL model, since we imposed an UV cutoff, here we will need to account for the Dirac sea in our calculations. Simply discarding that term is called the "no sea approximation" [31]. The rationale is that the parameters in our model can be tuned to suitably account for this approximation. Doing this (and also simplifying some terms) we have:

$$\begin{aligned} E = {} & 2 \sum_{i=p,n} \int \frac{\mathrm{d}^3\vec{p}}{(2\pi)^3} \omega_i (\rho_i + \bar{\rho}_i) \\ & + \frac{1}{2} m_\sigma^2 \sigma^2 + \frac{1}{2} m_\omega^2 \omega^2 + \frac{1}{2} m_\rho^2 \rho^2 + \frac{1}{3} \kappa (g_\sigma \sigma)^3 + \frac{1}{4} \lambda (g_\sigma \sigma)^4 \\ & + \frac{1}{8} \xi g_\omega^4 \omega^4 + 3\Lambda_{\omega\rho} (g_\omega^2 \omega^2)(g_\rho^2 \rho^2) - \Omega_0 \end{aligned} \tag{3.95}$$

$$\begin{aligned} P = {} & 2 \sum_{i=p,n} \int \frac{\mathrm{d}^3\vec{p}}{(2\pi)^3} \Big[T \ln\Big(1 + e^{-(\omega_i + \tilde{\mu}_i)/T}\Big) + T \ln\Big(1 + e^{-(\omega_i - \tilde{\mu}_i)/T}\Big) \Big] \\ & - \frac{1}{2} m_\sigma^2 \sigma^2 + \frac{1}{2} m_\omega^2 \omega^2 + \frac{1}{2} m_\rho^2 \rho^2 - \frac{1}{3} \kappa (g_\sigma \sigma)^3 - \frac{1}{4} \lambda (g_\sigma \sigma)^4 \\ & + \frac{1}{4!} \xi g_\omega^4 \omega^4 + \Lambda_{\omega\rho} (g_\omega^2 \omega^2)(g_\rho^2 \rho^2) + \Omega_0 \end{aligned} \tag{3.96}$$

$$\begin{aligned} S = {} & \frac{2}{T} \sum_{i=p,n} \int \frac{\mathrm{d}^3\vec{p}}{(2\pi)^3} \Big[\omega_i (\bar{\rho}_i + \rho_i) + \tilde{\mu}_i (\bar{\rho}_i - \rho_i) \\ & + T \ln\Big(1 + e^{-(\omega_i + \tilde{\mu}_i)/T}\Big) + T \ln\Big(1 + e^{-(\omega_i - \tilde{\mu}_i)/T}\Big) \Big] \end{aligned} \tag{3.97}$$

$$n_i = 2 \int \frac{\mathrm{d}^3\vec{p}}{(2\pi)^3} (\rho_i - \bar{\rho}_i), \quad i = p, n \tag{3.98}$$

$$2g_\sigma \sum_{i=p,n} \int \frac{\mathrm{d}^3\vec{p}}{(2\pi)^3} \frac{M_i}{\omega_i} [\ell_i + \bar{\ell}_i] = m_\sigma^2 \sigma + \kappa g_\sigma^3 \sigma^2 + \lambda g_\sigma^4 \sigma^3 \tag{3.99}$$

$$g_\omega (n_p + n_n) = m_\omega^2 \omega + \frac{1}{3!} \xi g_\omega^4 \omega^3 + 2\Lambda_{\omega\rho} (g_\omega^2 \omega)(g_\rho^2 \rho^2) \tag{3.100}$$

$$\frac{1}{2} g_\rho (n_p - n_n) = m_\rho^2 \rho + 2\Lambda_{\omega\rho} (g_\omega^2 \omega^2)(g_\rho^2 \rho) \tag{3.101}$$

There are other approaches to accounting for the contribution of the Dirac sea [33], but we will not explore them in this work.

3.2.3 Leptonic contribution

For purposes of charge conservation we again add a leptonic contribution, same as we did to the NJL model, with equal results. Refer to section 3.1.5.

3.2.4 Charge neutrality and chemical equilibrium

Again, we must impose that the matter be charge neutral. In this model this means

$$\begin{aligned} \sum q_i n_i &= q_p n_p + q_n n_n + q_e n_e + q_\mu n_\mu \\ &= n_p - n_e - n_\mu = 0 \end{aligned} \tag{3.102}$$

Similarly to what we had with the NJL model, we also need to enforce charge neutrality and beta equilibrium in this model. Detailed balance with respect to beta decay means

$$n \rightleftharpoons p + e^- + \overline{\nu_e} \Rightarrow \mu_n = \mu_p + \mu_e - \mu_{\nu_e} \tag{3.103}$$

Once again disregarding neutrinos we obtain

$$\mu_n = \mu_p + \mu_e \tag{3.104}$$

while detailed balance with respect to muon decay means the electron and muon chemical potentials are equal:

$$\mu_e = \mu_\mu \tag{3.105}$$

Of course, these relations also follow from writing the chemical potential of each particle in terms of the chemical potentials of conserved charges (see (3.56)), so we have:

$$\begin{cases} \mu_p = \mu_b + \mu_q \\ \mu_n = \mu_b \\ \mu_e = -\mu_q \\ \mu_\mu = -\mu_q \end{cases} \Rightarrow \begin{cases} \mu_n = \mu_p + \mu_e \\ \mu_e = \mu_\mu \end{cases} \tag{3.106}$$

3.3 Two-phase construction

We have now developed two models of neutron star matter: the NJL model, for deconfined quark matter, and the NL3$\omega\rho$ model, for confined hadronic matter. The question remains of how to combine these to build a single model of stellar matter.

In this work we consider that neutron star matter can exist in two phases: a confined phase and a deconfined phase, with properties given by the NJL model and by the NL3$\omega\rho$ model, respectively. We expect that at low baryonic densities matter exists in the confined state, as hadrons, and that at high densities it exists in the deconfined state. At some region in between there will be a phase transition.

At the phase transition, both phases coexist in a *mixed phase*, in chemical, thermal, and mechanical equilibrium:

$$\mu_{bQ} = \mu_{bH} \tag{3.107}$$
$$\mu_{qQ} = \mu_{qH} \tag{3.108}$$
$$T_Q = T_H \tag{3.109}$$
$$P_Q = P_H \tag{3.110}$$

with subscript Q denoting quantities in the quark phase and H in the hadronic phase, where μ_b and μ_q are the baryonic chemical potential and the electric charge chemical potential, respectively. Since all chemical potentials in the system can be written as a linear combination of only those two independent chemical potentials, the two conditions (3.107) and (3.108) suffice to impose chemical equilibrium.

For a single component substance (such as water and its familiar liquid–vapour transition), the phase transition takes place at constant pressure [34]. However in these models we work with a two-component substance, which means that the phase transition won't happen at constant pressure and constant fraction. Instead we will have an interval where both phases coexist, the mixed/hybrid region, with the volume fraction

$$\chi \equiv \frac{V_Q}{V_Q + V_H} \tag{3.111}$$

varying smoothly from 0 to 1 in this interval.

3.3.1 Thermodynamics

In the two-phase system in the mixed phase, the energy density, pressure, and entropy density are given by

$$E = \chi E_Q + (1-\chi)E_H + E_l \tag{3.112}$$
$$P = P_Q + P_l = P_H + P_l \tag{3.113}$$
$$S = \chi S_Q + (1-\chi)S_H + S_l \tag{3.114}$$

These are sometimes called the Gibbs conditions of phase equilibrium.

Recall that even though there are several particles and several associated chemical potentials, there are only two conserved charges/independent chemical potentials hence only two independent components.

where subscripts Q and H denote the energy/pressure/entropy of the quark and hardonic phases, respectively, and subscript l denotes the leptonic contribution.

3.3.2 Charge neutrality and chemical equilibrium

When considering the separate models these are the conditions of charge neutrality:

$$Q: \quad \tfrac{2}{3}n_u - \tfrac{1}{3}n_d - \tfrac{1}{3}n_s - n_e - n_\mu = 0 \tag{3.115}$$

$$H: \quad n_p - n_e - n_\mu = 0 \tag{3.116}$$

However there is no reason that in the mixed phase both phases must be separately charge neutral, but only that they are *globally* charge neutral. The weaker condition of global charge neutrality is expressed

$$\begin{aligned} &\chi Q_Q + (1-\chi)Q_H + Q_l \\ &= \chi(\tfrac{2}{3}n_u - \tfrac{1}{3}n_d - \tfrac{1}{3}n_s) + (1-\chi)n_p - n_e - n_\mu = 0 \end{aligned}$$

where $Q_{Q/H/l}$ denotes the charge density of the quark/hadronic/lepton portion, respectively.

The total number of independent chemical potentials in the mixture is two: the baryonic and electrical chemical potentials. The chemical potential of each species is, in terms of those:

$$\begin{cases} \mu_u = \frac{1}{3}\mu_b + \frac{2}{3}\mu_q \\ \mu_d = \frac{1}{3}\mu_b - \frac{1}{3}\mu_q \\ \mu_s = \frac{1}{3}\mu_b - \frac{1}{3}\mu_q \\ \mu_p = \mu_b + \mu_q \\ \mu_n = \mu_b \\ \mu_e = -\mu_q \\ \mu_\mu = -\mu_q \end{cases} \tag{3.117}$$

which yields, for example, the following constraints:

$$\begin{cases} \mu_n = \mu_u + \mu_d + \mu_s \\ \mu_n = \mu_p + \mu_e \\ \mu_e = \mu_d - \mu_u \\ \mu_e = \mu_\mu \end{cases} \tag{3.118}$$

3.3.3 Equation of state

The two models predict different pressures for the same chemical potential. We can represent this as two surfaces in a $P(\mu_n, \mu_e)$ diagram (Figure 3.2). The intersection of these surfaces is the set of configurations where the two phases are in chemical and mechanical equilibrium (it is assumed both models are calculated at the same temperature). The mixed phase will belong to this intersection.

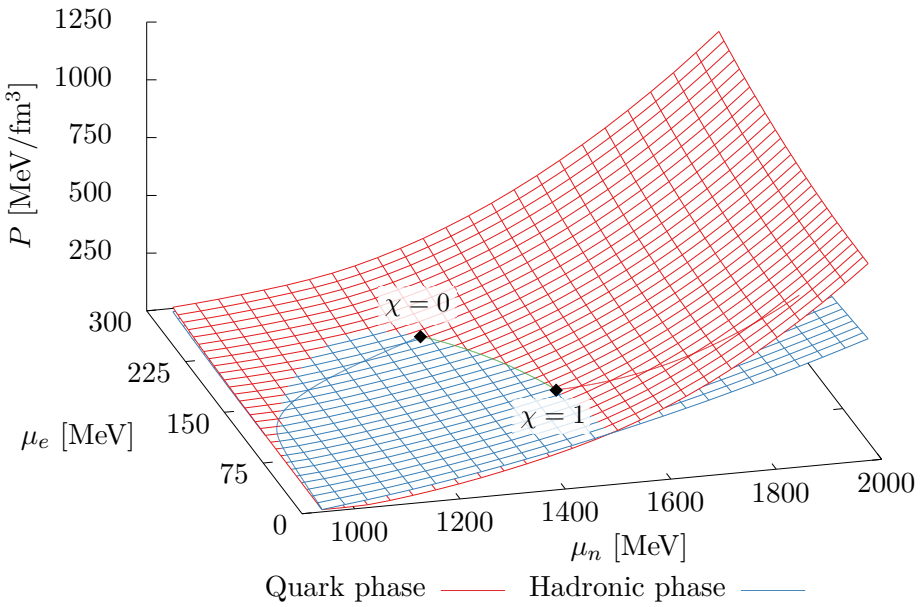

Figure 3.2: Pressure of the two phases as a function of chemical potentials.

At low densities, matter is purely hadronic. The equation of state lies in the surface for the hadronic phase. Charge neutrality constrains it to a curve along that surface (blue line on Figure 3.2). At some point it reaches the intersection of the two surfaces: this is the point where the mixed phase starts, with $\chi = 0$: now the constraint of charge neutrality of the hadronic phase is relaxed to the constraint of global charge neutrality (3.117). The equation of state continues along the intersection (green line) until such point as $\chi = 1$; then the system is in a pure quark phase, the restriction (3.109) ceases to make sense, and the constraint of global charge neutrality again reduces to the constraint of neutrality of the quark phase. The EoS continues along the red line. Schematically:

$$\text{Hadron} \quad \begin{cases} Q_H + Q_l = 0 \\ \chi = 0 \end{cases} \tag{3.119}$$

$$\Downarrow$$

$$\text{Mixed} \quad \begin{cases} \chi Q_Q + (1-\chi) Q_H + Q_l = 0 \\ P_Q = P_H \end{cases} \tag{3.120}$$

$$\Downarrow$$

$$\text{Quark} \quad \begin{cases} Q_Q + Q_l = 0 \\ \chi = 1 \end{cases} \tag{3.121}$$

3.4 Zero temperature limit

As mentioned in page 4, after only minutes from its formation a star cools down to temperatures way below the MeVs, insignificant on a nuclear scale [1]. Since this happens so quickly after formation, most observations will be of stars in this regime. As such, in our calculations, it is useful to take the $T = 0$ limit of the expressions derived in this chapter, for even though we could run set T to a typical temperature, such as 10^{-4} MeV, this would bring problems at a numerical level for no benefit at all. It is much more efficient to take the algebraic limit of these expressions when $T \to 0$, and work with those instead.

In the $T = 0$ limit the Fermi distributions become

$$\lim_{T\to 0} \not{f}(E,\mu,T) = H(\mu - E) \tag{3.122}$$

$$\lim_{T\to 0} \bar{\not{f}}(E,\mu,T) = 0 \tag{3.123}$$

where $H(x)$ is the Heaviside step function, defined in appendix B.5:

$$H(x) = \begin{cases} 1 & \text{if} \quad x \geq 0 \\ 0 & \text{if} \quad x < 0 \end{cases} \tag{3.124}$$

Writing the expressions for the thermodynamic properties in this limit is therefore a matter of removing the antiparticle distributions and substituting the particle Fermi distributions with a step function.

3.4.1 Nambu–Jona-Lasinio model

Taking this limit on expressions (3.42)–(3.47) we have

$$\begin{aligned} E = 6 \sum_{f=u,d,s} \int \frac{\mathrm{d}^3\vec{p}}{(2\pi)^3} \omega_f [H(\tilde{\mu}_f - \omega_f) - 1] \\ + 2G_S({\sigma_u}^2 + {\sigma_d}^2 + {\sigma_s}^2) + 2G_V({n_u}^2 + {n_d}^2 + {n_s}^2) - 4G_D\sigma_u\sigma_d\sigma_s + \Omega_0 \end{aligned} \tag{3.125}$$

$$\begin{aligned} P = 6 \sum_{f=u,d,s} \int \frac{\mathrm{d}^3\vec{p}}{(2\pi)^3} [\omega_f - (\omega_f - \tilde{\mu}_f) H(\tilde{\mu}_f - \omega_f)] \\ - 2G_S({\sigma_u}^2 + {\sigma_d}^2 + {\sigma_s}^2) + 2G_V({n_u}^2 + {n_d}^2 + {n_s}^2) + 4G_D\sigma_u\sigma_d\sigma_s - \Omega_0 \end{aligned} \tag{3.126}$$

$$S = 0 \tag{3.127}$$

$$n_i = 6 \int \frac{\mathrm{d}^3\vec{p}}{(2\pi)^3} H(\tilde{\mu}_i - \omega_i) \tag{3.128}$$

$$\sigma_i = 6 \int \frac{\mathrm{d}^3\vec{p}}{(2\pi)^3} \frac{M_i}{\omega_i} [H(\tilde{\mu}_i - \omega_i) - 1] \tag{3.129}$$

where the entropy is of course zero at absolute zero by the third law of thermodynamics.

Assuming the integration is spherically symmetric in momentum space, these expressions can be further developed by replacing the integration over $\mathrm{d}^3\vec{p}$ with $4\pi p^2\,\mathrm{d}p$, that is,

$$\frac{\mathrm{d}^3\vec{p}}{(2\pi)^3} = \frac{4\pi p^2\,\mathrm{d}p}{(2\pi)^3} = \frac{1}{2\pi^2}p^2\,\mathrm{d}p\,, \quad (p \equiv |\vec{p}|) \tag{3.130}$$

Let us also define the Fermi momentum p_F to be such that $\tilde{\mu} = \sqrt{p_F^2 + M^2} \Leftrightarrow p_F = \sqrt{\tilde{\mu}^2 - M^2}$. We then have that $H(\tilde{\mu} - \omega) = H(p_F - p)$.

We have:

$$\begin{aligned} E = \sum_{f=u,d,s} \frac{3}{\pi^2} \int \omega_f [H(p_{Ff} - p) - 1] p^2\,\mathrm{d}p + 2G_S({\sigma_u}^2 + {\sigma_d}^2 + {\sigma_s}^2) \\ + 2G_V({n_u}^2 + {n_d}^2 + {n_s}^2) - 4G_D\sigma_u\sigma_d\sigma_s + \Omega_0 \end{aligned} \tag{3.132}$$

$$n_i = \frac{3}{\pi^2} \int H(p_{Fi} - p) p^2\,\mathrm{d}p \tag{3.133}$$

$$\sigma_i = \frac{3}{\pi^2} \int \frac{M_i}{\omega_i} [H(p_{Fi} - p) - 1] p^2\,\mathrm{d}p \tag{3.134}$$

Recalling also that by our regularization procedure we cut off the integrals on $|\vec{p}| = \Lambda$, and that $p_{Ff} \ll \Lambda$,

$$\begin{aligned} E = -\frac{3}{\pi^2} \sum_{f=u,d,s} \int_{p_{Ff}}^{\Lambda} \sqrt{p^2 + M_f^2}\, p^2\,\mathrm{d}p + 2G_S({\sigma_u}^2 + {\sigma_d}^2 + {\sigma_s}^2) \\ + 2G_V({n_u}^2 + {n_d}^2 + {n_s}^2) - 4G_D\sigma_u\sigma_d\sigma_s + \Omega_0 \end{aligned} \tag{3.135}$$

$$n_i = \frac{3}{\pi^2} \int_0^{p_{Fi}} p^2\,\mathrm{d}p \tag{3.136}$$

$$\sigma_i = -\frac{3}{\pi^2} \int_{p_{Fi}}^{\Lambda} \frac{M_i}{\sqrt{p^2 + M_i^2}} p^2\,\mathrm{d}p \tag{3.137}$$

Notice we haven't calculated the limit for the pressure, nor do we have to. Instead of going through the trouble it's easier (and computationally more efficient) to use the following thermodynamic consistency relation (see (2.62)):

$$P = -E + \mathcal{T}\mathcal{S}^{0} + \sum_f \mu_f n_f \tag{3.138}$$

So we can calculate E, n_f, and σ_i by expressions (3.135)–(3.137), and then knowing those we calculate the pressure by the expression above.

p_F is a positive definite quantity, so more precisely,

$$p_F = \begin{cases} \sqrt{\tilde{\mu}^2 - M^2} & \text{if} \quad \tilde{\mu}^2 \geq M^2 \\ 0 & \text{if} \quad \tilde{\mu}^2 < M^2 \end{cases} \tag{3.131}$$

These integrals have closed-form solutions, included for reference in appendix A.9. Using these we finally have:

$$\begin{aligned} E = -\frac{3}{8\pi^2}\sum_{f=u,d,s}\Bigg[&\Lambda\sqrt{\Lambda^2+M_f^2}(2\Lambda^2+M_f^2) - p_{Ff}\tilde{\mu}_f(2p_{Ff}^2+M_f^2) \\ &- M_f^4\ln\left(\frac{\Lambda+\sqrt{\Lambda^2+M_f^2}}{p_{Ff}+\tilde{\mu}_f}\right)\Bigg] + 2G_S({\sigma_u}^2+{\sigma_d}^2+{\sigma_s}^2) \\ &+ 2G_V({n_u}^2+{n_d}^2+{n_s}^2) - 4G_D\sigma_u\sigma_d\sigma_s + \Omega_0 \end{aligned} \tag{3.139}$$

$$P = -E + \sum_{f=u,d,s}\mu_f n_f \tag{3.140}$$

$$n_i = \frac{p_{Fi}^3}{\pi^2} \tag{3.141}$$

$$\sigma_i = -\frac{3}{2\pi^2}M_i\left[\Lambda\sqrt{\Lambda^2+M_i^2} - M_i^2\ln\left(\frac{\Lambda+\sqrt{\Lambda^2+M_i^2}}{p_{Fi}+\tilde{\mu}_i}\right) - p_{Fi}\tilde{\mu}_i\right] \tag{3.142}$$

Applicability of the model

In the $T = 0$ limit, the domain of applicability of the model is when the Fermi momenta are below the cutoff:

$$p_{Fi} < \Lambda, \quad i = u, d, s \tag{3.143}$$

3.4.2 NL3$\omega\rho$ model

Applying the same procedure for expressions (3.95)–(3.98) and (3.99)–(3.101), we obtain the following zero temperature limits:

$$\begin{aligned} E = 2\sum_{i=p,n}\int\frac{\mathrm{d}^3\vec{p}}{(2\pi)^3}\omega_i H(\tilde{\mu}_i-\omega_i) \\ + \frac{1}{2}m_\sigma^2\sigma^2 + \frac{1}{2}m_\omega^2\omega^2 + \frac{1}{2}m_\rho^2\rho^2 + \frac{1}{3}\kappa(g_\sigma\sigma)^3 + \frac{1}{4}\lambda(g_\sigma\sigma)^4 \\ + \frac{1}{8}\xi g_\omega^4\omega^4 + 3\Lambda_{\omega\rho}(g_\omega^2\omega^2)(g_\rho^2\rho^2) + \Omega_0 \end{aligned} \tag{3.144}$$

$$n_i = 2\int\frac{\mathrm{d}^3\vec{p}}{(2\pi)^3}H(\tilde{\mu}_i-\omega_i) \tag{3.145}$$

and

$$2g_\sigma\sum_{i=p,n}\int\frac{\mathrm{d}^3\vec{p}}{(2\pi)^3}\frac{M_i}{\omega_i}H(\tilde{\mu}_i-\omega_i) = m_\sigma^2\sigma + \kappa g_\sigma^3\sigma^2 + \lambda g_\sigma^4\sigma^3 \tag{3.146}$$

$$g_\omega(n_p+n_n) = m_\omega^2\omega + \frac{1}{3!}\xi g_\omega^4\omega^3 + 2\Lambda_{\omega\rho}(g_\omega^2\omega)(g_\rho^2\rho^2) \tag{3.147}$$

$$\frac{1}{2}g_\rho(n_p - n_n) = m_\rho^2\rho + 2\Lambda_{\omega\rho}(g_\omega^2\omega^2)(g_\rho^2\rho) \tag{3.148}$$

Once again making the integration over $\frac{p^2\mathrm{d}p}{2\pi^2}$ instead of $\frac{\mathrm{d}^3\vec{p}}{(2\pi)^3}$ we have

$$\begin{aligned} E = &\sum_{i=p,n}\frac{1}{\pi^2}\int \omega_i H(\tilde{\mu}_i - \omega_i)p^2\,\mathrm{d}p \\ &+ \frac{1}{2}m_\sigma^2\sigma^2 + \frac{1}{2}m_\omega^2\omega^2 + \frac{1}{2}m_\rho^2\rho^2 + \frac{1}{3}\kappa(g_\sigma\sigma)^3 + \frac{1}{4}\lambda(g_\sigma\sigma)^4 \\ &+ \frac{1}{8}\xi g_\omega^4\omega^4 + 3\Lambda_{\omega\rho}(g_\omega^2\omega^2)(g_\rho^2\rho^2) + \Omega_0 \end{aligned} \tag{3.149}$$

$$n_i = \frac{1}{\pi^2}\int H(\tilde{\mu}_i - \omega_i)p^2\,\mathrm{d}p \tag{3.150}$$

that is

$$\begin{aligned} E = &\sum_{i=p,n}\frac{1}{\pi^2}\int_0^{p_{Fi}} \omega_i p^2\,\mathrm{d}p \\ &+ \frac{1}{2}m_\sigma^2\sigma^2 + \frac{1}{2}m_\omega^2\omega^2 + \frac{1}{2}m_\rho^2\rho^2 + \frac{1}{3}\kappa(g_\sigma\sigma)^3 + \frac{1}{4}\lambda(g_\sigma\sigma)^4 \\ &+ \frac{1}{8}\xi g_\omega^4\omega^4 + 3\Lambda_{\omega\rho}(g_\omega^2\omega^2)(g_\rho^2\rho^2) + \Omega_0 \end{aligned} \tag{3.151}$$

$$n_i = \frac{1}{\pi^2}\int_0^{p_{Fi}} p^2\,\mathrm{d}p \tag{3.152}$$

again, with the aid of the closed form integrals in appendix A.9, we have

$$\begin{aligned} E = &\frac{1}{8\pi^2}\sum_{i=p,n}\left[p_{Fi}\tilde{\mu}_i(2p_{Fi}^2 + M_i^2) - {M_i}^4\ln\left(\frac{p_{Fi}+\tilde{\mu}_i}{M_i}\right)\right] \\ &+ \frac{1}{2}m_\sigma^2\sigma^2 + \frac{1}{2}m_\omega^2\omega^2 + \frac{1}{2}m_\rho^2\rho^2 + \frac{1}{3}\kappa(g_\sigma\sigma)^3 + \frac{1}{4}\lambda(g_\sigma\sigma)^4 \\ &+ \frac{1}{8}\xi g_\omega^4\omega^4 + 3\Lambda_{\omega\rho}(g_\omega^2\omega^2)(g_\rho^2\rho^2) + \Omega_0 \end{aligned} \tag{3.153}$$

$$P = -E + \sum_{i=p,n}\mu_i n_i \tag{3.154}$$

$$n_i = \frac{p_{Fi}^3}{3\pi^2} \tag{3.155}$$

while the three equations (3.146), (3.147), and (3.148) become

$$g_\sigma\frac{1}{2\pi^2}\sum_{i=p,n}M_i\left[p_{Fi}\tilde{\mu}_i - M_i^2\ln\left(\frac{p_{Fi}+\tilde{\mu}_i}{M_i}\right)\right] = m_\sigma^2\sigma + \kappa g_\sigma^3\sigma^2 + \lambda g_\sigma^4\sigma^3 \tag{3.156}$$

$$g_\omega(n_p + n_n) = m_\omega^2\omega + \frac{1}{3!}\xi g_\omega^4\omega^3 + 2\Lambda_{\omega\rho}(g_\omega^2\omega)(g_\rho^2\rho^2) \tag{3.157}$$

$$\frac{1}{2}g_\rho(n_p - n_n) = m_\rho^2\rho + 2\Lambda_{\omega\rho}(g_\omega^2\omega^2)(g_\rho^2\rho) \tag{3.158}$$

3.4.3 Leptons

For the leptonic contribution the procedure is entirely analogous, and we have

$$E = \frac{1}{8\pi^2} \sum_{\ell=e,\mu} \left[p_{F\ell}\mu_\ell(2p_{F\ell}^2 + m_\ell^2) - {m_\ell}^4 \ln\left(\frac{p_{F\ell} + \mu_\ell}{m_\ell}\right)\right] \tag{3.159}$$

$$P = -E + \sum_{\ell=e,\mu} \mu_\ell n_\ell \tag{3.160}$$

$$n_i = \frac{p_{Fi}^3}{3\pi^2} \tag{3.161}$$

Chapter 4

Results

4.1 Parameterization

The models we studied depend on several parameters. These can be determined by fitting to known experimental, observational and theoretical data.

4.1.1 Nambu–Jona-Lasinio model

The NJL model has 7 parameters: the three bare quark masses, three coupling parameters, G_S, G_V, and G_D, and the momentum cutoff Λ. The parameters of the NJL model must reproduce known physical vacuum observables (such as meson masses and decay times). In this work, however, since we are studying a two-phase model, it is more important that the NJL model is compatible with the NL3$\omega\rho$ model, namely that the vacuum baryonic chemical potential in the NJL model matches the value in the NL3$\omega\rho$ model [35]. This implies that the parameters of the NJL model must reproduce a vacuum effective mass for up and down quarks compatible with the nucleon mass of the NL3$\omega\rho$ model.

Table 4.1: Nucleon masses [22].

Particle	Mass [MeV]
Proton (p)	938.272 081 3(58)
Neutron (n)	939.565 413 3(58)

The masses of the proton and neutron (Table 4.1) are almost equal, so we can take $m_{\text{nucleon}} \approx \frac{m_p+m_n}{2} = 938.9\,\text{MeV}$ (the nucleon mass used in the NL3$\omega\rho$ model). Since $p = (uud)$ and $n = (udd)$, we must have approximately $M_u \approx M_d \approx \frac{1}{3}m_{\text{nucleon}} \approx 313\,\text{MeV}$.

In this work we use the following parameter set (Table 4.2), which sacrifices some precision with regard to the vacuum meson masses and decay times in order to reproduce an effective nucleon mass compatible with the NL3$\omega\rho$ model (i.e. the same baryonic chemical potential):

Table 4.2: NJL model parameter set [35].

Λ [MeV]	m_u [MeV]	m_d [MeV]	m_s [MeV]	G_S [MeV^{-2}]	G_V [MeV^{-2}]	G_D [MeV^{-5}]
630.0	5.5	5.5	135.7	$1.781/\Lambda^2$	———	$9.29/\Lambda^5$

These predict the following vacuum constituent masses: $M_u = M_d = 311.955\,\text{MeV}$, $M_s = 508.123\,\text{MeV}$, close to the desired value of 313 MeV for the mass of u and d.

We can calculate the meson masses and decay constants and compare them with experimental data (Table 4.3).

Table 4.3: Meson masses and decay constants, from the NJL model [35] and from experiment [22].

	m_π [MeV]	f_π [MeV]	m_K [MeV]	f_K [MeV]	m_η [MeV]	$m_{\eta'}$ [MeV]
Model	138.5	90.7	493.5	96.3	478.2	953.7
Experimental	139.570 61(24)	92.1(12)	493.677(16)	110.0(3)	547.862(17)	957.78(6)

As discussed this parametrization yields worse values for some vacuum observables.

Note, however, that in this work G_V corresponds to a coupling with density, so we could not fix its value by fitting to values of observables in the vacuum, as we did for the other parameters (indeed the question of the value of G_V at finite density remains open; not even its sign is known with certainty [36]). Therefore in this work we chose to do our calculations with several different values of G_V and examine how this affects the properties of matter and the resulting neutron stars.

We will experiment with values of G_V in the order of magnitude of G_S. We will also try setting $G_V = 0$ to compare the results with the case of absent vector coupling. We will consider positive and negative values of G_V. A positive coupling means the energy increases with density, corresponding to a repulsive interaction, and vice versa, with a negative coupling corresponding to an attractive interaction.

4.1.2 NL3$\omega\rho$ model

The NL3$\omega\rho$ model described in section 3.2 has 11 parameters: the bare nucleon mass m, the meson masses, m_σ, m_ω, m_ρ, the scalar, vector, and isovector coupling constants g_σ, g_ω and g_ρ respectively, and four more coupling constants for the nonlinear interactions: κ, λ, ξ and $\Lambda_{\omega\rho}$.

We have several experimental quantities in nuclear physics that we want our model to reproduce, namely the saturation density, the binding energy per nucleon, and the incompressibility coefficient, for symmetric nuclear matter, and also the value and slope of the symmetry energy at the saturation density.

In this work we use the NL3$\omega\rho$ parametrization with symmetry energy slope $L = 55$.

Matter with an equal density of protons and neutrons.

The value of the symmetry energy slope isn't well fixed by experiment; acceptable values are roughly in the interval $30 < L < 120$ [17]. A value of $L = 55$ is targeted in this work.

Table 4.4: NL3$\omega\rho$ model parameter set [32,37].

m [MeV]	m_σ [MeV]	m_ω [MeV]	m_ρ [MeV]	g_σ	g_ω	g_ρ
938.918 747 3	508.194	782.501	763.0	10.2170	12.8680	11.2766

κ [MeV^{-1}]	λ	ξ	$\Lambda_{\omega\rho}$
1.930	-0.003	0	0.030

The model with this parameter set predicts the following nuclear properties at saturation density: the density n_0, the binding energy per nucleon B/A, the compression modulus K, the symmetry energy S_0, and the symmetry energy slope L.

Table 4.5: NL3$\omega\rho$ model nuclear properties [15].

n_0 [fm^{-3}]	B/A [MeV]	K [MeV]	S_0 [MeV]	L [MeV]
0.148	-16.30	272.0	31.7	55.2

4.1.3 Leptons

The model of a free gas of leptons depends of course only on the masses of the particles. They are known with a great deal of precision from experiment:

Table 4.6: Lepton masses [22].

Particle	Mass [MeV]
Electron (e^-)	0.510 998 946 1(31)
Muon (μ^-)	105.658 374 5(24)

4.2 Numerical algorithms

In order to solve the models, we have to solve a self-consistent system of equations for the effective masses and the effective chemical potentials, which in general depend on the fields and the densities, and the equations of motion for the auxiliary fields as well as the expressions for the densities, which in turn depend on the effective masses and chemical potentials. Together with these, we must also include the constraints of charge neutrality and beta equilibrium.

These systems are highly non-linear. In order to solve them numerically we opted to use a globally convergent variant Newton's method with a numerical Jacobian [38,39] . This is an iterative method that starts from an initial guess and uses the derivative of the function at that point (in the case of systems of equations, the Jacobian) to compute

a better approximation to the root of the function. Given a system of equations of the sort $\vec{f}(\vec{x}) = \vec{0}$, starting from a guess $\vec{x} = \vec{x}_0$, we iterate:

$$\vec{x}_{n+1} = \vec{x}_n - \mathbf{J}^{-1}(\vec{x}_n)\,\vec{f}(\vec{x}_n) \tag{4.1}$$

where $\mathbf{J}$ is the Jacobian of the system (it is calculated numerically due to the lack of analytic expressions for the derivatives).

This method is sensitive to the initial guess; arguably its biggest strength is that it converges quadratically when it satisfies a set of conditions that include being "sufficiently close" to the root. However, if the guess is not close to the true value, or if the function is not well behaved in the neighbourhood of the root, the method may converge slower than quadratically, or if a stationary point or cycle is encountered it may not converge at all. Since in this context we have physical values and intuition to guide us towards reasonable guesses, this was never a problem we couldn't overcome "by hand" during the course of this work; nevertheless the option remained to use a slower and more robust method first, to approach the root, switching to Newton's method when the value was close enough.

The "globally convergent" variant is a strategy that ensures that even if we are outside the neighbourhood of the root we can still make *some* progress in each iteration. This approach combines the rapid local convergence of the plain Newton's method with a more robust strategy that ensures eventual convergence from almost all starting points.

In the case when we are solving a system several times while varying a parameter in small steps along an interval, something we do often in this work, we can use the result from the preceding step of the parameter as the new guess for the current step, provided (i) the step size in the parameter is small and (ii) the change in the functions when varying that parameter is not discontinuous or very large in that interval.

For integration, we opted to use a Gaussian quadrature with a default of 128 points, further subdividing the interval, applying the algorithm for each subinterval, and summing, whenever the interval was too large, or falling back to a smaller number of quadrature points when the interval was very small, for performance. When performing integrals from 0 to ∞, we use the same method with the following substitution:

$$\int_0^{+\infty} f(x)\,\mathrm{d}x = \int_0^{\frac{\pi}{2}} f(\tan u)\frac{\mathrm{d}u}{\cos^2 u} = 2\int_0^{\frac{\pi}{2}} \frac{f(\tan u)}{\cos(2u) - 1}\,\mathrm{d}u \tag{4.2}$$

A particular difficulty arose when performing integrals at very low temperatures. Since the Fermi distributions approach a step function as the temperature approaches zero, the integration algorithm could give very inaccurate results in the region where near $E \approx \mu$ (where the "drop" happens), while wasting time in the other regions, where the distribution is nearly constant. The problem was solved with an adaptive-style scheme: the lower the temperature, the more points would be taken near $E = \mu$, and less in the other regions. At any rate, when the temperature is very low, it is preferred to

This can be proven and "sufficiently close" can be made mathematically rigorous; see [39].

I.e. first derivative exists, is continuous, and is nonzero, and second derivative exists; also that the derivative is not too small and the second derivative not too large

use directly the limits derived for zero temperature, since we are incurring in a totally negligible error for the typical values of T in a neutron star post-formation.

Throughout the algorithms, whenever a sum with a large number of terms was to be performed, we took care to use the Kahan summation algorithm to minimize the error due to floating point rounding in the computer. When making a sum of a large number of terms we iterate through a sequence of terms and accumulate to a variable. Eventually the running sum grows very large compared to the next term to be summed, and when summing two floating point values of very different scales the lower order bits are lost (truncated or rounded), therefore the worst-case error grows with $\mathcal{O}(N)$, where N is the number of elements to be summed. The Kahan summation algorithm takes care of this problem by keeping a running compensation for the lost bits and adding it to the sum. This way the error is bounded by the floating point precision instead of growing with the number of terms.

In pseudocode:

```
fn kahan(terms):
    sum = 0.0
    err = 0.0
    for i in terms:
        y = i - err  # Subtract the accumulated error
        t = sum + y
        err = (t - sum) - y  # Should be 0 algebrically but
                             # isn't due to fp errors
        sum = t
    return sum
```

Be sure to mark `y` and `t` as `volatile` in C/C++ (or equivalent) else the compiler may optimize it away.

The programs were implemented in the C++ programming language and used the Eigen linear algebra library [40].

4.3 Equations of state

4.3.1 Results in the NJL model

The system to be solved for the NJL model contains 14 unknowns: 3 quark effective masses, 3 quark chemical potentials, 3 quark effective chemical potentials, 3 quark scalar densities, 2 lepton chemical potentials. It is determined by 13 equations: 3 expressions for the effective masses, 3 expressions for the effective chemical potential, 3 expressions for the scalar densities, 3 independent constraints on the chemical potentials, one constraint on the charge neutrality. In order for the system to be completely determined we must supply one additional constraint, for example, fixing the baryonic number density:

$$n_b = \frac{n_u + n_d + n_s}{3} \tag{4.3}$$

In order to obtain points for an equation of state, we proceed as follows: for a number of values of n_b in an interval, solve the system and output the corresponding energy

density and pressure. Repeating for several values of n_b, we obtain several points (E, P) of the equation of state.

We repeat this process with varying values of G_V, which enables us to see the effects this unfixed parameter has on the equation of state. Let $\alpha \equiv \frac{G_V}{G_S}$. Running this algorithm for $\alpha = -0.25, 0.00, 0.25, 0.50, 0.75$, for baryon densities in the interval $[0.01 : 1.60]\,\mathrm{fm}^{-3}$, we obtain the equations of state in Figure 4.1.

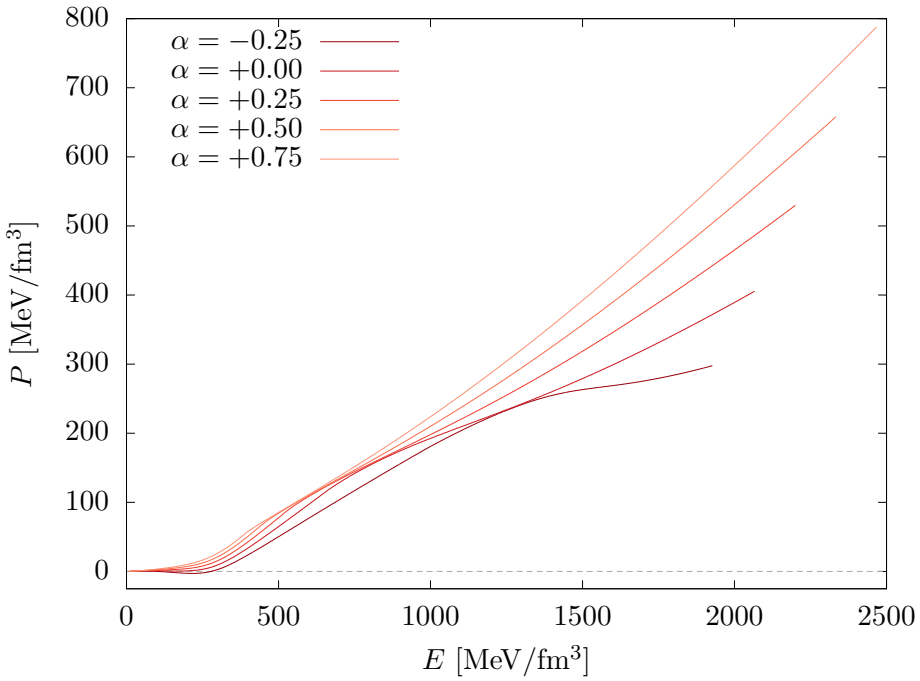

Figure 4.1: Equations of state obtained in the NJL model, for different values of G_V.

As expected, a higher value of G_V gives a stiffer equation of state. Furthermore, we can also observe that each EoS has a "bend" at some energy, and that this "bend" happens earlier for higher G_V. We can identify this phenomenon with the appearance of strange quarks. We can see this by plotting the slope of the EoS together with the density of strange quarks (Figure 4.2) and noting that the onset of strange quarks coincides with a dip in the slope of the EoS. Since they are much more massive than the u and d quarks they will not appear until a sufficiently high density, and since the vector coupling has the effect of shifting the the threshold for the appearance of strange quarks (Figure 4.4), this change will occur at lower energies as we increase G_V.

We can plot the relative densities of each species of particle, as a function of density (for example when $\alpha = 0.5$: Figure 4.3). In order to see how they vary with G_V, see Figure 4.4 (leptons omitted for simplicity).

We take care to verify that even at the highest density we were in the domain of applicability of the model, that is, $p_F < \Lambda$ for all flavours.

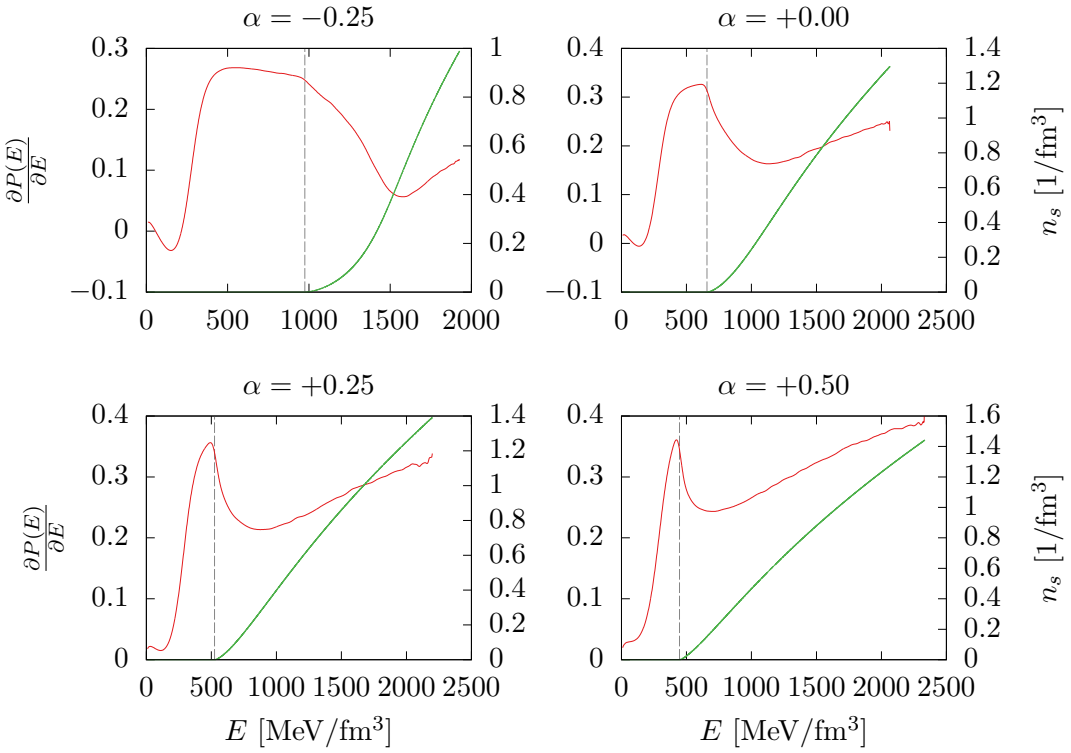

Figure 4.2: Slope of the NJL equation of state (red curve) superimposed with strange quark density (green curve), for different values of G_V.

The electron fraction never goes above 0.01%, and muons almost never appear; of the values of G_V considered, only with $G_V = 0.75\,G_S$ do muons appear at all, briefly after the onset of strangeness, and only in quantities never exceeding $10^{-3}n_b$. As such we have roughly $2n_u \approx n_d + n_s$ throughout the density range. Because of this and of beta equilibrium, the up quark density is nearly constant throughout the density range, at $Y_u \approx \frac{1}{3}$, while the onset of strangeness prompts an equal decrease in the down quark density.

The spontaneous chiral symmetry breaking and subsequent restoration at high densities is also a visible feature of the quark model; we can see the dynamical mass generation from the nonvanishing scalar densities at work by looking at the effective quark masses (Figure 4.3). In the vacuum they are several times larger than the bare masses ($\sigma_i \neq 0$), and as the density increases they tend to their bare value, indicating that the symmetry is restored, at least partially (fully restored in the light sector (u and d) and partially restored in the strange quark).

Finally we note that at lower densities the model predicts negative pressures (this can be seen in Figure 4.1). This indicates that the model breaks down at very low densities. This is mostly not a problem since at those densities the model is in the hadronic phase anyway, but it can cause some issues in the mixed phase (like in Figure 4.15).

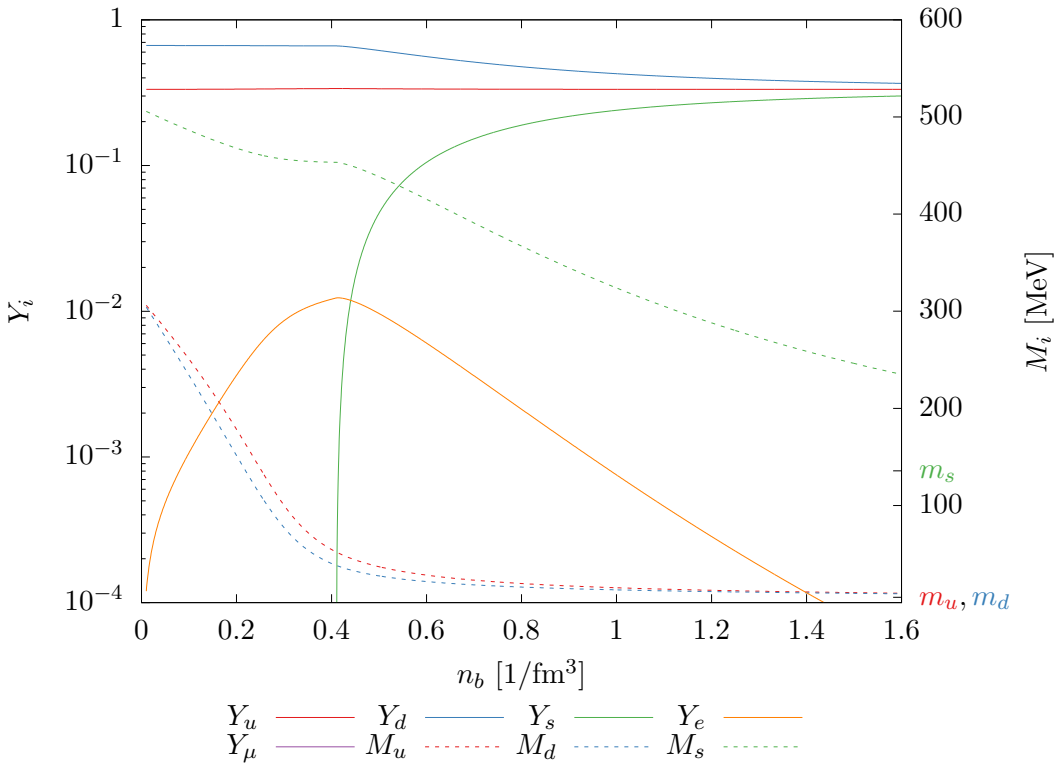

Figure 4.3: Fraction of particle densities with respect to baryonic density, and effective quark masses, in the NJL model with $G_V = 0.5\,G_S$.

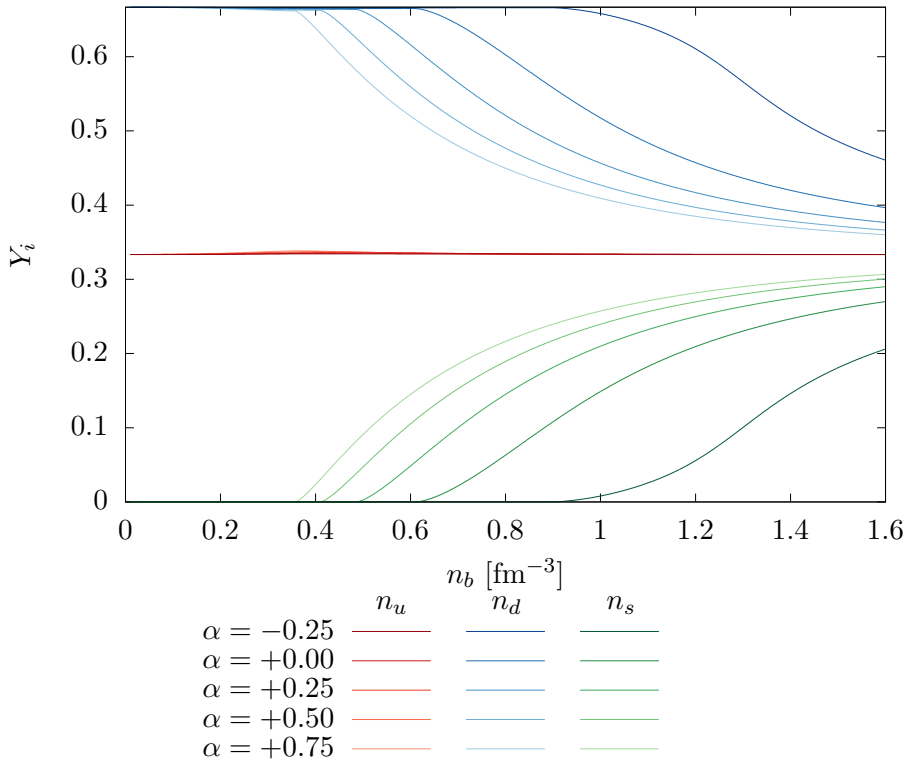

Figure 4.4: Fraction of particle densities, for different values of G_V.

4.3.2 Results in the NL3$\omega\rho$ model

The system to be solved for the NL3$\omega\rho$ model contains 10 unknowns: the effective nucleon mass, 2 hadron chemical potentials, 2 hadron effective chemical potentials, 3 mean meson fields, 2 lepton chemical potentials. It is determined by 9 equations: the expression for the effective nucleon mass, 2 expressions for the effective chemical potentials, 3 expressions for the meson fields, 2 independent constraints on the chemical potentials, one constraint on the charge neutrality.

We run an equivalent procedure to obtain points for the NL3$\omega\rho$ equation of state. Here,

$$n_b = n_n + n_p \tag{4.4}$$

Running in the interval $n_b \in [0.01 : 1.00]\,\mathrm{fm}^{-3}$ we obtain the equation of state in Figure 4.5.

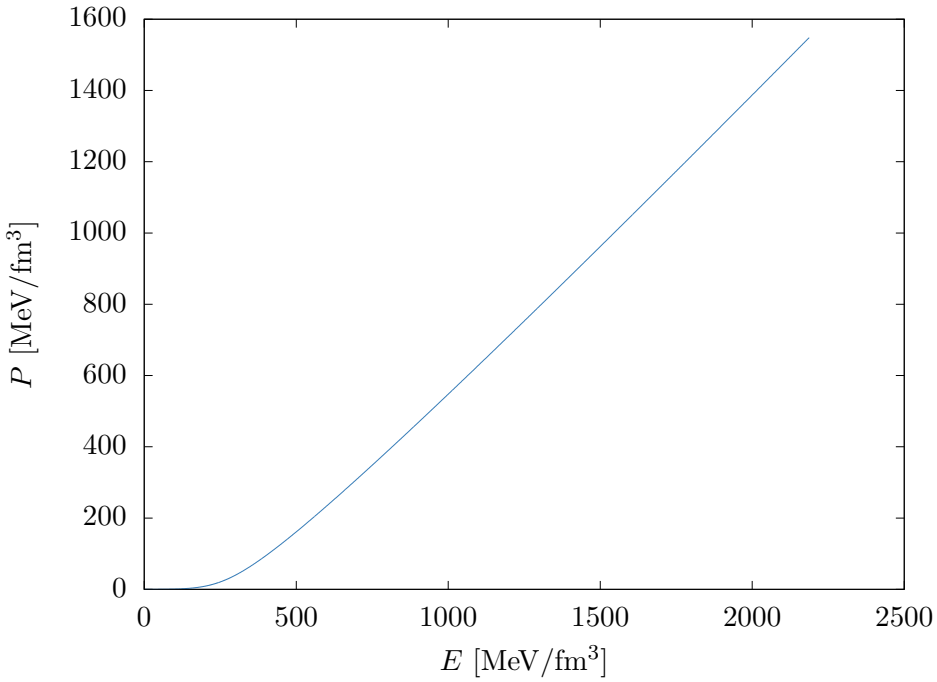

Figure 4.5: Equation of state obtained in the NL3$\omega\rho$ model.

We can see this EoS is much stiffer at high densities than the one in the NJL model. This points in the direction that, in a two-phase approach, we will indeed find that at sufficiently high densities the quark EoS will be preferred. At low densities, however, we expect this to be the preferred phase.

As expected, neutrons are much more abundant than protons in beta-equilibrated matter (Figure 4.6). At sufficiently high densities (around saturation density) muons can appear, which means that protons and electrons are no longer constrained to have the same density.

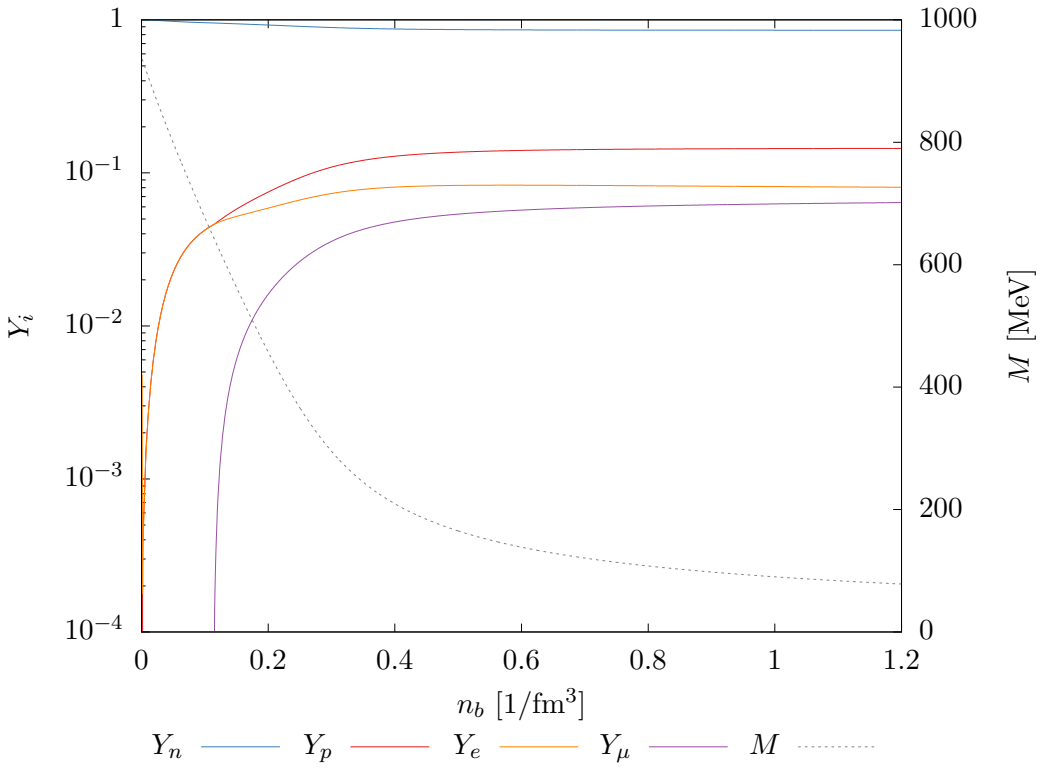

Figure 4.6: Fraction of particle densities with respect to baryonic density, and effective nucleon mass, in the NL3$\omega\rho$ model.

4.3.3 Results in the mixed phase

The system to be solved for the mixed model contains 23 unknowns: 3 quark effective masses, 3 quark chemical potentials, 3 quark effective chemical potentials, 3 quark scalar densities, the effective nucleon mass, 2 hadron chemical potentials, 2 hadron effective chemical potentials, 3 mean meson fields, 2 lepton chemical potentials, and the phase fraction. It is determined by 22 equations: 3 expressions for the effective quark masses, 3 expressions for the effective quark chemical potentials, 3 expressions for the quark scalar densities, the expression for the effective nucleon mass, 2 expressions for the effective chemical potentials, 3 expressions for the meson fields, 5 independent constraints on the chemical potentials, one constraint on the charge neutrality, one constraint on matching phase pressures.

We run the calculations for the full, two-phase model, again by fixing one quantity and varying across a range. For practical reasons, it is more convenient to fix the baryonic chemical potential instead of the baryonic density, as we did in the preceding sections.

Having obtained an equation of state for each of the models, we can plot the predicted pressure as a function of the baryonic chemical potential and superimpose them.

The process to calculate the two-phase model EoS is as follows: we start at low den-

sities/chemical potential where the model predicts a purely hadronic phase. We impose charge neutrality of the hadronic phase, but calculate the two phases simultaneously (printing the quantities of the hadronic phase, of course). Eventually, the two phases predict the same pressure: this is the start of the mixed phase, with $\chi = 0$. We switch to imposing global charge neutrality (3.117) and matching pressure between the two phases (3.110). The fraction χ rises monotonically with density, until eventually reaching $\chi = 1$, signifying the end of the mixed phase and the start of the pure quark phase. We switch to only demanding charge neutrality of the quark phase and calculate until the end. Using this procedure, and again varying the vector coupling of the NJL model, we obtain an equation of state for the two-phase model (Figure 4.7).

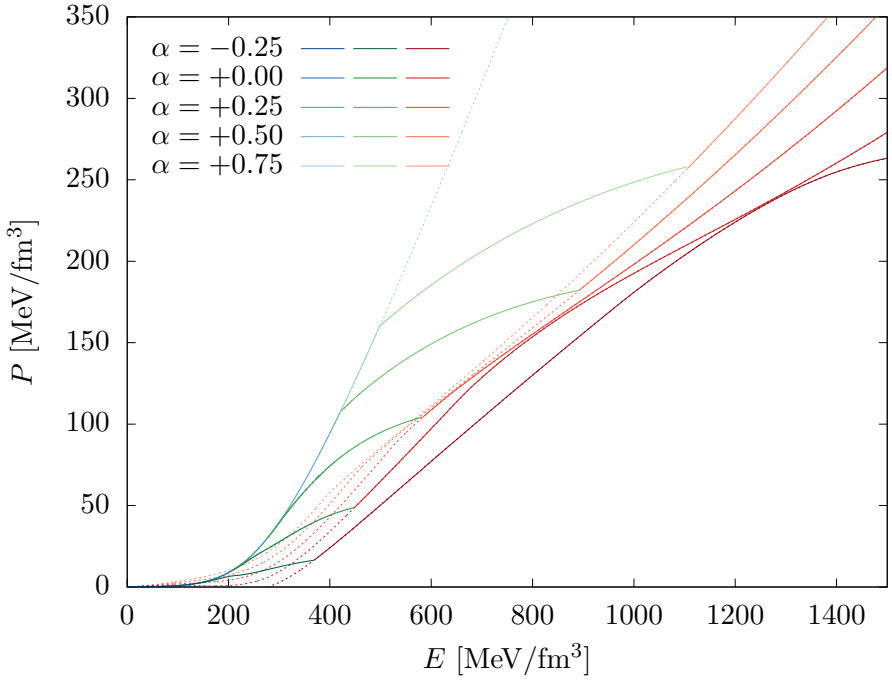

Figure 4.7: Equations of state obtained in the two-phase model, for different values of G_V. Red: Quark phase, blue: hadronic phase, green: mixed phase. Continuations of the pure EoSs shown in dashed line.

As we can see, the EoS in the two-phase model transitions smoothly from the hadronic EoS into the quark EoS, with an interval where matter is described by a mixed phase. Given that increasing the vector coupling stiffens the quark EoS, the transition is pushed to higher densities when G_V is increased. The extension of the mixed phase is also greater when G_V is large and smaller when it is smaller.

The particle densities also vary smoothly with density. (Figures 4.8 and 4.9). With the onset of the mixed phase the nucleons are replaced by the quarks. The lepton density also falls when the transition happens. At extremely high densities matter is almost

See (3.119)–(3.121).

purely quarks, with no electrons.

The phase transition densities are summarized in Table 4.7. We say that deconfinement starts to occur at the onset of the mixed phase ($n_{H\text{-}M}$).

Table 4.7: Phase transition densities (start and end of mixed phase, $n_{H\text{-}M}$ and $n_{M\text{-}Q}$ respectively), in units of fm^{-3} and in multiples of saturation density.

α	$n_{H\text{-}M}$ [fm^{-3}]	$n_{M\text{-}Q}$ [fm^{-3}]	$n_{H\text{-}M}/n_0$	$n_{M\text{-}Q}/n_0$
−0.25	0.1435	0.3757	0.97	2.54
0.00	0.2172	0.4373	1.47	2.95
0.25	0.2812	0.5317	1.90	3.59
0.50	0.4016	0.7353	2.71	4.97
0.75	0.4580	0.8543	3.09	5.77

We can see the choice of G_V makes a huge difference in the deconfinement density predicted by the model. A vector coupling of $-0.25G_V$, for example, predicts that deconfinement starts to happen at less than nuclear saturation density, which is not physically plausible. Other vector couplings predict higher deconfinement densities. This constrains the values G_V can take; if a too low deconfinement density is predicted, that value of the parameter may not be correct.

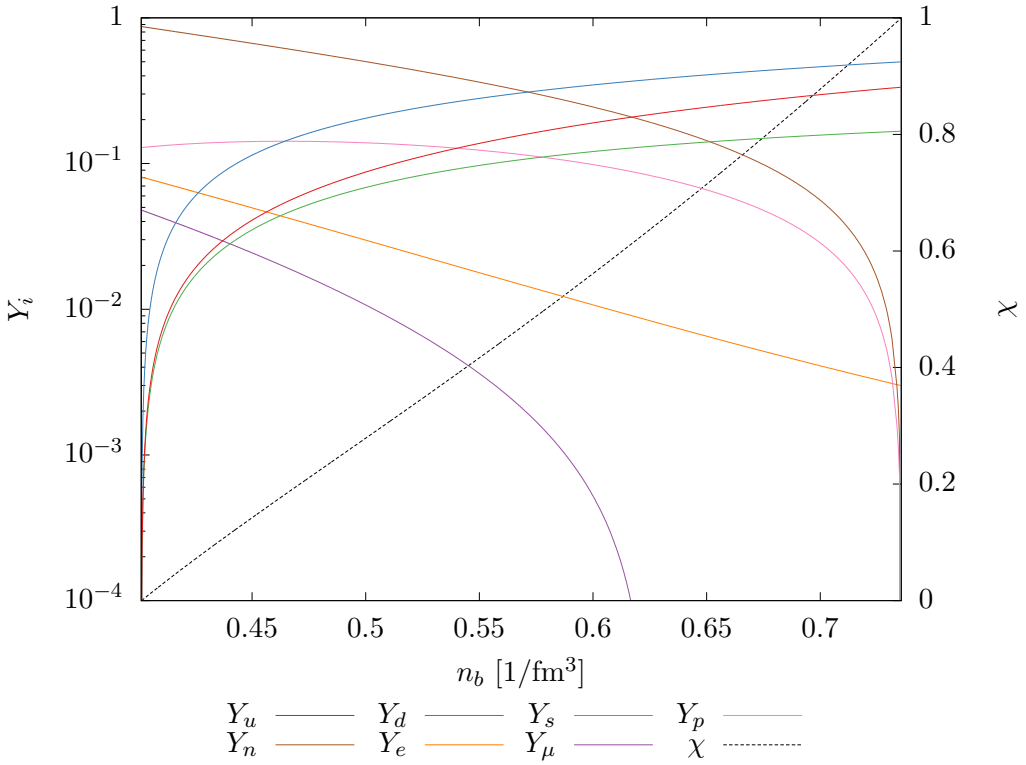

Figure 4.8: Fraction of particle densities with respect to baryonic density, and quark phase volume fraction, in the mixed phase with $G_V = 0.5\,G_S$.

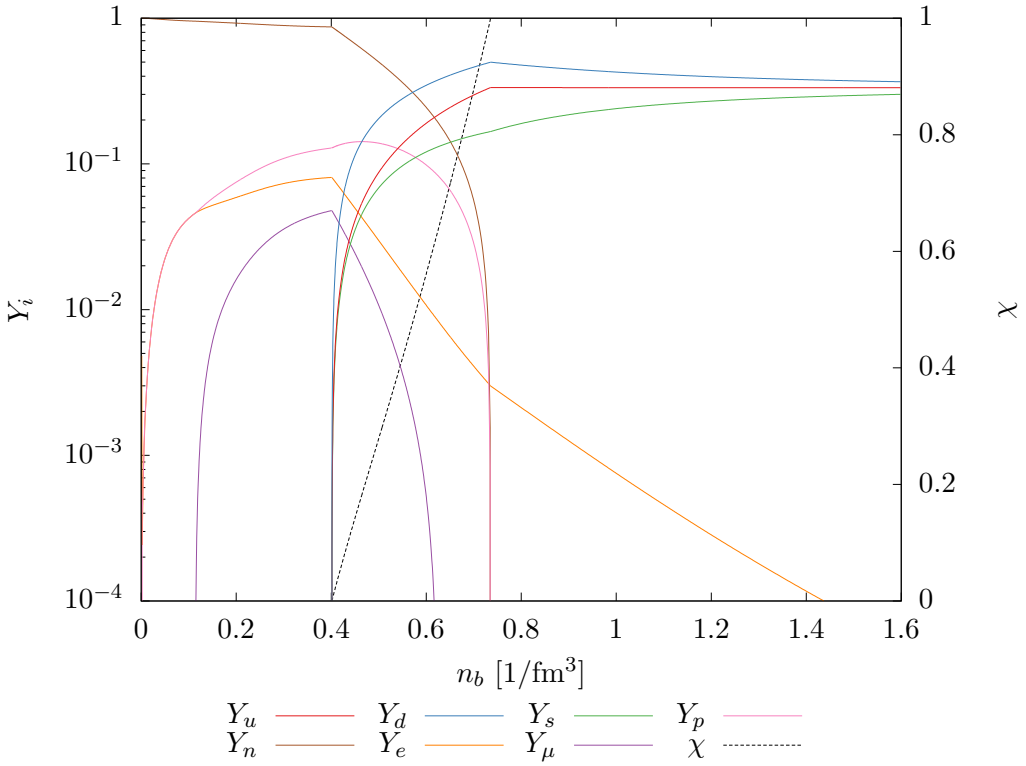

Figure 4.9: Fraction of particle densities with respect to baryonic density, and quark phase volume fraction, in the two-phase model with $G_V = 0.5\,G_S$.

4.4 Star sequences

Having calculated the equation of state that relates density and pressure we can solve the Tolman–Oppenheimer–Volkoff equations to determine the star structure, as per the procedure explained in section 1.4.2. Using the equations of state we derived for the full two-phase model we obtain mass–radius curves shown in Figure 4.10.

As discussed, we account for the crust with the method presented in section 1.8. The transition density is taken to be $n_* = 0.5n_0 = 0.074\,\mathrm{fm}^{-3}$. As discussed in section 1.8, this approximation can be bad for very low masses, way below $1\,\mathrm{M}_\odot$.

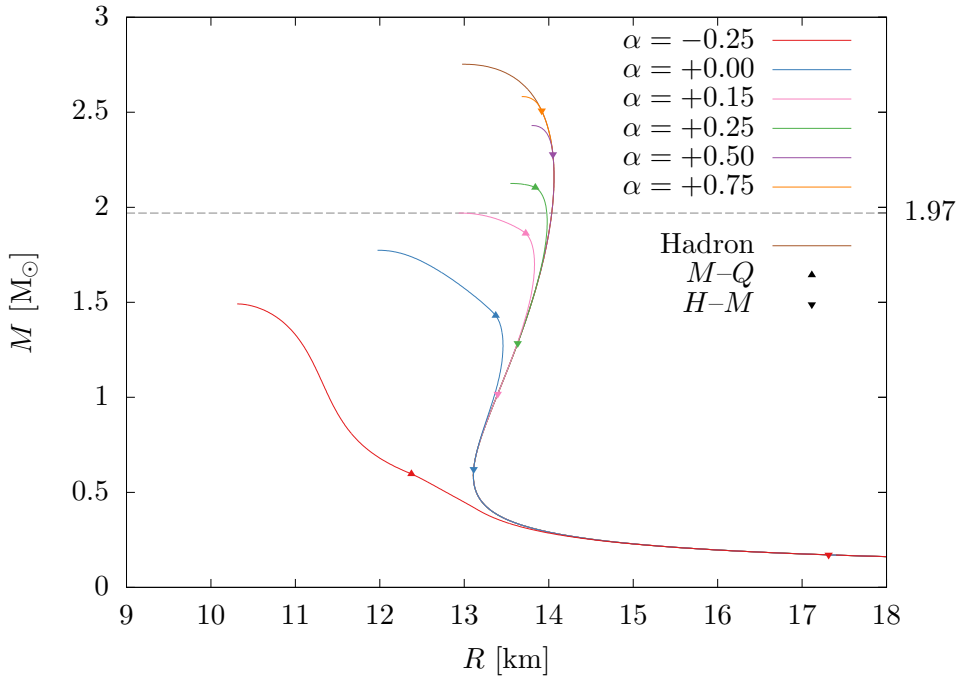

Figure 4.10: Sequence of stable stars by radius, with the two-phase EoS, with varying G_V.

The maximum masses, corresponding radii and central density, as well as the radius and central density of the $1.4\,\mathrm{M}_\odot$ star, for each value of G_V are summarized in Table 4.8.

As expected, since the transition to the quark phase above a certain density softens the EoS compared to a purely hadronic one, the model produces lower mass stars whenever the central density is enough that there is some quark content in the star's core, either in a mixed phase or, if the density is high enough, in a pure quark phase. As we've seen in Figure 4.7, a higher value of the vector coupling G_V shifts the transition density to higher values, which corresponds to a stiffer EoS, which corresponds to a higher maximum mass. Note also that because of this, for $\alpha = 0.5$ and 0.75 there exist no stable stars in the sequence with a high enough density to have a pure quark core, only a hybrid one.

The observations detailed in section 1.2 provide constraints for the validity of our model, namely on the value of the free parameter G_V. The latest observations have

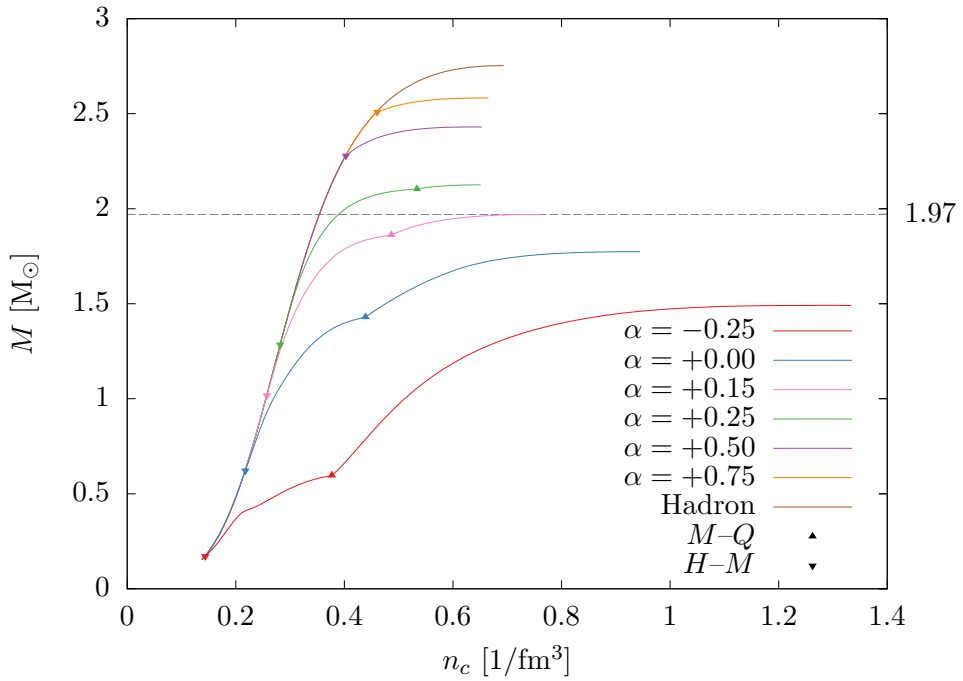

Figure 4.11: Sequence of stable stars by central density, with the two-phase EoS, with varying G_V.

discovered stars with masses of at least 1.97 solar masses, maybe more. As such, we conclude that it is impossible, in the context of this model, that the quark vector coupling constant takes values $G_V = 0$ or $G_V = -0.25\,G_S$. This excludes not only attractive vector interactions, but also a model without a vector coupling: some such coupling is indispensable in the quark phase of this model for satisfying experimental observations of neutron stars, all other parameters being equal. We can search the parameter space for the least value of G_V that gives a maximum mass above $1.97\,\mathrm{M}_\odot$; this corresponds to $G_V = 0.15\,G_S$. We plot the curves for this value of G_V too, in Figures 4.10 and 4.11.

In turn, of course, this also places an upper limit on the densities of the stars (since the maximum central density decreases with increasing G_V and the latter has a minimum admissible value). Nevertheless, the higher mass stable stars have enough central density to support matter in the mixed phase at its centre and, if the vector coupling isn't too large, even a pure quark core.

Other less precise and/or unconfirmed measurements have proposed masses as high as $2.7\,\mathrm{M}_\odot$. Nevertheless reference [4] is quoted as concluding "The largest NS mass can rule out the EoSs that have maximum masses that fall below this value. The current record holder on this front is J0348+0432 with a mass of $2.01(4)\,\mathrm{M}_\odot$". Thus the least maximum mass compatible with observations so far is $2.01 - 0.04 = 1.97\,\mathrm{M}_\odot$

Table 4.8: Mass and radius of most massive stable star, radius of the $1.4\,M_\odot$ star, and central density of the most massive and $1.4\,M_\odot$ stars, as a function of α.

α	$M_{\max}$ [$M_\odot$]	$R_{\max}$ [km]	$n_{c\,\max}$ [fm^{-3}]	$R_{1.4}$ [km]	$n_{c\,1.4}$ [fm^{-3}]
-0.25	1.4913	10.3177	1.3026	10.8378	0.8064
0.00	1.7739	11.9841	0.9357	13.4091	0.4036
0.15	1.9702	12.9470	0.7545	13.7170	0.3016
0.25	2.1253	13.5576	0.6463	13.7252	0.2927
0.50	2.4301	13.8054	0.6417	13.7255	0.2925
0.75	2.5823	13.6888	0.6557	13.7255	0.2925
H	2.7527	12.9871	0.6901	13.7255	0.2925

4.5 Finite temperature

In this section we will show how the EoS changes with temperature. We plot the EoS of the NJL and NL3$\omega\rho$ models at increasing temperatures, and compare them to the $T = 0$ baseline (Figure 4.12 and Figure 4.13 respectively).

In the quark model, increasing temperature generally leads to a stiffer equation of state; also the "kink" at the onset of strange quarks is less pronounced. This is because at $T \neq 0$ there are states above the Fermi level which are occupied, that is, even at the lowest densities there already exists some strange quark content, thus the effect (the one summarized in Figure 4.2) is less pronounced. The higher the temperature the more particles are excited above the Fermi energy, so the less pronounced is that bend.

In the NL3$\omega\rho$ model, the equation becomes more stiff, with increasing temperature, at low densities and softer at high densities.

Constant temperature stars, however, are not realistic. The assumption of constant temperature throughout the star is not a physically reasonable one, except at a very low temperature. As explained before, neutron stars cool very rapidly after formation until reaching temperatures way below the MeV scale [1]. As such, during the cooling stage there are temperature gradients in the star. Only when it cools enough to apply the zero temperature approximation can we say the star is in uniform thermal equilibrium. As such it is not physically meaningful to construct stars using these EoSs.

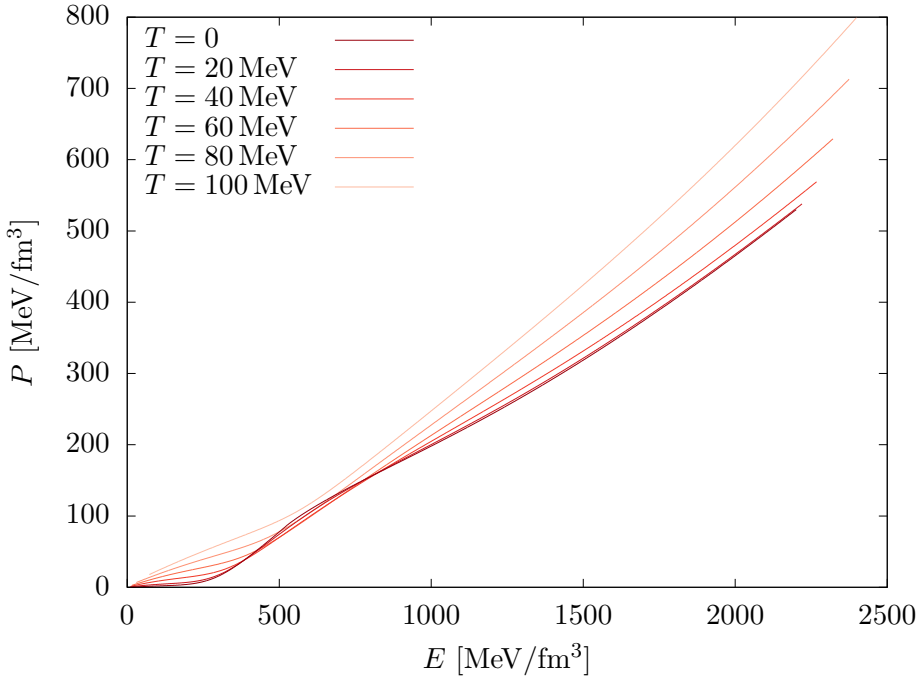

Figure 4.12: Equation of state for the NJL model at increasing temperature, with $G_V = 0.25\,G_S$.

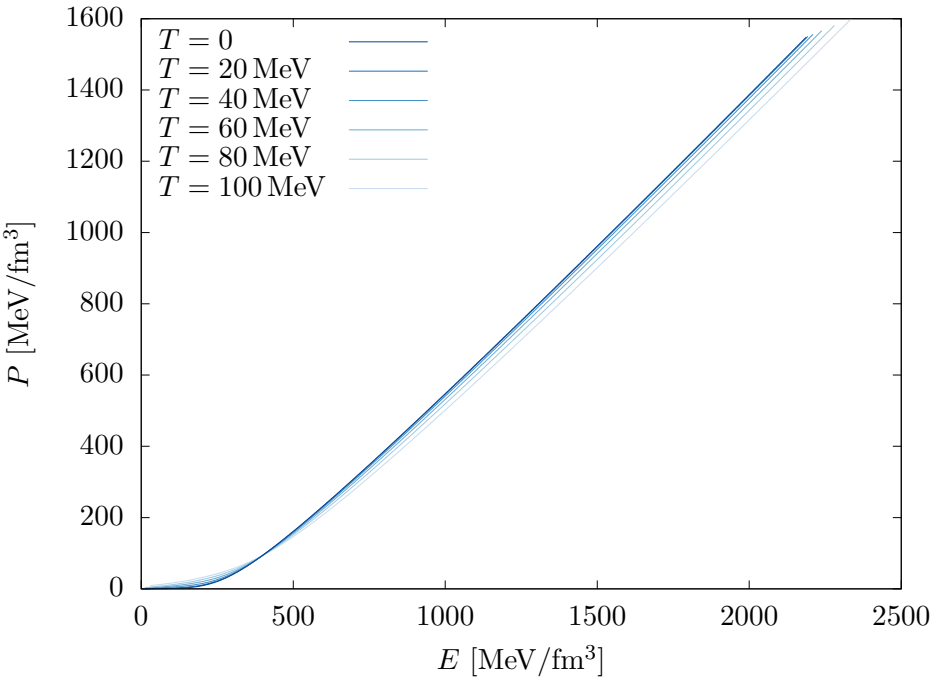

Figure 4.13: Equation of state for the NL3$\omega\rho$ model at increasing temperature.

4.6 Proto-neutron stars

Even though constant-temperature stars are not realistic, constant *entropy* stars are. Indeed, when a neutron star is born, we expect there to be an entropy per baryon of approximately 1 (it is estimated in supernova calculations that neutrons stars may be formed with almost-constant entropy throughout the star, with an entropy per baryon in that order [41]). As mentioned before, it takes on the order of 20 seconds for neutrinos to diffuse out. In this diffusion process, the neutrinos deposit energy in the star material, heating it. By the time they have diffused, they have heated the star to its maximum, corresponding to an entropy per baryon of about 2; it then quickly cools down to temperatures negligible on a nuclear scale.

In order to study this process, it is interesting to study proto-neutron stars by idealising them as constant-entropy stars, and calculating the properties of these kinds of stars at different values of entropy per baryon, corresponding to subsequent stages in the star formation process, and comparing them with the cold stars studied in the preceding sections. Let $s \equiv S/n_b$ be the entropy per baryon. Let also Y_i be the fraction of particle i, as a fraction of the baryonic density, that is

$$Y_i \equiv \frac{n_i}{n_b} \tag{4.5}$$

We will study stars at three stages [41]: first, the star immediately after formation, with a constant entropy of 1 throughout the star and with trapped neutrinos; this amounts to fixing the electronic lepton fraction at about $Y_e + Y_{\nu_e} = 0.4$. Then the maximally heated star, just after neutrinos have diffused, then the usual zero-temperature star after it has cooled way below nuclear energies.

Summarizing:

Table 4.9: Proto-neutron star evolution stages.

$s = 1$	$Y_e + Y_{\nu_e} = 0.4$	$Y_\mu + Y_{\nu_\mu} = 0$
$s = 2$	$Y_{\nu_e} = 0$	$Y_{\nu_\mu} = 0$
$T = 0$	$Y_{\nu_e} = 0$	$Y_{\nu_\mu} = 0$

We can calculate the EoSs and draw mass–radius curves for each stage. In the calculations in this section we take $G_V = 0.25\, G_S$. Note that this is a somewhat rudimentary analysis; more detailed dynamical and evolutionary calculations are necessary to confirm the results obtained via this reasoning.

We can observe in Figures 4.14 and 4.15 that the temperature tends to increase with density, for if the density increases, in order to maintain a given entropy, the temperature must be higher. However, the temperature falls when the transition to the quark phase happens. This is because quark matter has many more degrees of freedom than hadronic

This figure is obtained by estimating the efficiency of the electron capture processes during the supernova collapse that precedes the formation of the neutron star [41].

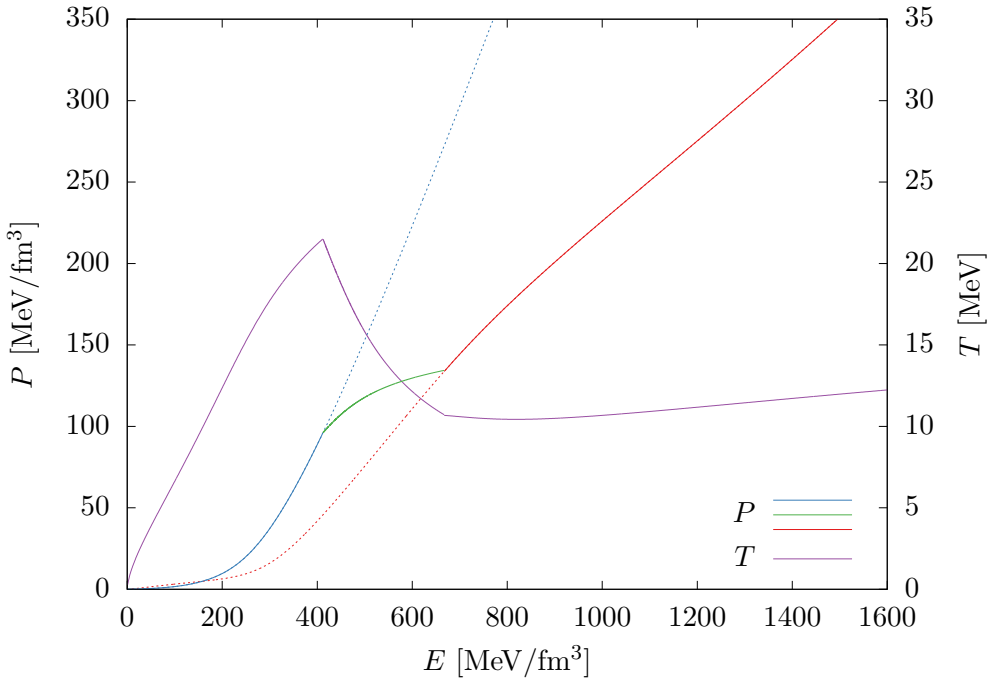

Figure 4.14: Equation of state at constant entropy ($s = 1$) with trapped neutrinos ($Y_e + Y_{\nu_e} = 0.4$), with $G_V = 0.25\, G_S$.

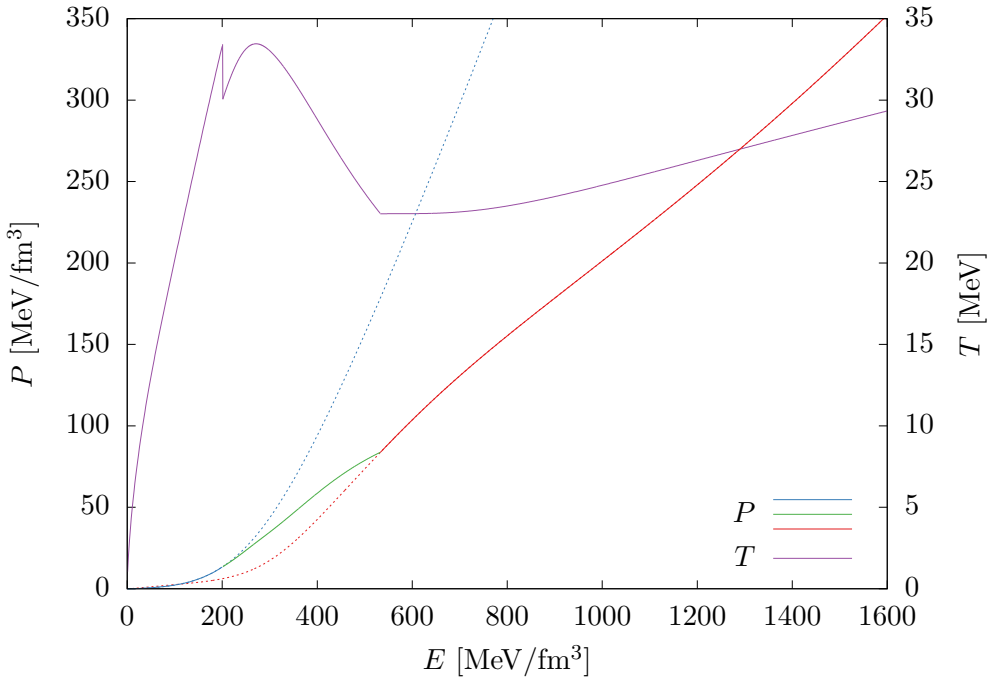

Figure 4.15: Equation of state at constant entropy ($s = 2$) after neutrinos have escaped ($Y_{\nu_e} = Y_{\nu_\mu} = 0$), with $G_V = 0.25\, G_S$.

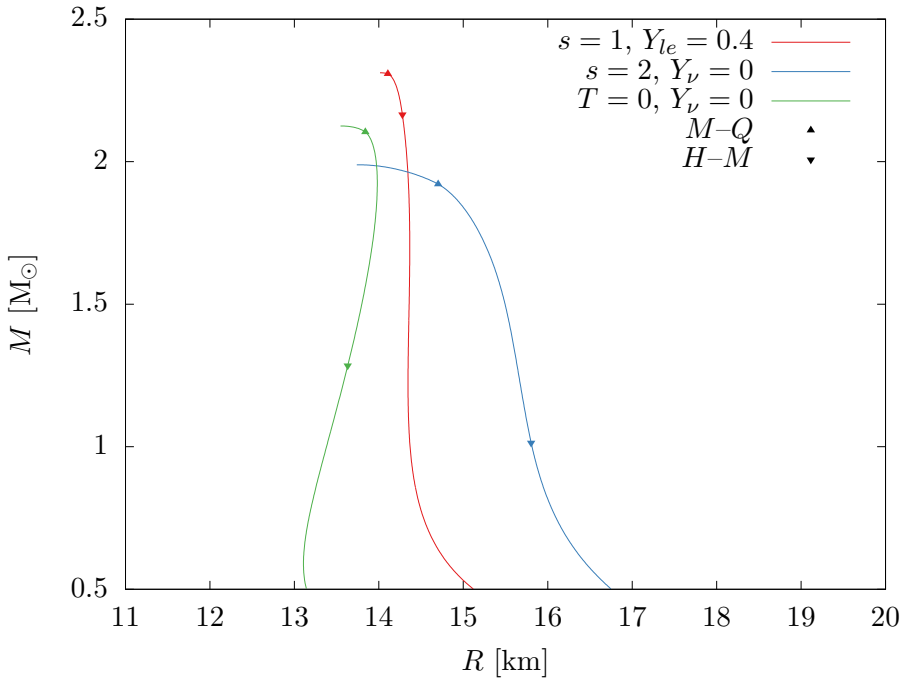

Figure 4.16: Sequence of stable stars by radius, for the three considered stages of neutron star evolution, with $G_V = 0.25\, G_S$.

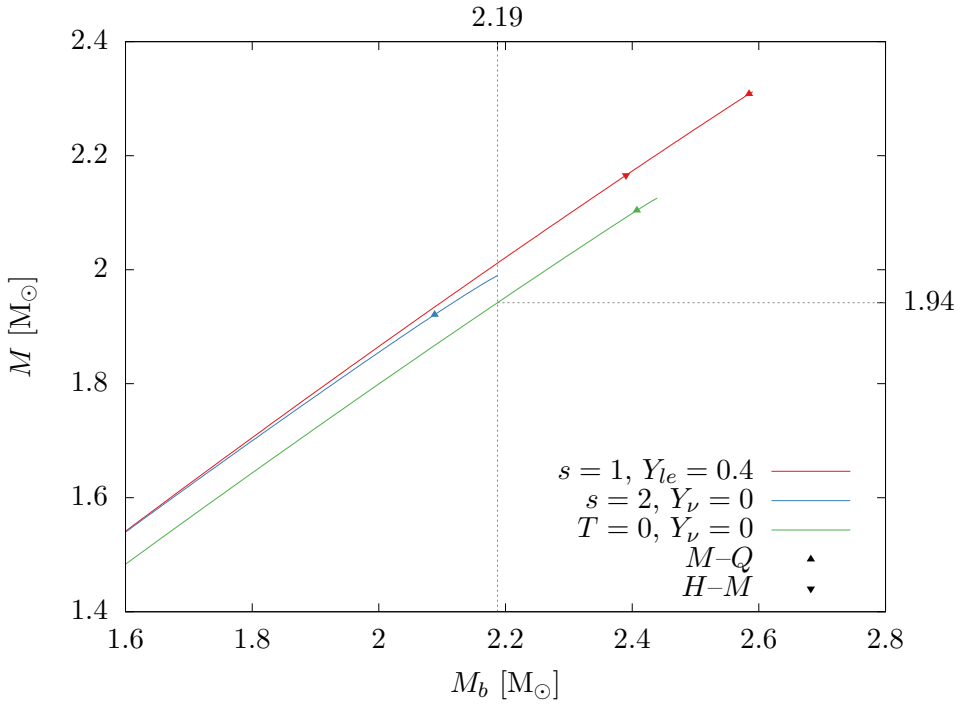

Figure 4.17: Gravitational mass as a function of baryonic mass, for the three considered stages of neutron star evolution, with $G_V = 0.25\, G_S$.

matter: three quarks *vs* two nucleons, and the quarks exist in 3 colors. Thus in the mixed phase we register a drop in the temperature.

In Figure 4.16 we can compare the mass–radius curves of neutron stars at each stage. As expected, a higher thermal pressure will yield larger stars, hence why the maximally heated stars are bigger than the freshly formed proto-neutron stars, which in turn are bigger than the cold stars. On the other hand, the predicted maximum mass has to do with the stiffness of the equation of state: when $s = 1$ with neutrinos the transition into quark matter happens at comparatively high densities, and since it is the appearance of quark matter that softens the EoS the result is that the predicted maximum mass is higher. The opposite happens when $s = 2$ without neutrinos.

We can also plot the stars' mass as a function of the total *baryonic* mass (Figure 4.17). This enables us to make the following analysis:

Assume that as it evolves a star doesn't lose or gain mass, i.e. it evolves along a line of constant M_b. When it is formed it is in a stable configuration corresponding to a point in the red curve in Figure 4.17 ($s = 1, Y_{le} = 0.4$). Given that its baryonic mass is conserved, if the star has $M_b > 2.19\,\mathrm{M}_\odot$ then there is no stable star in the next stage ($s = 2, Y_\nu = 0$) corresponding to that baryonic mass, meaning when the star evolves to this stage it will become unstable and collapse into a low mass black hole. This threshold corresponds to a final mass of $1.94\,\mathrm{M}_\odot$ (total mass at the final stage). This puts an upper limit on the baryonic mass that a proto-neutron star can have to "survive" into a neutron star, and therefore an upper limit on the mass of the stars that can evolve in this model. This upper limit is smaller than what one obtains by simply taking the maximum mass in the sequence of stable stars, as we did before. As such, this approach suggests a stricter criterion for a realistic model than usually thought: it not only has to predict a maximum mass above observational constraints, but it also must predict an upper limit on the mass of stars which are endpoints of proto-neutron star evolution greater than that same constraint. By this analysis, the star's final mass must correspond to a baryonic mass that lies in the stable sequence for each stage of evolution. This analysis is predicated on the star not losing or accreting mass during the formation process. Also, accretion phenomena after the initial formation period may allow a star to reach a higher mass.

We can do these calculations again varying G_V. The results are summarised in Table 4.10.

Table 4.10: Maximum baryonic mass for which the model predicts a stable star at all three stages, and corresponding final mass, as well as the maximum stable mass, for different values of G_V.

α	M_b [$\mathrm{M}_\odot$]	M [$\mathrm{M}_\odot$]	M_{max} [$\mathrm{M}_\odot$]
0.15	2.0516	1.8367	1.9702
0.25	2.1876	1.9423	2.1253
0.28	2.2326	1.9734	2.1742
0.50	2.5562	2.2137	2.4301
0.75	2.8241	2.4017	2.5823

The smallest value of G_V that produces a maximum final star mass, from the set of masses which correspond to a baryonic mass in the stable region for all three formation stages, above the observational constraint of $1.97\,\mathrm{M}_\odot$ is $G_V = 0.28\,G_S$ (included in Table 4.10).

Therefore we conclude that, by requiring that not only does the maximum mass in the stable sequence have to lie above $1.97\,\mathrm{M}_\odot$, but also that the maximum final mass for which there corresponds a stable PNS with the same baryonic mass in the stable sequence at all stages of formation also has to be above this limit, we have a new criterion for the validity of a neutron star model. In this case, the minimum value of G_V is $0.28\,G_S$, higher than the $0.15\,G_S$ limit deduced in section 4.4.

However, accretion of mass after formation may allow a less massive star to reach higher masses (above the limit imposed by this new constraint but below the maximum stable star mass), even if it cannot reach those masses directly after the aforementioned formation process. If these phenomena play an important role in the mass of neutron stars, it may mean this is not a good constraint (since the masses we observe are overwhelmingly more probable to be of stars many millions of years after formation).

Chapter 5

Conclusions and outlook

Conclusions

The results about the mass–radius relation of stars in this work indicate that this model, consisting of two phases described by the NJL and the NL3$\omega\rho$ models, is a valid model to describe dense matter in neutron stars. In particular, the constraint imposed by the observation of $\approx 2\,\mathrm{M}_\odot$ neutron stars is satisfied, provided that the quark vector coupling constant is such that the predicted maximum mass star is above this limit. In particular, an attractive or absent vector interaction is ruled out. This provides important clues about the behaviour of dense matter at higher than saturation density, since the deconfinement transition in this model depends critically on the exact value of this coupling.

The mass of the heaviest neutron star in this model is constrained from below by observations, and from above by the value predicted in a purely hadronic star (a hybrid model with quarks will never exceed that value since the quark EoS is softer than the hadronic one). The least value of G_V that predicts a maximum mass above the measured J0348+0432 pulsar mass ($M^- = 1.97\,\mathrm{M}_\odot$) is $G_V = 0.15\,G_S$.

This model predicts that the heaviest stars will, depending on the value of the vector coupling, have either hybrid matter or pure quark matter in their centre. If the vector coupling is too high it will eventually suppress the appearance of quarks altogether. Therefore, we conclude there is evidence to consider it realistic to propose that the heaviest neutron stars in the universe (masses close to $2\,\mathrm{M}_\odot$) do contain deconfined quark matter in their inner core. If this is true, it is possible that they are the only places in the universe where there exists bulk cold quark matter.

Furthermore, by idealising proto-neutron stars in subsequent stages of evolution as constant-entropy stars, possibly with trapped neutrinos, and assuming stars don't gain or lose mass in the process, we can deduce a maximum mass for stars which are the endpoint of this evolution, by finding the maximum baryonic mass for which all stages of evolution predict stable stars, then finding the final mass corresponding to it. Since this mass is lower than the maximum mass in the sequence, this suggests a stricter criterion for a realistic model than previously thought: the model has not only to predict maximum masses above experimental constraints, but it also must predict those masses

as endpoints of proto-neutron star evolution. By requiring this criterion to be satisfied as well, the minimum admissible value of G_V is bumped to $G_V = 0.28\,G_S$. However, if the accretion of material after the initial formation process has a significant impact on the mass of a neutron star, it may mean this criterion is not good for comparison with observations, since simply by virtue of the lifetime of neutron stars and their rate of formation we are overwhelmingly more likely to observe stars after a significant amount of time has passed from formation. Then a star can reach higher masses than it has immediately after formation, which negates this criterion as regards comparison with general observations. If the effect of accretion on the total mass is small, the criterion is at least approximately valid.

Outlook

There are several interesting avenues of research available to develop this model further. For instance, hyperons were not considered in this work, but a more complete treatment of the hadronic phase should include these strange baryons. These would "compete" with the strange quarks in the mixed phase. In this work we consider that strangeness appears only in quark matter, with the appearance of strange quarks, but not in the hadronic phase. A more complete treatment would allow the possibility of the appearance of strangeness in the hadronic phase in hyperons. It would be interesting to study the effect that allowing hyperons to appear has on the EoS.

One effect that was also neglected is the crystalline structure of the mixed phase and the contribution of surface energy in the arrangement of the matter in the mixed phase regime. Since we have two coexisting, charged phases, it will be energetically favourable for matter to be in an ordered configuration. Even though these effects are orders of magnitude weaker than the rest of the energy contribution [1], a rigorous treatment of the structure of the neutron star must include this analysis. Regardless, the effect on the mass–radius curves is negligible.

It would be important to ascertain whether or not the mass gain via accretion, after formation, is sufficiently small for the criterion we introduced in section 4.6 to be valid.

Finally, as noted in section 3.1.1, there is more freedom to tune the quark interaction while keeping it invariant under transformations of the quark field from the group $\mathrm{U}(1)_V \otimes \mathrm{SU}(N_f)_L \otimes \mathrm{SU}(N_f)_R$. This gives us more parameters to experiment with. It would be important to study how the mass–radius relationship changes with the variation of these parameters (as we did with G_V in this work), explore the parameter space and deduce an admissible region of parameter sets compatible with observations, just like we deduced an interval of admissible G_V in this work.

Appendix A

Auxiliary calculations

A.1 Small crust approximation

Calculating the structure of the crust often requires special attention, and needs to be treated in a suitable framework. If we are only interested in the broad properties of the crust, however, such as its mass and radius, and not in studying its detailed internal structure, we may not need to perform those calculations. We present such an alternative approach, put forward in [16].

This approach hinges on the fact that the crust of a neutron star is small in thickness and mass compared to the star, namely $l_{\text{crust}}/R \sim 0.1$ and $M_{\text{crust}}/M \sim 0.01$, where l_{crust} is the thickness of the crust and M_{crust} is the mass of the crust, compared to the radius of the star R and its mass M. Therefore, for the region $r \in [R_{\text{core}}; R]$ (that is, inside the crust) the TOV equation can be simplified via the following approximations:

$$\begin{cases} m(r) \approx M \\ \dfrac{4\pi r^3 P(r)}{m(r)} \ll 1 \end{cases} \tag{A.1}$$

so that the TOV simplifies to

$$\begin{aligned} \frac{\mathrm{d}P(r)}{\mathrm{d}r} &= -\Big(\rho(r) + P(r)\Big)\left(1 - \frac{2GM}{r}\right)^{-1} \frac{GM}{r^2} \\ \Leftrightarrow \frac{\mathrm{d}P}{\rho + P} &= -\frac{1}{2}\frac{R_s/r^2}{1 - R_s/r}\,\mathrm{d}r\,, \quad R_s \equiv 2GM \end{aligned} \tag{A.2}$$

where R_s is the Schwarzschild radius of the star.

Let P_*, n_* e μ_* be the pressure, baryonic density, and baryonic chemical potential, respectively, in the core–crust interface. For P and r inside the crust, that is, $P_* > P > 0$ e $r_* < r < R$,

$$\begin{aligned} \int_0^P \frac{\mathrm{d}P}{\rho + P} &= -\frac{1}{2}\int_R^r \frac{R_s/r^2}{1 - R_s/r}\,\mathrm{d}r \\ &= \frac{1}{2}\ln\left(\frac{1 - R_s/R}{1 - R_s/r}\right) \end{aligned} \tag{A.3}$$

As for the left-hand side, note that in thermodynamic equilibrium the (baryonic) chemical potential can be written

$$\mu = \frac{\mathrm{d}\rho}{\mathrm{d}n} \overset{T=0}{=} \frac{P+\rho}{n} \tag{A.4}$$

from which

$$\frac{\mathrm{d}P}{P+\rho} = \frac{\mathrm{d}P}{\mathrm{d}\mu}\frac{\mathrm{d}\mu}{P+\rho} = \frac{\mathrm{d}\mu}{\mu} \tag{A.5}$$

In other words the left-hand side of (A.3) is equivalent to $\ln\left(\frac{\mu(P)}{\mu(0)}\right)$. This enables us to relate two radial positions with the ratio of the chemical potential between those points:

$$\frac{\sqrt{1-R_s/r_1}}{\sqrt{1-R_s/r_2}} = \frac{\mu_2}{\mu_1} \tag{A.6}$$

This in turn lets us easily calculate the properties of the crust (namely mass and thickness). For instance, by relating R and R_{core} via the relation above, we have

$$\begin{aligned} &\frac{\sqrt{1-R_s/R}}{\sqrt{1-R_s/R_{\mathrm{core}}}} = \frac{\mu_*}{\mu_0} \\ \Leftrightarrow\ &R = \frac{R_{\mathrm{core}}}{1-(\alpha-1)(R_{\mathrm{core}}/R_s-1)}, \quad \alpha \equiv \left(\frac{\mu_*}{\mu_0}\right)^2 \end{aligned} \tag{A.7}$$

and

$$\boxed{l_{\mathrm{crust}} = R - R_{\mathrm{core}} = \gamma R_{\mathrm{core}}\frac{1-R_s/R_{\mathrm{core}}}{1-\gamma(1-R_s/R_{\mathrm{core}})}}, \quad \gamma \equiv (\alpha-1)\frac{R_{\mathrm{core}}}{R_s} \tag{A.8}$$

In order to determine the mass we can even go further and neglect the term $\frac{2GM(r)}{r}$ in the TOV, so that we have

$$\frac{\mathrm{d}P(r)}{\mathrm{d}r} = -\rho(r)\frac{Gm(r)/r^2}{1-2Gm(r)/r} \tag{A.9}$$

$$\Leftrightarrow \frac{\mathrm{d}P}{\mathrm{d}m} = -\frac{Gm}{4\pi r^4(1-2Gm/r)} \tag{A.10}$$

The mass of the crust is by then by this approximation

$$\boxed{M_{\mathrm{crust}} = \frac{4\pi P_* R_{\mathrm{core}}^4}{GM_{\mathrm{core}}}\left(1-\frac{2GM_{\mathrm{core}}}{R_{\mathrm{core}}}\right)} \tag{A.11}$$

The contribution of the crust mass to the total mass is an order of magnitude smaller than the contribution of the crust thickness to the overall radius of the star. As such, we can get away with making a more severe approximation in determining the former, by also assuming $\frac{P}{\rho} \ll 1$ so we can drop all terms in P in the TOV equation, in addition to the approximations we did above in determining an expression for the thickness of the crust.

Both these expressions enable us to calculate the mass and thickness of the crust knowing only: the mass and radius of the core and the core–crust transition density/pressure, as well as the baryonic chemical potential in the vacuum (at $P = 0$). No further information is needed.

The total mass and radius of the star are

$$M = M_{\text{core}} + M_{\text{crust}} \tag{A.12}$$

$$R = R_{\text{core}} + l_{\text{crust}} \tag{A.13}$$

A.2 Noether's theorem

Theorem. To every continuous symmetry of the Lagrangian there corresponds a conserved current j^μ such that

$$\partial_\mu j^\mu = 0 \tag{A.14}$$

Proof. We'll do this by supposing an infinitesimal transformation, which we can do because we are considering a continuous symmetry. Consider a number of fields ϕ_a. We say that a transformation of the sort

$$\phi_a \to \phi_a + \delta\phi_a \tag{A.15}$$

where the infinitesimal transformation $\delta\phi_a$ is some function of the fields $X_a(\phi)$, is a symmetry if the corresponding change in the Lagrangian,

$$\mathcal{L} \to \mathcal{L} + \delta\mathcal{L} \tag{A.16}$$

is at most a total derivative of some function.

$$\delta\mathcal{L} = \partial_\mu F^\mu \tag{A.17}$$

Let us calculate the change $\delta\mathcal{L}$ in terms of the transformation $\delta\phi$.

$$\delta\mathcal{L} = \frac{\partial\mathcal{L}}{\partial\phi_a}\delta\phi_a + \frac{\partial\mathcal{L}}{\partial(\partial_\mu\phi_a)}\partial_\mu(\delta\phi_a) \tag{A.18}$$

$$= \left[\frac{\partial\mathcal{L}}{\partial\phi_a} - \partial_\mu\frac{\partial\mathcal{L}}{\partial(\partial_\mu\phi_a)}\right]\delta\phi_a + \partial_\mu\left(\frac{\partial\mathcal{L}}{\partial(\partial_\mu\phi_a)}\delta\phi_a\right) \tag{A.19}$$

But the first term in brackets is simply the Euler–Lagrange equations, which vanish when the equations of motion are satisfied. In this case we're simply left with

$$\delta\mathcal{L} = \partial_\mu\left(\frac{\partial\mathcal{L}}{\partial(\partial_\mu\phi_a)}\delta\phi_a\right) \tag{A.20}$$

But if the transformation is a symmetry then $\delta\mathcal{L} = \partial_\mu F^\mu$, so

$$\partial_\mu F^\mu = \partial_\mu\left(\frac{\partial\mathcal{L}}{\partial(\partial_\mu\phi_a)}\delta\phi_a\right) \tag{A.21}$$

$$\Leftrightarrow \boxed{\partial_\mu j^\mu = 0, \quad j^\mu = \frac{\partial\mathcal{L}}{\partial(\partial_\mu\phi_a)}X_a(\phi) - F^\mu} \tag{A.22}$$

■

A.3 Goldstone theorem

Theorem. For every spontaneously broken continuous symmetry there corresponds one massless spin-0 particle, called a *Goldstone boson*, one for each of the generators of the broken symmetry.

Proof. Consider a theory with a number of fields ϕ_a and a Lagrangian:

$$\mathcal{L} = T(\partial_\mu \phi) - V(\phi) \tag{A.23}$$

where T represents the terms with derivatives and V the potential. Let ϕ_0 denote the configuration that minimizes V:

$$\left.\frac{\partial V}{\partial \phi_a}\right|_{\phi_0} = 0 \tag{A.24}$$

Expanding V around this minimum:

$$V(\phi) = V(\phi_0) + \frac{1}{2}(\phi_a - \phi_{0a})(\phi_b - \phi_{0b})\underbrace{\left(\frac{\partial^2 V}{\partial \phi_a \partial \phi_b}\right)}_{{m_{ab}}^2} + \dots \tag{A.25}$$

the coefficient of the quadratic term is a symmetric matrix whose eigenvalues correspond to the masses of the fields [20]. These eigenvalues must be positive, since we are expanding around a minimum.

Consider a continuous transformation, in an infinitesimal form:

$$\phi_a \to \phi_a + \delta\phi_a \tag{A.26}$$

where $\delta\phi_a$ is an infinitesimal amount, some function of the fields $X_a(\phi)$. Suppose also now that the fields are constant. If this transformation is a symmetry, then the Lagrangian must be invariant, but if the fields are constant, the derivative terms are automatically zero so this amounts to the potential alone being invariant, that is

$$V(\phi_a) = V(\phi_a + X_a) \Leftrightarrow \frac{\partial V}{\partial \phi_a} X_a = 0 \tag{A.27}$$

Then

$$\frac{\partial}{\partial \phi_b}\left(\frac{\partial V}{\partial \phi_a} X_a\right)\bigg|_{\phi_0} = 0 \tag{A.28}$$

$$\Leftrightarrow \left.\frac{\partial^2 V}{\partial \phi_a \partial \phi_b} X_a\right|_{\phi_0} + \left.\frac{\partial V}{\partial \phi_a}\frac{\partial X_a}{\partial \phi_b}\right|_{\phi_0} = 0 \tag{A.29}$$

The second term vanishes since ϕ_0 is a minimum of V, so the first term must also vanish:

$$\Leftrightarrow {m_{ab}}^2 X_a(\phi_0) = 0 \tag{A.30}$$

Now, if the symmetry is a good symmetry, then the minimum of the potential is preserved, that is, $X_a(\phi_0) = 0$, so no constraint is imposed on m_{ab}. If, however, the

symmetry is spontaneously broken, that is, it is not a symmetry of the ground state, then $X_a(\phi_0) \neq 0$, which necessarily means the matrix has one zero eigenvalue (from eigenvector $X_a(\phi_0)$),

$$m_{ab}{}^2 X_a(\phi_0) = 0\, X_a(\phi_0) \tag{A.31}$$

which implies the existence of a massless particle (once for each linearly independent spontaneously broken continuous symmetry). ■

A.4 Linearized products of operators

Linearizing products of operators means writing as an expectation value plus a perturbation,

$$\hat{A} = \langle \hat{A} \rangle + \delta\hat{A} \tag{A.32}$$

multiplying, and discarding terms that are second-order or more in the perturbation. The product of two operators becomes

$$\begin{aligned}
\hat{A}\hat{B} &= \Big(\langle \hat{A} \rangle + \delta\hat{A}\Big)\Big(\langle \hat{B} \rangle + \delta\hat{B}\Big) \\
&= \langle \hat{A} \rangle\langle \hat{B} \rangle + \langle \hat{A} \rangle\delta\hat{B} + \delta\hat{A}\langle \hat{B} \rangle + \delta\hat{A}\delta\hat{B} \\
&\approx \langle \hat{A} \rangle\langle \hat{B} \rangle + \langle \hat{A} \rangle\delta\hat{B} + \delta\hat{A}\langle \hat{B} \rangle \\
&= \langle \hat{A} \rangle\langle \hat{B} \rangle + \langle \hat{A} \rangle[\hat{B} - \langle \hat{B} \rangle] + [\hat{A} - \langle \hat{A} \rangle]\langle \hat{B} \rangle \\
&= \langle \hat{A} \rangle\hat{B} + \hat{A}\langle \hat{B} \rangle - \langle \hat{A} \rangle\langle \hat{B} \rangle
\end{aligned} \tag{A.33}$$

while the product of three operators becomes

$$\begin{aligned}
\hat{A}\hat{B}\hat{C} &= \Big(\langle \hat{A} \rangle + \delta\hat{A}\Big)\Big(\langle \hat{B} \rangle + \delta\hat{B}\Big)\Big(\langle \hat{C} \rangle + \delta\hat{C}\Big) \\
&= \Big(\langle \hat{A} \rangle\langle \hat{B} \rangle + \langle \hat{A} \rangle\delta\hat{B} + \delta\hat{A}\langle \hat{B} \rangle + \delta\hat{A}\delta\hat{B}\Big)\Big(\langle \hat{C} \rangle + \delta\hat{C}\Big) \\
&= \langle \hat{A} \rangle\langle \hat{B} \rangle\langle \hat{C} \rangle + \langle \hat{A} \rangle\delta\hat{B}\langle \hat{C} \rangle + \delta\hat{A}\langle \hat{B} \rangle\langle \hat{C} \rangle + \delta\hat{A}\delta\hat{B}\langle \hat{C} \rangle \\
&\quad + \langle \hat{A} \rangle\langle \hat{B} \rangle\delta\hat{C} + \langle \hat{A} \rangle\delta\hat{B}\delta\hat{C} + \delta\hat{A}\langle \hat{B} \rangle\delta\hat{C} + \delta\hat{A}\delta\hat{B}\delta\hat{C} \\
&\approx \langle \hat{A} \rangle\langle \hat{B} \rangle\langle \hat{C} \rangle + \langle \hat{A} \rangle\delta\hat{B}\langle \hat{C} \rangle + \delta\hat{A}\langle \hat{B} \rangle\langle \hat{C} \rangle + \langle \hat{A} \rangle\langle \hat{B} \rangle\delta\hat{C} \\
&= \langle \hat{A} \rangle\langle \hat{B} \rangle\langle \hat{C} \rangle + \langle \hat{A} \rangle[\hat{B} - \langle \hat{B} \rangle]\langle \hat{C} \rangle + [\hat{A} - \langle \hat{A} \rangle]\langle \hat{B} \rangle\langle \hat{C} \rangle + \langle \hat{A} \rangle\langle \hat{B} \rangle[\hat{C} - \langle \hat{C} \rangle] \\
&= \langle \hat{A} \rangle\hat{B}\langle \hat{C} \rangle + \hat{A}\langle \hat{B} \rangle\langle \hat{C} \rangle + \langle \hat{A} \rangle\langle \hat{B} \rangle\hat{C} - 2\langle \hat{A} \rangle\langle \hat{B} \rangle\langle \hat{C} \rangle
\end{aligned} \tag{A.34}$$

A.5 Fierz identities

The Fierz identities are frequently used in quantum field theory calculations to analyse four-fermion operators such as current–current operators of the sort we use in the NJL interaction Lagrangian. These reordering identities enable us to express a product of Dirac bilinears (or indeed two matrices from a set that forms a basis of or spans some vector space, of which the Dirac bilinears are but an example) as a linear combination of other products of bilinears (or matrices from the basis, in general) with the four

constituent spinors (or members of the target vector space, in general) in a different order.

In other words, given a term

$$(\overline{\psi}_1 A\psi_2)(\overline{\psi}_3 B\psi_4) \tag{A.35}$$

we want to write it as

$$(\overline{\psi}_1 M\psi_4)(\overline{\psi}_3 N\psi_2) \tag{A.36}$$

How do the matrices A and B relate to M and N, if these are expressed in terms of some basis? The answer is given by the Fierz identities.

Since in this work we wish to perform these calculations for quantities of the form $(\overline{\psi}A\psi)^2$, the reordering of the spinors is trivial. What this will do is enable us to expand an interaction term of the form above in its constituent terms.

We will make use of the Fierz identities for two cases in concrete: the operators in Dirac spaces and the $\mathfrak{u}(n)$ matrices.

Dirac operators

The set $\{\mathbb{1}, i\gamma^5, \gamma^\mu, \gamma^5\gamma^\mu, \sigma^{\mu\nu}\}$ of Dirac bilinears forms a basis for the space of 4×4 matrices. For these we have:

$$(\overline{\psi}_1 A_i\psi_2)(\overline{\psi}_3 A_i\psi_4) = \sum_j k_{ij}(\overline{\psi}_1 B_j\psi_4)(\overline{\psi}_3 B_j\psi_2) \tag{A.37}$$

where the coefficients k_{ij} are

Table A.1: Fierz coefficients k_{ij} for expanding Dirac bilinears.

A_i \ B_j	$\mathbb{1}$	$i\gamma^5$	γ^μ	$\gamma^5\gamma^\mu$	$\sigma^{\mu\nu}$
$\mathbb{1}$	$\frac{1}{4}$	$-\frac{1}{4}$	$\frac{1}{4}$	$-\frac{1}{4}$	$\frac{1}{8}$
$i\gamma^5$	$-\frac{1}{4}$	$\frac{1}{4}$	$\frac{1}{4}$	$-\frac{1}{4}$	$-\frac{1}{8}$
γ^μ	1	1	$-\frac{1}{2}$	$-\frac{1}{2}$	0
$\gamma^5\gamma^\mu$	-1	-1	$-\frac{1}{2}$	$-\frac{1}{2}$	0
$\sigma^{\mu\nu}$	3	-3	0	0	$-\frac{1}{2}$

$\mathfrak{u}(N)$ matrices

Let t_a, $a = 1, \ldots, N^2 - 1$ be the generators of $\mathrm{SU}(N)$, normalized such that $\mathrm{Tr}(t_a t_b) = 2\delta_{ab}$. Together with the identity, these form a basis for the space of $N \times N$ hermitian matrices. The Fierz coefficients for this basis are:

Reference [42] gives a clear derivation from first principles of the form of the general Fierz-type identities for any N-dimensional vector space.

The algebra of the generators of $\mathrm{U}(N)$

Table A.2: Fierz coefficients k_{ij} for expanding $\mathfrak{u}(1)$.

A_i \ B_j	$\mathbb{1}$	t_a
$\mathbb{1}$	$\frac{1}{N}$	$\frac{1}{2}$
t_a	$\frac{2(N^2-1)}{N^2}$	$-\frac{1}{N}$

A.6 Thermodynamic quantities for the NJL model in the mean field approximation

The grand canonical potential of the linearized NJL model is (see (3.41)):

$$\begin{aligned}\Omega = -6T \sum_{f=u,d,s} \int \frac{\mathrm{d}^3\vec{p}}{(2\pi)^3} \left[\frac{\omega_f}{T} + \ln\!\left(1 + e^{-(\omega_f+\tilde{\mu}_f)/T}\right) + \ln\!\left(1 + e^{-(\omega_f-\tilde{\mu}_f)/T}\right)\right] \\ + 2G_S({\sigma_u}^2 + {\sigma_d}^2 + {\sigma_s}^2) - 2G_V({n_u}^2 + {n_d}^2 + {n_s}^2) - 4G_D\sigma_u\sigma_d\sigma_s + \Omega_0\end{aligned} \tag{A.38}$$

From this quantity we can calculate all quantities of interest (see the expressions (2.59)–(2.62)). The calculations follow:

The particle densities are

$$\begin{aligned} n_i &= -\frac{\partial\Omega}{\partial\mu_i} \\ &= 6T \int \frac{\mathrm{d}^3\vec{p}}{(2\pi)^3} \left[\frac{-\frac{1}{T} e^{-(\omega_i+\tilde{\mu}_i)/T}}{1 + e^{-(\omega_i+\tilde{\mu}_i)/T}} + \frac{\frac{1}{T} e^{-(\omega_i-\tilde{\mu}_i)/T}}{1 + e^{-(\omega_i-\tilde{\mu}_i)/T}} \right] \\ &= 6 \int \frac{\mathrm{d}^3\vec{p}}{(2\pi)^3} \left[-\frac{1}{1 + e^{(\omega_i+\tilde{\mu}_i)/T}} + \frac{1}{1 + e^{(\omega_i-\tilde{\mu}_i)/T}} \right] \\ &= 6 \int \frac{\mathrm{d}^3\vec{p}}{(2\pi)^3} \left(\not{\ell}_i - \bar{\not{\ell}}_i \right), \quad i = u, d, s \end{aligned} \tag{A.39}$$

The pressure is

$$\begin{aligned} P &= -\frac{\partial(\Omega V)}{\partial V} = -\Omega \frac{\partial V}{\partial V} = -\Omega \\ &= 6 \sum_{f=u,d,s} \int \frac{\mathrm{d}^3\vec{p}}{(2\pi)^3} \left[\omega_f + T \ln\!\left(1 + e^{-(\omega_f+\tilde{\mu}_f)/T}\right) + T \ln\!\left(1 + e^{-(\omega_f-\tilde{\mu}_f)/T}\right)\right] \\ &\quad - 2G_S({\sigma_u}^2 + {\sigma_d}^2 + {\sigma_s}^2) + 2G_V({n_u}^2 + {n_d}^2 + {n_s}^2) + 4G_D\sigma_u\sigma_d\sigma_s - \Omega_0 \end{aligned} \tag{A.40}$$

The entropy density is

$$\begin{aligned} S &= -\frac{\partial\Omega}{\partial T} \\ &= 6 \sum_{f=u,d,s} \int \frac{\mathrm{d}^3\vec{p}}{(2\pi)^3} \left[\frac{\omega_f}{T} + \ln\!\left(1 + e^{-(\omega_f+\tilde{\mu}_f)/T}\right) + \ln\!\left(1 + e^{-(\omega_f-\tilde{\mu}_f)/T}\right)\right] \\ &\quad + 6T \sum_{f=u,d,s} \int \frac{\mathrm{d}^3\vec{p}}{(2\pi)^3} \left[-\frac{\omega_f}{T^2} + \frac{\frac{\omega_f+\tilde{\mu}_f}{T^2} e^{-(\omega_f+\tilde{\mu}_f)/T}}{1 + e^{-(\omega_f+\tilde{\mu}_f)/T}} + \frac{\frac{\omega_f-\tilde{\mu}_f}{T^2} e^{-(\omega_f-\tilde{\mu}_f)/T}}{1 + e^{-(\omega_f-\tilde{\mu}_f)/T}} \right] \end{aligned}$$

$$
\begin{aligned}
&= -\frac{\Omega + U - \Omega_0}{T} \\
&\quad + 6 \sum_{f=u,d,s} \int \frac{\mathrm{d}^3\vec{p}}{(2\pi)^3} \Big[-\frac{\omega_f}{T} + \frac{\omega_f + \tilde{\mu}_f}{T} \frac{1}{1 + e^{(\omega_f + \tilde{\mu}_f)/T}} + \frac{\omega_f - \tilde{\mu}_f}{T} \frac{1}{1 + e^{(\omega_f - \tilde{\mu}_f)/T}} \Big] \\
&= 6 \sum_{f=u,d,s} \int \frac{\mathrm{d}^3\vec{p}}{(2\pi)^3} \Big[-\frac{\omega_f}{T} + \frac{\omega_f + \tilde{\mu}_f}{T} \bar{\ell}_f + \frac{\omega_f - \tilde{\mu}_f}{T} \ell_f \Big] - \frac{\Omega + U - \Omega_0}{T} \\
&= \frac{6}{T} \sum_{f=u,d,s} \int \frac{\mathrm{d}^3\vec{p}}{(2\pi)^3} \Big[\omega_f (\bar{\ell}_f + \ell_f) + \tilde{\mu}_f (\bar{\ell}_f - \ell_f) + T \ln\Big(1 + e^{-(\omega_f + \tilde{\mu}_f)/T}\Big) + T \ln\Big(1 + e^{-(\omega_f - \tilde{\mu}_f)/T}\Big) \Big]
\end{aligned}
\tag{A.41}
$$

Finally the energy density is

$$
\begin{aligned}
E &= -P + TS + \sum_f \mu_f n_f \\
&= \Omega + T \left[6 \sum_{f=u,d,s} \int \frac{\mathrm{d}^3\vec{p}}{(2\pi)^3} \Big[-\frac{\omega_f}{T} + \frac{\omega_f + \tilde{\mu}_f}{T} \bar{\ell}_f + \frac{\omega_f - \tilde{\mu}_f}{T} \ell_f \Big] - \frac{\Omega + U - \Omega_0}{T} \right] + \sum_{f=u,d,s} \mu_f n_f \\
&= 6 \sum_{f=u,d,s} \left[\int \frac{\mathrm{d}^3\vec{p}}{(2\pi)^3} \Big[-\omega_f + (\omega_f + \tilde{\mu}_f) \bar{\ell}_f + (\omega_f - \tilde{\mu}_f) \ell_f \Big] + \mu_f n_f \right] - U + \Omega_0 \\
&= 6 \sum_{f=u,d,s} \int \frac{\mathrm{d}^3\vec{p}}{(2\pi)^3} \Big[-\omega_f + (\omega_f + \tilde{\mu}_f) \bar{\ell}_f + (\omega_f - \tilde{\mu}_f) \ell_f + \mu_f \Big(\ell_f - \bar{\ell}_f \Big) \Big] - U + \Omega_0 \\
&= 6 \sum_{f=u,d,s} \int \frac{\mathrm{d}^3\vec{p}}{(2\pi)^3} \Big[\omega_f (\overline{n_f} + n_f - 1) + (\tilde{\mu}_f - \mu_f)(\bar{\ell}_f - \ell_f) \Big] - U + \Omega_0 \\
&= 6 \sum_{f=u,d,s} \int \frac{\mathrm{d}^3\vec{p}}{(2\pi)^3} \Big[\omega_f (\bar{\ell}_f + \ell_f - 1) - 4 G_V n_f (\bar{\ell}_f - \ell_f) \Big] - U + \Omega_0 \\
&= 6 \sum_{f=u,d,s} \int \frac{\mathrm{d}^3\vec{p}}{(2\pi)^3} \omega_f (\bar{\ell}_f + \ell_f - 1) + \sum_{f=u,d,s} 4 G_V {n_f}^2 - U + \Omega_0 \\
&= 6 \sum_{f=u,d,s} \int \frac{\mathrm{d}^3\vec{p}}{(2\pi)^3} \omega_f (\bar{\ell}_f + \ell_f - 1) \\
&\qquad + 2 G_S ({\sigma_u}^2 + {\sigma_d}^2 + {\sigma_s}^2) + 2 G_V ({n_u}^2 + {n_d}^2 + {n_s}^2) - 4 G_D \sigma_u \sigma_d \sigma_s + \Omega_0
\end{aligned}
\tag{A.42}
$$

As for the condensates $\sigma_i = \langle \overline{\psi}_i \psi_i \rangle$, these are found by imposing that the grand canonical potential be stationary with respect to the vacuum expectation values of the fields:

$$
\frac{\partial \Omega}{\partial \sigma_i} = 0, \quad i = u, d, s \tag{A.43}
$$

If these all vanish then we can write

$$
\frac{\partial \Omega}{\partial \sigma_i} + \sum_{j=u,d,s} \frac{\partial \Omega}{\partial \sigma_i} = \frac{\partial \Omega}{\partial \sigma_i} + \sum_{j=u,d,s} \frac{\partial \Omega}{\partial M_j} \frac{\partial M_j}{\partial \sigma_i} = 0, \quad i = u, d, s \tag{A.44}
$$

Recall the gap equations for the constituent mass M (equation (3.36) or (3.38)):

$$M_i = m_i - 4G_S\sigma_i + 2G_D\sigma_j\sigma_k \tag{A.45}$$

with i,j,k even permutations of u,d,s. Therefore:

$$\frac{\partial\Omega}{\partial\sigma_i} = 4G_S\sigma_i - 4G_D\sigma_j\sigma_k, \quad i,j,k \text{ even permutations of } u,d,s \tag{A.46}$$

$$\begin{aligned}\frac{\partial\Omega}{\partial M_i} &= -6T\int\frac{\mathrm{d}^3\vec{p}}{(2\pi)^3}\frac{\partial}{\partial\omega_i}\left[\frac{\omega_i}{T} + \ln\left(1+e^{-(\omega_i+\tilde{\mu}_i)/T}\right) + \ln\left(1+e^{-(\omega_i-\tilde{\mu}_i)/T}\right)\right]\frac{\partial\omega_i}{\partial M_i} \\ &= -6\int\frac{\mathrm{d}^3\vec{p}}{(2\pi)^3}\left[1 + T\frac{-\frac{1}{T}e^{-(\omega_i+\tilde{\mu}_i)/T}}{1+e^{-(\omega_i+\tilde{\mu}_i)/T}} + T\frac{-\frac{1}{T}e^{-(\omega_i-\tilde{\mu}_i)/T}}{1+e^{-(\omega_i-\tilde{\mu}_i)/T}}\right]\frac{M_i}{\omega_i} \\ &= -6\int\frac{\mathrm{d}^3\vec{p}}{(2\pi)^3}\frac{M}{E}[1-\ell_i-\bar{\ell}_i] \equiv \mathcal{I}_i\end{aligned} \tag{A.47}$$

$$\frac{\partial M_i}{\partial\sigma_j} = \begin{cases} -4G_S & i=j \\ 2G_D\sigma_k & i\neq j\neq k \end{cases} \tag{A.48}$$

Assembling equation (A.44) we have

$$\begin{aligned} & 4G_S\sigma_i - 4G_D\sigma_j\sigma_k - 4G_S\mathcal{I}_i + 2G_D\mathcal{I}_j\sigma_k + 2G_D\mathcal{I}_k\sigma_j = 0 \\ \Leftrightarrow\ & 4G_S(\sigma_i-\mathcal{I}_i) + 2G_D(\mathcal{I}_j\sigma_k + \mathcal{I}_k\sigma_j - 2\sigma_j\sigma_k) = 0 \\ \Leftrightarrow\ & 4G_S(\sigma_i-\mathcal{I}_i) - 2G_D[(\sigma_j-\mathcal{I}_j)\sigma_k + (\sigma_k-\mathcal{I}_k)\sigma_j] = 0 \end{aligned} \tag{A.49}$$

where i,j,k are even permutations of u,d,s, from which we conclude

$$\sigma_i - \mathcal{I}_i = 0 \Leftrightarrow \sigma_i = 6\int\frac{\mathrm{d}^3\vec{p}}{(2\pi)^3}\frac{M_i}{E_i}[\ell_i + \bar{\ell}_i - 1] \tag{A.50}$$

for $i = u,d,s$.

A.7 Thermodynamic quantities for the NL3$\omega\rho$ model in the mean field approximation

The grand canonical potential density for the NL3$\omega\rho$ model in the mean field approximation is

$$\begin{aligned}\Omega = & -2T\sum_{i=p,n}\int\frac{\mathrm{d}^3\vec{p}}{(2\pi)^3}\left[\ln\left(1+e^{-(\omega_i+\tilde{\mu}_i)/T}\right) + \ln\left(1+e^{-(\omega_i-\tilde{\mu}_i)/T}\right)\right] \\ & + \frac{1}{2}m_\sigma^2\sigma^2 - \frac{1}{2}m_\omega^2\omega^2 - \frac{1}{2}m_\rho^2\rho^2 + \frac{1}{3}\kappa(g_\sigma\sigma)^3 + \frac{1}{4}\lambda(g_\sigma\sigma)^4 \\ & - \frac{1}{4!}\xi g_\omega^4\omega^4 - \Lambda_{\omega\rho}(g_\omega^2\omega^2)(g_\rho^2\rho^2) + \Omega_0\end{aligned} \tag{A.51}$$

That is: (u,d,s), (d,s,u), (s,u,d). See appendix B.4.

From this quantity we can calculate all quantities of interest (see the expressions (2.59)–(2.62)). The calculations follow:

$$\begin{aligned} n_i &= -\frac{\partial\Omega}{\partial\mu_i} \\ &= 2T\int\frac{\mathrm{d}^3\vec{p}}{(2\pi)^3}\left[\frac{-\frac{1}{T}e^{-(E_i+\tilde{\mu}_i)/T}}{1+e^{-(E_i+\tilde{\mu}_i)/T}}+\frac{\frac{1}{T}e^{-(E_i-\tilde{\mu}_i)/T}}{1+e^{-(E_i-\tilde{\mu}_i)/T}}\right] \\ &= 2\int\frac{\mathrm{d}^3\vec{p}}{(2\pi)^3}\left[-\frac{1}{1+e^{(E_i+\tilde{\mu}_i)/T}}+\frac{1}{1+e^{(E_i-\tilde{\mu}_i)/T}}\right] \\ &= 2\int\frac{\mathrm{d}^3\vec{p}}{(2\pi)^3}\left(\ell_i-\bar{\ell}_i\right), \quad i=p,n \end{aligned} \tag{A.52}$$

$$\begin{aligned} P &= -\frac{\partial(\Omega V)}{\partial V} = -\Omega\frac{\partial V}{\partial V} = -\Omega \\ &= 2\sum_{i=p,n}\int\frac{\mathrm{d}^3\vec{p}}{(2\pi)^3}\left[T\ln\left(1+e^{-(\omega_i+\tilde{\mu}_i)/T}\right)+T\ln\left(1+e^{-(\omega_i-\tilde{\mu}_i)/T}\right)\right] \\ &\quad -\frac{1}{2}m_\sigma^2\sigma^2+\frac{1}{2}m_\omega^2\omega^2+\frac{1}{2}m_\rho^2\rho^2-\frac{1}{3}\kappa(g_\sigma\sigma)^3-\frac{1}{4}\lambda(g_\sigma\sigma)^4 \\ &\quad +\frac{1}{4!}\xi g_\omega^4\omega^4+\Lambda_{\omega\rho}(g_\omega^2\omega^2)(g_\rho^2\rho^2)-\Omega_0 \end{aligned} \tag{A.53}$$

$$\begin{aligned} S &= -\frac{\partial\Omega}{\partial T} \\ &= 2\sum_{i=p,n}\int\frac{\mathrm{d}^3\vec{p}}{(2\pi)^3}\left[\ln\left(1+e^{-(\omega_i+\tilde{\mu}_i)/T}\right)+\ln\left(1+e^{-(\omega_i-\tilde{\mu}_i)/T}\right)\right] \\ &\quad +2T\sum_{i=p,n}\int\frac{\mathrm{d}^3\vec{p}}{(2\pi)^3}\left[\frac{\frac{\omega_i+\tilde{\mu}_i}{T^2}e^{-(\omega_i+\tilde{\mu}_i)/T}}{1+e^{-(\omega_i+\tilde{\mu}_i)/T}}+\frac{\frac{\omega_i-\tilde{\mu}_i}{T^2}e^{-(\omega_i-\tilde{\mu}_i)/T}}{1+e^{-(\omega_i-\tilde{\mu}_i)/T}}\right] \\ &= -\frac{\Omega+U-\Omega_0}{T} \\ &\quad +2\sum_{i=p,n}\int\frac{\mathrm{d}^3\vec{p}}{(2\pi)^3}\left[\frac{\omega_i+\tilde{\mu}_i}{T}\frac{1}{1+e^{(\omega_i+\tilde{\mu}_i)/T}}+\frac{\omega_i-\tilde{\mu}_i}{T}\frac{1}{1+e^{(\omega_i-\tilde{\mu}_i)/T}}\right] \\ &= 2\sum_{i=p,n}\int\frac{\mathrm{d}^3\vec{p}}{(2\pi)^3}\left[\frac{\omega_i+\tilde{\mu}_i}{T}\bar{\ell}_i+\frac{\omega_i-\tilde{\mu}_i}{T}\ell_i\right]-\frac{\Omega+U-\Omega_0}{T} \\ &= \frac{2}{T}\sum_{i=p,n}\int\frac{\mathrm{d}^3\vec{p}}{(2\pi)^3}\left[\omega_i(\bar{\ell}_i+\ell_i)+\tilde{\mu}_i(\bar{\ell}_i-\ell_i)+T\ln\left(1+e^{-(\omega_i+\tilde{\mu}_i)/T}\right)+T\ln\left(1+e^{-(\omega_i-\tilde{\mu}_i)/T}\right)\right] \end{aligned} \tag{A.54}$$

$$
\begin{aligned}
E &= -P + TS + \sum_i \mu_i n_i \\
&= \Omega + T\left[2\sum_{i=p,n}\int \frac{\mathrm{d}^3\vec{p}}{(2\pi)^3}\left[\frac{\omega_i+\tilde{\mu}_i}{T}\bar{\not{f}}_i + \frac{\omega_i-\tilde{\mu}_i}{T}\not{f}_i\right] - \frac{\Omega+U-\Omega_0}{T}\right] + \sum_{i=p,n}\mu_i n_i \\
&= 2\sum_{i=p,n}\int \frac{\mathrm{d}^3\vec{p}}{(2\pi)^3}\Big[(\omega_i+\tilde{\mu}_i)\bar{\not{f}}_i + (\omega_i-\tilde{\mu}_i)\not{f}_i\Big] + \mu_i n_i - U + \Omega_0 \\
&= 2\sum_{i=p,n}\int \frac{\mathrm{d}^3\vec{p}}{(2\pi)^3}\Big[\omega_i(\not{f}_i+\bar{\not{f}}_i) - \tilde{\mu}_i(\not{f}_i-\bar{\not{f}}_i)\Big] + \mu_i n_i - U + \Omega_0 \\
&= 2\sum_{i=p,n}\int \frac{\mathrm{d}^3\vec{p}}{(2\pi)^3}\omega_i(\not{f}_i+\bar{\not{f}}_i) - (\tilde{\mu}_i-\mu_i)n_i - U + \Omega_0 \\
&= 2\sum_{i=p,n}\int \frac{\mathrm{d}^3\vec{p}}{(2\pi)^3}\omega_i(\not{f}_i+\bar{\not{f}}_i) - (-g_\omega\omega - \tfrac{1}{2}g_\rho\rho)n_p - (-g_\omega\omega + \tfrac{1}{2}g_\rho\rho)n_n - U + \Omega_0 \\
&= 2\sum_{i=p,n}\int \frac{\mathrm{d}^3\vec{p}}{(2\pi)^3}\omega_i(\not{f}_i+\bar{\not{f}}_i) + g_\omega\omega(n_p+n_n) + \frac{1}{2}g_\rho\rho(n_p-n_n) \\
&\quad + \frac{1}{2}m_\sigma^2\sigma^2 - \frac{1}{2}m_\omega^2\omega^2 - \frac{1}{2}m_\rho^2\rho^2 + \frac{1}{3}\kappa(g_\sigma\sigma)^3 + \frac{1}{4}\lambda(g_\sigma\sigma)^4 \\
&\quad - \frac{1}{4!}\xi g_\omega^4\omega^4 - \Lambda_{\omega\rho}(g_\omega^2\omega^2)(g_\rho^2\rho^2) + \Omega_0
\end{aligned}
\tag{A.55}
$$

Once again, the values of the auxiliary fields are obtained by imposing that they minimize the grand canonical potential.

$$\frac{\partial\Omega}{\partial\sigma} = 0 \tag{A.56}$$

$$\frac{\partial\Omega}{\partial\omega} = 0 \tag{A.57}$$

$$\frac{\partial\Omega}{\partial\rho} = 0 \tag{A.58}$$

We have three equations:

$$
\begin{aligned}
\frac{\partial\Omega}{\partial\sigma} &= -2T\sum_{i=p,n}\int \frac{\mathrm{d}^3\vec{p}}{(2\pi)^3}\frac{\partial}{\partial\omega_i}\Big[\ln\Big(1+e^{-(\omega_i+\tilde{\mu}_i)/T}\Big) + \ln\Big(1+e^{-(\omega_i-\tilde{\mu}_i)/T}\Big)\Big]\frac{\partial\omega_i}{\partial M}\frac{\partial M}{\partial\sigma} \\
&\quad + m_\sigma^2\sigma + \kappa g_\sigma^3\sigma^2 + \lambda g_\sigma^4\sigma^3 \\
&= -2T\sum_{i=p,n}\int \frac{\mathrm{d}^3\vec{p}}{(2\pi)^3}\left[\frac{-\frac{1}{T}e^{-(\omega_i+\tilde{\mu}_i)/T}}{1+e^{-(\omega_i+\tilde{\mu}_i)/T}} + \frac{-\frac{1}{T}e^{-(\omega_i-\tilde{\mu}_i)/T}}{1+e^{-(\omega_i-\tilde{\mu}_i)/T}}\right]\left(\frac{M}{\omega_i}\right)(-g_\sigma) \\
&\quad + m_\sigma^2\sigma + \kappa g_\sigma^3\sigma^2 + \lambda g_\sigma^4\sigma^3 \\
&= -2g_\sigma\sum_{i=p,n}\int \frac{\mathrm{d}^3\vec{p}}{(2\pi)^3}\frac{M}{\omega_i}\Big[\not{f}_i+\bar{\not{f}}_i\Big] + m_\sigma^2\sigma + \kappa g_\sigma^3\sigma^2 + \lambda g_\sigma^4\sigma^3 = 0
\end{aligned}
\tag{A.59}
$$

$$\begin{aligned}
\frac{\partial\Omega}{\partial\omega} &= -2T\sum_{i=p,n}\int\frac{\mathrm{d}^3\vec{p}}{(2\pi)^3}\frac{\partial}{\partial\tilde{\mu}_i}\Big[\ln\Big(1+e^{-(\omega_i+\tilde{\mu}_i)/T}\Big)+\ln\Big(1+e^{-(\omega_i-\tilde{\mu}_i)/T}\Big)\Big]\frac{\partial\tilde{\mu}_i}{\partial\omega}\\
&\quad - m_\omega^2\omega - \frac{1}{3!}\xi g_\omega^4\omega^3 - 2\Lambda_{\omega\rho}(g_\omega^2\omega)(g_\rho^2\rho^2)\\
&= -2T\sum_{i=p,n}\int\frac{\mathrm{d}^3\vec{p}}{(2\pi)^3}\left[\frac{-\frac{1}{T}e^{-(\omega_i+\tilde{\mu}_i)/T}}{1+e^{-(\omega_i+\tilde{\mu}_i)/T}}+\frac{\frac{1}{T}e^{-(\omega_i-\tilde{\mu}_i)/T}}{1+e^{-(\omega_i-\tilde{\mu}_i)/T}}\right](-g_\omega)\\
&\quad - m_\omega^2\omega - \frac{1}{3!}\xi g_\omega^4\omega^3 - 2\Lambda_{\omega\rho}(g_\omega^2\omega)(g_\rho^2\rho^2)\\
&= 2g_\omega\sum_{i=p,n}\int\frac{\mathrm{d}^3\vec{p}}{(2\pi)^3}\Big[\not{\ell}_i-\bar{\not{\ell}}_i\Big] - m_\omega^2\omega - \frac{1}{3!}\xi g_\omega^4\omega^3 - 2\Lambda_{\omega\rho}(g_\omega^2\omega)(g_\rho^2\rho^2) = 0\\
&= g_\omega(n_p+n_n) - m_\omega^2\omega - \frac{1}{3!}\xi g_\omega^4\omega^3 - 2\Lambda_{\omega\rho}(g_\omega^2\omega)(g_\rho^2\rho^2) = 0
\end{aligned}\tag{A.60}$$

$$\begin{aligned}
\frac{\partial\Omega}{\partial\rho} &= -2T\sum_{i=p,n}\int\frac{\mathrm{d}^3\vec{p}}{(2\pi)^3}\frac{\partial}{\partial\tilde{\mu}_i}\Big[\ln\Big(1+e^{-(\omega_i+\tilde{\mu}_i)/T}\Big)+\ln\Big(1+e^{-(\omega_i-\tilde{\mu}_i)/T}\Big)\Big]\frac{\partial\tilde{\mu}_i}{\partial\rho}\\
&\quad - m_\rho^2\rho - 2\Lambda_{\omega\rho}(g_\omega^2\omega^2)(g_\rho^2\rho)\\
&= -2\int\frac{\mathrm{d}^3\vec{p}}{(2\pi)^3}\Big(\Big[\not{\ell}_p-\bar{\not{\ell}}_p\Big]\Big(-\tfrac{1}{2}g_\rho\Big)+\Big[\not{\ell}_n-\bar{\not{\ell}}_n\Big]\Big(+\tfrac{1}{2}g_\rho\Big)\Big)\\
&\quad - m_\rho^2\rho - 2\Lambda_{\omega\rho}(g_\omega^2\omega^2)(g_\rho^2\rho)\\
&= g_\rho\int\frac{\mathrm{d}^3\vec{p}}{(2\pi)^3}\Big[\not{\ell}_p-\bar{\not{\ell}}_p\Big] - g_\rho\int\frac{\mathrm{d}^3\vec{p}}{(2\pi)^3}\Big[\not{\ell}_n-\bar{\not{\ell}}_n\Big] - m_\rho^2\rho - 2\Lambda_{\omega\rho}(g_\omega^2\omega^2)(g_\rho^2\rho) = 0\\
&= \frac{1}{2}g_\rho(n_p-n_n) - m_\rho^2\rho - 2\Lambda_{\omega\rho}(g_\omega^2\omega^2)(g_\rho^2\rho) = 0
\end{aligned}\tag{A.61}$$

The latter two also let us write the energy in the following way:

$$\begin{aligned}
E = 2\sum_{i=p,n}\int\frac{\mathrm{d}^3\vec{p}}{(2\pi)^3}&\omega_i(\not{\ell}_i+\bar{\not{\ell}}_i)\\
&+\frac{1}{2}m_\sigma^2\sigma^2+\frac{1}{2}m_\omega^2\omega^2+\frac{1}{2}m_\rho^2\rho^2+\frac{1}{3}\kappa(g_\sigma\sigma)^3+\frac{1}{4}\lambda(g_\sigma\sigma)^4\\
&+\frac{1}{8}\xi g_\omega^4\omega^4+3\Lambda_{\omega\rho}(g_\omega^2\omega^2)(g_\rho^2\rho^2)+\Omega_0
\end{aligned}\tag{A.62}$$

A.8 Thermodynamic quantities for a free gas of leptons

The Lagrangian of a free fermion gas of non-interacting leptons is trivially the same as its mean field "approximation", so the results derived in that formalism are exact. The grand canonical potential density for this model is

$$\Omega = -2T\sum_{\ell=e,\mu}\int\frac{\mathrm{d}^3\vec{p}}{(2\pi)^3}\left[\frac{\omega_\ell}{T}+\ln\Big(1+e^{-(\omega_\ell+\mu_\ell)/T}\Big)+\ln\Big(1+e^{-(\omega_\ell-\mu_\ell)/T}\Big)\right]+\Omega_0 \tag{A.63}$$

Following expressions (2.59)–(2.62) yields

$$n_i = -\frac{\partial\Omega}{\partial\mu_i} = 2\int \frac{\mathrm{d}^3\vec{p}}{(2\pi)^3}\Big(\fermi_i - \bar{\fermi}_i\Big), \quad \ell = e,\mu \tag{A.64}$$

$$\begin{aligned} P &= -\frac{\partial(\Omega V)}{\partial V} = -\Omega\frac{\partial V}{\partial V} = -\Omega \\ &= 2T\sum_{\ell=e,\mu}\int \frac{\mathrm{d}^3\vec{p}}{(2\pi)^3}\left[\frac{\omega_\ell}{T} + \ln\Big(1+e^{-(\omega_\ell+\mu_\ell)/T}\Big) + \ln\Big(1+e^{-(\omega_\ell-\mu_\ell)/T}\Big)\right] - \Omega_0 \end{aligned} \tag{A.65}$$

$$\begin{aligned} S &= -\frac{\partial\Omega}{\partial T} \\ &= \frac{2}{T}\sum_{\ell=e,\mu}\int \frac{\mathrm{d}^3\vec{p}}{(2\pi)^3}\Big[\omega_\ell(\bar{\fermi}_\ell + \fermi_\ell) + \tilde{\mu}_\ell(\bar{\fermi}_\ell - \fermi_\ell) + T\ln\Big(1+e^{-(\omega_\ell+\tilde{\mu}_\ell)/T}\Big) + T\ln\Big(1+e^{-(\omega_\ell-\tilde{\mu}_\ell)/T}\Big)\Big] \end{aligned} \tag{A.66}$$

$$\begin{aligned} E &= -P + TS + \sum_\ell \mu_\ell n_\ell \\ &= \Omega + T\left[2\sum_{\ell=e,\mu}\int \frac{\mathrm{d}^3\vec{p}}{(2\pi)^3}\left[-\frac{\omega_i}{T} + \frac{\omega_\ell+\tilde{\mu}_\ell}{T}\bar{\fermi}_\ell + \frac{\omega_\ell-\tilde{\mu}_\ell}{T}\fermi_\ell\right] - \frac{\Omega+U-\Omega_0}{T}\right] + \sum_{\ell=e,\mu}\mu_\ell n_\ell \\ &= 2\sum_{\ell=e,\mu}\int \frac{\mathrm{d}^3\vec{p}}{(2\pi)^3}\Big[-\omega_\ell + (\omega_\ell+\tilde{\mu}_\ell)\bar{\fermi}_\ell + (\omega_\ell-\tilde{\mu}_\ell)\fermi_\ell\Big] + \mu_\ell n_\ell - U + \Omega_0 \\ &= 2\sum_{\ell=e,\mu}\int \frac{\mathrm{d}^3\vec{p}}{(2\pi)^3}\Big[\omega_\ell(\fermi_\ell + \bar{\fermi}_\ell - 1) - \tilde{\mu}_\ell(\fermi_\ell - \bar{\fermi}_\ell)\Big] + \mu_\ell n_\ell - U + \Omega_0 \\ &= 2\sum_{\ell=e,\mu}\int \frac{\mathrm{d}^3\vec{p}}{(2\pi)^3}\omega_\ell(\fermi_\ell + \bar{\fermi}_\ell - 1) - (\tilde{\mu}_\ell - \mu_\ell)n_\ell - U + \Omega_0 \\ &= 2\sum_{\ell=e,\mu}\int \frac{\mathrm{d}^3\vec{p}}{(2\pi)^3}\omega_\ell(\fermi_\ell + \bar{\fermi}_\ell - 1) + \Omega_0 \end{aligned} \tag{A.67}$$

A.9 Useful closed-form integrals

These integrals were obtained with the aid of computer algebra systems:

$$\int x^2\sqrt{x^2+a^2}\,\mathrm{d}x = \frac{1}{8}\Big(x\sqrt{x^2+a^2}(2x^2+a^2) - a^4\log\Big(x+\sqrt{x^2+a^2}\Big)\Big) \tag{A.68}$$

$$\int \frac{x^2 a}{\sqrt{x^2+a^2}}\,\mathrm{d}x = \frac{1}{2}a\Big(x\sqrt{x^2+a^2} - a^2\log\Big(x+\sqrt{x^2+a^2}\Big)\Big) \tag{A.69}$$

We do not repeat calculations which are totally analogous to previous ones.

Appendix B

Definitions

B.1 Gamma matrices and the algebra of spinors

The gamma matrices are a set of matrices that are such that they obey a specific anticommutation relation.

$$\{\gamma^\mu, \gamma^\nu\} = 2\eta^{\mu\nu} \tag{B.1}$$

Formally, they generate a representation of the $C\ell_{1,3}(\mathbb{R})$ Clifford algebra. The matrices act on the space of spinors. In the Dirac basis, the four (contravariant) gamma matrices are

$$\begin{aligned} \gamma^0 &= \begin{pmatrix} 1 & 0 & 0 & 0 \\ 0 & 1 & 0 & 0 \\ 0 & 0 & -1 & 0 \\ 0 & 0 & 0 & -1 \end{pmatrix} \quad \gamma^1 = \begin{pmatrix} 0 & 0 & 0 & 1 \\ 0 & 0 & 1 & 0 \\ 0 & -1 & 0 & 0 \\ -1 & 0 & 0 & 0 \end{pmatrix} \\ \gamma^2 &= \begin{pmatrix} 0 & 0 & 0 & -i \\ 0 & 0 & i & 0 \\ 0 & i & 0 & 0 \\ -i & 0 & 0 & 0 \end{pmatrix} \quad \gamma^3 = \begin{pmatrix} 0 & 0 & 1 & 0 \\ 0 & 0 & 0 & -1 \\ -1 & 0 & 0 & 0 \\ 0 & 1 & 0 & 0 \end{pmatrix} \end{aligned} \tag{B.2}$$

while the covariant matrices are obtained by lowering the indices as usual

$$\gamma_\mu = \eta_{\mu\nu}\gamma^\nu = \{\gamma^0, -\gamma^1, -\gamma^2, -\gamma^3\} \tag{B.3}$$

The γ^0 matrix is hermitian, while the $\gamma^1, \gamma^2, \gamma^3$ are anti-hermitian.

$$(\gamma^0)^\dagger = \gamma^0 \tag{B.4}$$

$$\gamma^{i\dagger} = -\gamma^i \tag{B.5}$$

A useful definition is that of the fifth gamma matrix.

$$\gamma^5 = \gamma_5 \equiv i\gamma^0\gamma^1\gamma^2\gamma^3 = \begin{pmatrix} 0 & 0 & 1 & 0 \\ 0 & 0 & 0 & 1 \\ 1 & 0 & 0 & 0 \\ 0 & 1 & 0 & 0 \end{pmatrix} \tag{B.6}$$

The fifth gamma matrix has the following useful properties:

$$\{\gamma^\mu, \gamma^5\} = 0 \tag{B.7}$$
$$(\gamma^5)^2 = \mathbb{1}_4 \tag{B.8}$$
$$\gamma^{5\dagger} = \gamma^5 \tag{B.9}$$

B.2 Generators and structure constants of SU(3)

SU(3) is the special unitary group of degree 3. It is the Lie group of unitary 3×3 matrices with determinant $+1$. The generators of SU(3) are denoted t_a, and can be written

$$t_a = \frac{\lambda_a}{2} \tag{B.10}$$

where λ_a are the Gell-Mann matrices, traceless Hermitian matrices, the analogues of the Pauli matrices of SU(2) for SU(3). They form a basis for the space of traceless 3×3 Hermitian matrices. They are:

$$\begin{aligned} \lambda_1 &= \begin{pmatrix} 0 & 1 & 0 \\ 1 & 0 & 0 \\ 0 & 0 & 0 \end{pmatrix} \quad \lambda_2 = \begin{pmatrix} 0 & -i & 0 \\ i & 0 & 0 \\ 0 & 0 & 0 \end{pmatrix} \quad \lambda_3 = \begin{pmatrix} 1 & 0 & 0 \\ 0 & -1 & 0 \\ 0 & 0 & 0 \end{pmatrix} \\ \lambda_4 &= \begin{pmatrix} 0 & 0 & 1 \\ 0 & 0 & 0 \\ 1 & 0 & 0 \end{pmatrix} \quad \lambda_5 = \begin{pmatrix} 0 & 0 & -i \\ 0 & 0 & 0 \\ i & 0 & 0 \end{pmatrix} \\ \lambda_6 &= \begin{pmatrix} 0 & 0 & 0 \\ 0 & 0 & 1 \\ 0 & 1 & 0 \end{pmatrix} \quad \lambda_7 = \begin{pmatrix} 0 & 0 & 0 \\ 0 & 0 & -i \\ 0 & i & 0 \end{pmatrix} \quad \lambda_8 = \frac{1}{\sqrt{3}} \begin{pmatrix} 1 & 0 & 0 \\ 0 & 1 & 0 \\ 0 & 0 & -2 \end{pmatrix} \end{aligned} \tag{B.11}$$

The generators (which form the $\mathfrak{su}(3)$ algebra) obey

$$[t_a, t_b] = i f_{abc} t^c \tag{B.12}$$
$$\{t_a, t_b\} = \frac{1}{3}\delta_{ab} + 4 d_{abc} t^c \tag{B.13}$$

Although not really one of the gamma matrices the notation stuck.

where f_{abc} are the structure constants of the algebra,

$$\begin{aligned} &f_{123} = 1 \\ &f_{147} = -f_{156} = f_{246} = f_{257} = f_{345} = -f_{367} = \frac{1}{2} \\ &f_{458} = f_{678} = \frac{\sqrt{3}}{2} \\ &\text{zero otherwise} \end{aligned} \tag{B.14}$$

and d_{abc} are the symmetric coefficients,

$$\begin{aligned} &d_{118} = d_{228} = d_{338} = -d_{888} = \frac{1}{\sqrt{3}} \\ &d_{448} = d_{558} = d_{668} = d_{778} = -\frac{1}{2\sqrt{3}} \\ &d_{146} = d_{157} = -d_{247} = d_{256} = d_{344} = d_{355} = -d_{366} = -d_{377} = \frac{1}{2} \\ &\text{zero otherwise} \end{aligned} \tag{B.15}$$

Any matrix of SU(3) can be written as $\exp(i\theta^i t_i)$, where $\theta^i \in \mathbb{R}$.

B.3 Generators of SU(2)

SU(2) is the special unitary group of degree 2. It is the Lie group of unitary 2×2 matrices with determinant $+1$. Analogously to the previous section, we present the generators, denoted τ_i:

$$\tau_i = \frac{\sigma_i}{2} \tag{B.16}$$

where σ_i are the Pauli matrices which form a basis for the space of 2×2 traceless Hermitian matrices. They are:

$$\sigma_1 = \begin{pmatrix} 0 & 1 \\ 1 & 0 \end{pmatrix} \quad \sigma_2 = \begin{pmatrix} 0 & -i \\ i & 0 \end{pmatrix} \quad \sigma_3 = \begin{pmatrix} 1 & 0 \\ 0 & -1 \end{pmatrix} \tag{B.17}$$

They obey

$$[\tau_i, \tau_j] = i\varepsilon_{ijk}\tau^k \tag{B.18}$$

$$\{\tau_i, \tau_j\} = \frac{1}{2}\delta_{ij} \tag{B.19}$$

Here the structure constants of the $\mathfrak{su}(2)$ algebra are the Levi-Civita symbol (see next section) and the symmetric coefficients are all zero.

B.4 The Levi-Civita symbol

The Levi-Civita symbol, also known as the completely antisymmetric tensor, denoted $\varepsilon_{i_1,i_2,\ldots,i_n}$ is a rank n tensor defined over an ordered alphabet of symbols $a_1, a_2, \ldots, a_n$, and has the following properties:

- $\varepsilon_{i_1,i_2,\ldots,i_n} = 1$ if $i_1, i_2, \ldots, i_n = a_1, a_2, \ldots, a_n$ respectively
- $\varepsilon_{\ldots,i_p,\ldots,i_q,\ldots} = -\varepsilon_{\ldots,i_q,\ldots,i_p,\ldots}$
- $\varepsilon_{i_1,i_2,\ldots,i_n} = 0$ if any $i_p = i_q, p \neq q$

That is, the symbol of the ordered alphabet is defined as 1, it flips sign under a permutation of two indices, and is equal to zero if there are any repeated indices. In other words, the symbol is equal to the sign of the permutation, if all indices are different, and zero if any indices are repeated.

The sign of a permutation is $+1$ for an even permutation (even number of permutations) and -1 for an odd permutation (odd number of permutations).

For the particular case where the alphabet is (u, d, s) the Levi-Civita symbol is

$$\begin{cases} \varepsilon_{uds} = \varepsilon_{dsu} = \varepsilon_{sud} = +1 \\ \varepsilon_{sdu} = \varepsilon_{usd} = \varepsilon_{dus} = -1 \\ \text{zero otherwise} \end{cases} \tag{B.20}$$

The determinant of an $N \times N$ matrix can be written by contracting the Levi-Civita symbol with its components. Let

$$A = \begin{pmatrix} a_{11} & a_{12} & \ldots & a_{1N} \\ a_{21} & a_{22} & \ldots & a_{2N} \\ \vdots & \vdots & \ddots & \vdots \\ a_{N1} & a_{N2} & \ldots & a_{NN} \end{pmatrix} \tag{B.21}$$

The determinant of A is

$$\det A = \sum_{i_1=0}^{N} \sum_{i_2=0}^{N} \cdots \sum_{i_N=0}^{N} \varepsilon_{i_1,i_2,\ldots,i_N} a_{1i_1} a_{2i_2} \ldots a_{Ni_N} \tag{B.22}$$

For the particular case where A is a 3×3 square matrix over indices u, d, s, the determinant can be written

$$\begin{aligned} \det A &= \sum_{\substack{i=\{u,d,s\} \\ j=\{u,d,s\}}} \sum_{k=\{u,d,s\}} \varepsilon_{ijk} a_{ui} a_{dj} a_{sk} \\ &= a_{uu}a_{dd}a_{ss} + a_{ud}a_{ds}a_{su} + a_{us}a_{du}a_{sd} \\ &\quad - a_{us}a_{dd}a_{su} - a_{uu}a_{ds}a_{sd} - a_{ud}a_{du}a_{ss} \end{aligned} \tag{B.23}$$

B.5 Heaviside step functon

The Heaviside step function is defined as

$$H(x) = \begin{cases} 1 & \text{if} \quad x \geq 0 \\ 0 & \text{if} \quad x < 0 \end{cases} \tag{B.24}$$

which means that

$$\int_a^b f(x)H(x-c)\,\mathrm{d}x = \int_{\max\{a,c\}}^b f(x)\,\mathrm{d}x \tag{B.25}$$

$$\int_a^b f(x)H(c-x)\,\mathrm{d}x = \int_a^{\min\{b,c\}} f(x)\,\mathrm{d}x \tag{B.26}$$

Appendix C

Data files

The data files with the results from this work can be viewed and downloaded at:

`https://github.com/andrepd/masterthesis-data`

List of Figures

List of Tables

Acronyms

EoS Equation of state.

NJL Nambu–Jona-Lasinio.

NS Neutron atar.

PNS Proto-neutron star.

QCD Quantum chromodynamics.

QFT Quantum field theory.

TOV Tolman–Oppenheimer–Volkoff.

UV Ultraviolet.

Bibliography

[1] Norman K. Glendenning. *Compact stars: nuclear physics, particle physics, and general relativity*. Astronomy and astrophysics library. Springer, New York, 2nd ed edition, 2000. 1, 4, 5, 8, 10, 11, 14, 40, 42, 43, 44, 45, 53, 74, 82

[2] N. Chamel, P. Haensel, J. L. Zdunik, and A. F. Fantina. On the maximum mass of neutron stars. *International Journal of Modern Physics E*, 22(07):1330018, Jul 2013. arXiv:1307.3995, doi:10.1142/s021830131330018x. 2

[3] P. A. Mazzali, F. K. Ropke, S. Benetti, and W. Hillebrandt. A common explosion mechanism for type ia supernovae. *Science*, 315(5813):825–828, Feb 2007. arXiv:astro-ph/0702351v1, doi:10.1126/science.1136259. 2

[4] Feryal Özel and Paulo Freire. Masses, radii, and the equation of state of neutron stars. *Annual Review of Astronomy and Astrophysics*, 54(1):401–440, Sep 2016. doi:10.1146/annurev-astro-081915-023322. 2, 4, 8, 73

[5] I. Bombaci. The maximum mass of a neutron star. *AAP*, 305:871, Jan 1996. 2

[6] Feryal Özel. Observations and models of compact stars. http://xtreme.as.arizona.edu/NeutronStars/. Accessed: 2017-04-28. 2, 3

[7] Feryal Özel, Dimitrios Psaltis, Tolga Güver, Gordon Baym, Craig Heinke, and Sebastien Guillot. The dense matter equation of state from neutron star radius and mass measurements. *The Astrophysical Journal*, 820(1):28, Mar 2016. arXiv:1505.05155v2, doi:10.3847/0004-637x/820/1/28. 2

[8] J. W. T. Hessels, S. M. Ransom, I. H. Stairs, P. C. C. Freire, V. M. Kaspi, and F. Camilo. A Radio Pulsar Spinning at 716 Hz. *Science*, 311:1901–1904, Mar 2006. arXiv:astro-ph/0601337, doi:10.1126/science.1123430. 4

[9] B. P. Abbott et al. Observation of Gravitational Waves from a Binary Black Hole Merger. *Physical Review Letters*, 116(6), Feb 2016. arXiv:1602.03837, doi:10.1103/physrevlett.116.061102. 5

[10] V. E. Zavlin and G. G. Pavlov. Modeling neutron star atmospheres. 2002. arXiv:astro-ph/0206025. 5

[11] S.M. Carroll. *Spacetime and Geometry: An Introduction to General Relativity*. Addison Wesley, 2004. URL: https://books.google.pt/books?id=1SKFQgAACAAJ. 6, 7, 11

[12] J. R. Oppenheimer and G. M. Volkoff. On massive neutron cores. *Physical Review*, 55(4):374–381, Feb 1939. doi:10.1103/physrev.55.374. 8

[13] Nikolaos Stergioulas and John L. Friedman. Comparing models of rapidly rotating relativistic stars constructed by two numerical methods. *The Astrophysical Journal*, 444:306, May 1995. arXiv:astro-ph/9411032, doi:10.1086/175605. 8

[14] Scott Hughes. 8.022 — Lecture 1, Feb 2005. URL: http://web.mit.edu/sahughes/www/8.022/lec01.pdf. 12

[15] Fabrizio Grill, Helena Pais, Constança Providência, Isaac Vidaña, and Sidney S. Avancini. Equation of state and thickness of the inner crust of neutron stars. *Phys. Rev. C*, 90:045803, Oct 2014. arXiv:1404.2753, doi:10.1103/PhysRevC.90.045803. 14, 61

[16] J. L. Zdunik, M. Fortin, and P. Haensel. Neutron star properties and the equation of state for its core. 2016. arXiv:1611.01357. 14, 16, 83

[17] Camille Ducoin, Jérôme Margueron, Constança Providência, and Isaac Vidaña. Core-crust transition in neutron stars: Predictivity of density developments. *Physical Review C*, 83(4), Apr 2011. arXiv:arXiv:1102.1283, doi:10.1103/physrevc.83.045810. 15, 60

[18] P. A. M. Dirac. *The Principles of Quantum Mechanics (International Series of Monographs on Physics)*. Clarendon Press, 1982. 17

[19] David Tong. Lectures on quantum field theory. URL: http://www.damtp.cam.ac.uk/user/tong/qft.html. 17, 18

[20] M.E. Peskin and D.V. Schroeder. *An Introduction to Quantum Field Theory*. Advanced book classics. Avalon Publishing, 1995. URL: https://books.google.pt/books?id=i35LALN0GosC. 18, 19, 20, 24, 34, 86

[21] D. Griffiths. *Introduction to Elementary Particles*. Physics textbook. Wiley, 2008. URL: https://books.google.pt/books?id=Wb9DYrjcoKAC. 19, 24

[22] C. Patrignani et al. Review of Particle Physics. *Chin. Phys.*, C40(10):100001, 2016. URL: http://pdg.lbl.gov/2017/listings/contents_listings.html, doi:10.1088/1674-1137/40/10/100001. 21, 25, 41, 59, 60, 61

[23] G. 't Hooft. How instantons solve the U(1) problem. *Physics Reports*, 142(6):357–387, Sep 1986. doi:10.1016/0370-1573(86)90117-1. 23, 25, 34

[24] C. McNeile, A. Bazavov, C. T. H. Davies, R. J. Dowdall, K. Hornbostel, G. P. Lepage, and H. D. Trottier. Direct determination of the strange and light quark condensates from full lattice QCD. *Physical Review D*, 87(3), Feb 2013. arXiv:1211.6577, doi:10.1103/physrevd.87.034503. 24

[25] S. Scherer. Introduction to Chiral Perturbation Theory. Oct 2002. arXiv:hep-ph/0210398. 25

[26] J.I. Kapusta and C. Gale. *Finite-Temperature Field Theory: Principles and Applications*. Cambridge Monographs on Mathematical Physics. Cambridge University Press, 2006. URL: https://books.google.pt/books?id=rll8dJ2iTpsC. 26, 27, 29, 40, 42

[27] V. G. Vaks and A. I. Larkin. On the application of the methods of superconductivity theory to the problem of the masses of elementary particles. *Sov. Phys. JETP. (English edition)*, 13:192–193, 1961. URL: http://www.jetp.ac.ru/cgi-bin/dn/e_013_01_0192.pdf. 31

[28] Y. Nambu and G. Jona-Lasinio. Dynamical model of elementary particles based on an analogy with superconductivity. i. *Phys. Rev.*, 122:345–358, Apr 1961. doi:10.1103/PhysRev.122.345. 31

[29] U. Vogl and W. Weise. The Nambu and Jona-Lasinio model: Its implications for hadrons and nuclei. *Progress in Particle and Nuclear Physics*, 27:195–272, 1991. doi:10.1016/0146-6410(91)90005-9. 31, 32, 33, 34

[30] J.D. Walecka. A theory of highly condensed matter. *Annals of Physics*, 83(2):491–529, Apr 1974. doi:10.1016/0003-4916(74)90208-5. 44

[31] P. G. Reinhard. The relativistic mean-field description of nuclei and nuclear dynamics. *Reports on Progress in Physics*, 52(4):439–514, apr 1989. URL: https://doi.org/10.1088/0034-4885/52/4/002, doi:10.1088/0034-4885/52/4/002. 45, 48

[32] C. J. Horowitz and J. Piekarewicz. Neutron star structure and the neutron radius of ^{208}Pb. *Physical Review Letters*, 86(25):5647–5650, Jun 2001. doi:10.1103/physrevlett.86.5647. 45, 61

[33] Felix Karbstein. Integrating out the Dirac sea in the Walecka model. *Physical Review C*, 81(4), Apr 2010. arXiv:0908.2759, doi:10.1103/physrevc.81.045206. 49

[34] Manuel Fiolhais. Aulas de termodinâmica, 2011. 50

[35] R. C. Pereira, P. Costa, and C. Providência. Two-solar-mass hybrid stars: A two model description using the Nambu–Jona-Lasinio quark model. *Physical Review D*, 94(9), Nov 2016. arXiv:1610.06435, doi:10.1103/physrevd.94.094001. 59, 60

[36] Kenji Fukushima. Phase diagrams in the three-flavor Nambu–Jona-Lasinio model with the Polyakov loop. *Physical Review D*, 77(11), Jun 2008. arXiv:0803.3318, doi:10.1103/physrevd.77.114028. 60

[37] J. Piekarewicz. Validating relativistic models of nuclear structure against theoretical, experimental, and observational constraints. *Physical Review C*, 76(6), Dec 2007. arXiv:0709.2699, doi:10.1103/physrevc.76.064310. 61

[38] William Press. *Numerical Recipes: The Art of Scientific Computing*. Cambridge University Press, Cambridge, UK New York, 2007. 61

[39] Endre Süli and David F. Mayers. *An Introduction to Numerical Analysis*. Cambridge University Press, 2003. 61, 62

[40] Gaël Guennebaud, Benoît Jacob, et al. Eigen v3. http://eigen.tuxfamily.org, 2017. 63

[41] A.W. Steiner, M. Prakash, and J.M. Lattimer. Quark-hadron phase transitions in young and old neutron stars. *Physics Letters B*, 486(3-4):239–248, Aug 2000. arXiv:nucl-th/0003066, doi:10.1016/s0370-2693(00)00780-2. 76

[42] C. C. Nishi. Simple derivation of general Fierz-type identities. *American Journal of Physics*, 73(12):1160–1163, Dec 2005. arXiv:hep-ph/0412245v4, doi:10.1119/1.2074087. 88